

Quantifizierung von Rauschen basierend auf zwei visuellen Modellansätze.

Diplomarbeit an der Fachhochschule Köln
Fachbereich Photoingenieurswesen und Medientechnik

vorgelegt von
Johanna Kleinmann
Matr.-Nr. 11034000

Referent
Prof. Dr. Gregor Fischer

Koreferent
Dipl. Ing. Dietmar Wüller, Image Engineering, Frechen

Köln, 15^{ten} August 2006

Quantification of noise based on two visual Models

Thesis of the Department of
Imaging Science and Media Technology
University of Applied Sciences of Cologne

Author

Johanna Kleinmann

Matr.-Nr. 11034000

First Reviewer

Prof. Dr. Gregor Fischer

Second Reviewer

Dipl.-Ing. Dietmar Wüller, Image Engineering, Frechen

Cologne, 15th of August 2006

Table of content

1 .Chapter 1: Different Methods to measure and quantify noise.....	1
1.1 Setting the Context.....	1
1.1.1 Noise Definition.....	1
1.1.2 Signal to Noise Ratio Measurement Method.....	1
1.1.3 Alternative Approach: CIELab and CIELuv Colour Space.....	5
1.1.3.1 The Actual Perception of Noise.....	5
1.1.3.2 Noise seen as a Colour Difference.....	5
1.2 Description of the Experiment and Development of a new Approach.....	8
1.2.1 Shiraz Experiment.....	8
1.2.2 Thesis: the Threshold Images should get the same Noise Value.....	9
1.2.3 Overview of the Thesis.....	10
2 .Chapter2: The Human Visual System and the Human Visual Model.....	11
2.1 Definition of Colour.....	11
2.2 Eye's Light Sensitivity System: the Photoreceptors.....	12
2.2.1 Sensitivity of the Photoreceptors.....	12
2.2.2 Chromatic Adaptation.....	13
2.2.3 Mosaic and Spatial Arrangement of the Photoreceptors.....	14
2.3 Visual Signal Processing.....	15
2.3.1 Colour Sensation requires an Interaction between the Photoreceptors..	15
2.3.2 Structure of the Photoreceptors and Neurons Interconnections.....	16
2.3.3 Distribution of the Nerves' Fibres throughout the Photoreceptors.....	17
2.3.4 Processing of the Signals: Opponent Colour Signals.....	17

2.4 Spatial Properties of Colour Vision: the Contrast Sensitivity Function	19
2.4.1 Contrast Sensitivity Function and Spatial Frequency.....	19
2.4.2 Restrictions of the Model of the Contrast Sensitivity Function.....	20
2.4.3 Achromatic or Luminance Contrast Sensitivity Function.....	21
2.4.4 Chromatic Contrast Sensitivity Function.....	22
2.5 Human Visual Model and its Algorithm.....	23
2.5.1 Human Visual Model.....	23
2.5.2 Algorithm of the Human Visual System.....	25
3 .Chapter 3:Visual Noise Measurements Model.....	34
3.1 Visual Noise Value Formula.....	34
3.1.1 The Formula.....	34
3.1.1.1 The Formula from the CIELuv1976 Colour Space.....	34
3.1.1.2 The Formula from the CIELab1976 Colour Space.....	35
3.1.1.3 CIELuv1976 vs. CIELab1976.....	36
3.2 Results of the Visual Noise Measurement Model.....	38
3.2.1 Noise Evaluation for Colour Difference in the Luminance Channel.....	40
3.2.2 Noise Evaluation for Colour Difference in the Chroma Channel.....	42
3.2.3 Noise Evaluation for Colour Difference in the Hue Channel.....	46
3.2.4 First Conclusions.....	47
3.3 Praxis oriented Tests of the Visual Noise Measurement Model.....	50
3.3.1 Test of the two Grey Patches.....	50
3.3.2 Example of the Visual Noise Measurement Model used in the Image Engineering Analyser®.....	51
3.3.2.1 OECF20-Chart photographed with the Camera Canon ix65 at sensitivity of 100ISO and 400ISO.....	52
3.3.2.2 Brief analysis.....	54

4 .Chapter 4: S-CIELabDE2000 Model.....	56
4.1 S-CIELabDE2000 Formula: Comparison of a "Noisy" Image with a "Noise-free" Image.....	56
4.2 Investigation of the S-CIELabDE2000 Model.....	63
4.2.1 Investigation with Threshold Images with rectangular spatial Patterns with different Contrast.....	63
4.2.1.1 Noise Input as a Colour difference in the Luminance Channel.....	64
4.2.1.2 Noise Input as Colour Difference in the Chroma Channel.....	65
4.2.1.3 Noise Input as Colour Difference in the Hue Channel.....	66
4.2.2 Further Investigation: Colour Difference in function of the Contrast and the Frequency Patterns.....	68
4.3 Investigation of the Colour Difference for Uniform Patches.....	69
4.3.1 Investigation with Threshold Images.....	69
4.3.2 Brief conclusion.....	70
5 .Chapter 5: Noise Scaling as a Description of the Eye Sensitivity.....	71
5.1 Visual Noise as a Function of the Noise Input.....	71
5.1.1 Visual Noise Scaling along the Luminance Channel.....	72
5.1.2 Visual Noise Scaling along the Chroma Channel.....	74
5.1.3 Visual Noise Scaling along the Hue Channel.....	77
5.1.4 Comparing Noise Scaling and Facility to determine Threshold Images	79
5.2 Noise Scaling between the Chroma and Hue Noise Input.....	81
5.3 Brief conclusion.....	84

6 .Chapter 6: Conclusion.....	85
6.1 Quantification of noise: The Stand of the Research and the new Approach: an Algorithm describing the Human Visual System.....	85
6.1.1 Stand of the Research.....	85
6.1.2 The new Approach: an Algorithm describing the Human Visual System	86
6.2 Results of the Noise Quantification with the two Models.....	86
6.2.1 Quantification of Noise with the Visual Noise Measurement Model....	87
6.2.1.1 Tools of the Visual Noise Measurement Model.....	87
6.2.1.2 Evaluation of the Threshold Images with the Visual Noise Measurement Model.....	87
6.2.2 Noise Quantification with the S-CIELabDE2000 Model.....	88
6.2.2.1 Tool of the S-CIELabDE2000 Model.....	88
6.2.2.2 Evaluation of the Threshold images with the S-CIELabDE200 Model....	88
6.2.3 Conclusion for both Models.....	89
6.3 Does the human visual Algorithm used match the Eye's Sensitivity?....	89
6.3.1 Eye's Sensitivity between Colours in term of Luminance, Chroma, and Hue.....	89
6.3.2 Eye's Sensitivity between Luminance, Chroma and Hue in term of Colour.....	90
6.3.3 Brief conclusion.....	90
6.4 Improvement of the Measurements and of the Method.....	91
6.4.1 Improvement of the Measurements.....	91
6.4.2 Improvement of the Human Visual Algorithm.....	92
7 .Bibliography.....	95
8 .Declaration.....	98
9 .Appendix.....	99

1 .Chapter 1: Different Methods to measure and quantify noise

1.1 Setting the Context

1.1.1 Noise Definition

Colour noise is a current phenomenon in digital image technology. It has many sources [10 pp18-19] [11 pp23-24], and despite the steady improvement of digital imaging technology, noise can not be totally eradicated because of its inherent nature and its statistical, random characteristics.

According to the normative part *ISO 15739:2002(E)* [16], noise is defined as an "*unwanted variations in the response of an imaging system.*" It means that the pixel value is not the one it should be according to the ambient or incident light, the object colours and the camera settings. Consequently colour noise artefacts are image errors that can be observed as brightness or colour changes. [11 p26].

1.1.2 Signal to Noise Ratio Measurement Method

Noise can be measured with the signal to noise ratio[16]:

The signal to noise ratio is determined from the data captured from the uniform density patches of block 13 of the OECF-chart (refer to figure 3.01 [paragraph 3.3.2]) defined by the ISO-standard (in the normative part of *ISO 15739:2002(E)* [16] in Annex A). Lighted under given and specific conditions, the middle grey patch 13b should have a density of 0,9 and refers to the "18% signal level".

The signal to noise ratio is determined by [16]:

$$SNR = \frac{L_{Sat} \cdot 0,18 \cdot \text{incremental gain}}{\sigma_{total\ noise}} \quad (1.01)$$

- Where L_{Sat} is the target luminance that gives the maximum unclipped output from the camera (for an eight bit system, this is 255) [16].
- The 0,18 is the 18% reflectance of the target at a density of 0,9, with respect to a maximum level of 140% (predefined light condition) [16].
- The incremental gain is the first derivative of the OECF, determined by the method in ISO 14524 [16].
- The digital noise is calculated from the standard deviations of the pixel values over the uniform patch. [16]

In practice it can be observed that the more signal, the more noise. But the signal amplitude increases quicker than the noise amplitude, consequently the signal to noise ratio increases when the patches' density decreases.

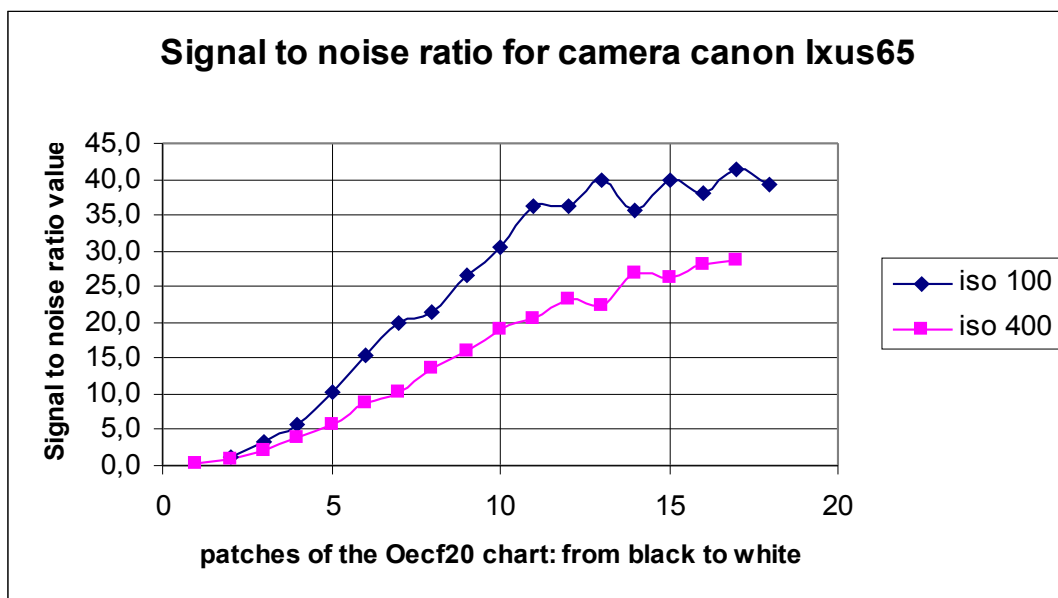


Figure 1.03: Signal to noise ratio values of the patches of the OECF-20 chart photographed with the camera Canon® Ixus65 at a sensor sensitivity of 100ISO and 400ISO.

To characterise the noise behaviour of digital cameras, the ISO-standard has only set the signal to noise ratio of the middle-grey patch of density of 0,9 as reference. But the quantification of noise with this method does not always accurately represent the visual impression of noise, as shown in the following example.

The two middle grey patches of density 0,9 of the test chart OECF20 have been photographed with the digital still camera: *Panasonic® DMC-TZ1G* at sensitivity of 100ISO (figure 1.01) and of 400ISO (figure 1.02).

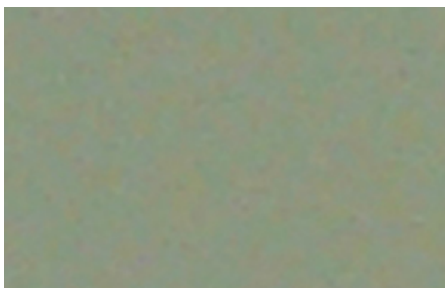


Figure 1.01: Sensitivity of 100ISO

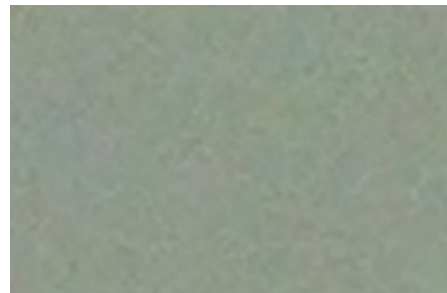


Figure 1.02: Sensitivity of 400ISO

Looking at the patches, it is obvious that for each patch the appearance of noise is different, the noise is from a different kind. At a sensor sensitivity of 100ISO, the noise is chromatic, with red and yellow appearance, and has coarse structures. At a sensitivity of 400ISO, the noise is achromatic, since the grey colour differences seems to take place as luminance differences.

So in comparing both patches, it is clear that visually it is the patch with the sensor sensitivity of 400ISO that it is the most distorted by noise and the most disturbing for the human eye. So in quantifying noise, we would expect that the noise value for the patch photographed at 400ISO would be greater than the noise value for the patch photographed at 100ISO. However, this is not the case when using the signal to noise ratio method: the signal to noise ratio values are the same for both patches: at 100ISO, the SNR is 27,9 and at 400ISO, the SNR is 29,1 (the signal to noise ratio being a linear function).

The signal to noise ratio fails by quantifying the noise seen impression, because first of all, it does not take into account that noise can be from different kind: noise has many sources **[10 pp18-19] [11 pp23-24]**, so it can have different appearances depending on the sensor characteristics and imaging digital processing. Moreover it does not cover the whole dynamic range of the camera, if the lighter and darker patches were evaluated it could be shown, that the seen noise behaves differently over the densities.

Since the signal to noise ratio method is not giving satisfying results regarding the expectations, other methods have to be investigated.

1.1.3 Alternative Approach: CIELab and CIELuv Colour Space

1.1.3.1 The Actual Perception of Noise

It is well documented that the human eye discriminates small differences in luminance more easily than in chroma, and that colour differences are more noticeable in uniform pattern than in high frequency pattern. This suggests that the eye reacts differently depending to the kind of noise: only luminance noise, colour noise, high or low frequency noise, and depending where the noise occurs: uniform surface or complex pattern. The clarity of noise to observers depends on “*the magnitude of the noise, the apparent tone of the area containing the noise, and the spatial frequency of the noise*”. [16]

That is why the noise can not be described just as a physical grandeur, as the signal to noise ratio method does, but it should be described as a physiological one. Indeed the visual noise level can vary depending on the viewing distance, spatial frequency, density, colour and viewing conditions [16].

1.1.3.2 Noise seen as a Colour Difference

Colour noise can be seen as a colour difference, since a pixel becomes "noisy" when it differs from the original colour it should be. So at first it could have been assumed to use the recommended CIE colour spaces for this purpose. Indeed, the CIE has been searching for a uniform colour space that would match the perception of the human visual system.

Two colour spaces should fulfil this requirement: CIE L*u*v* 1976 and the CIE L*a*b*. However, as it is explained in Robertson's paper, *The CIE 1976 Color-Difference Formulae* [22], both colour spaces are not entirely uniform as they were supposed to be; they are only approximately uniform. Investigating their uniformity with the Munsell Color System and the MacAdam Ellipses would show interesting characteristics for each colour space.

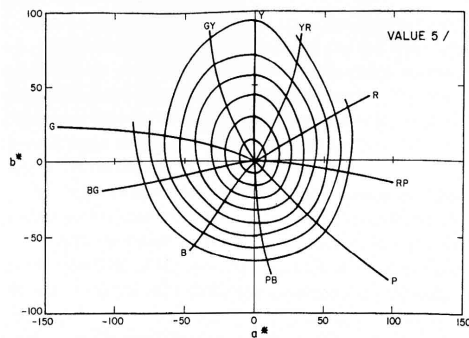


Figure 1.03: Munsell loci of constant hue and chroma plotted in the CIE 1976 a^*b^* diagram.

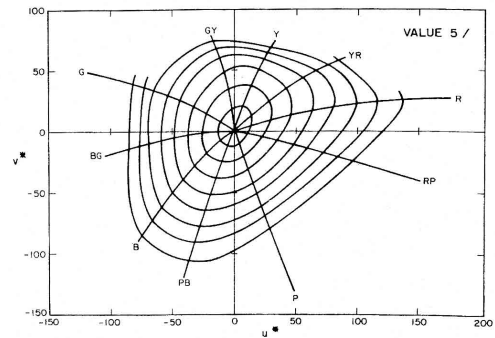


Figure 1.04: Munsell loci of constant hue and chroma plotted in the CIE 1976 u^*v^* diagram.

“Figure 1.03 and 1.04 show Munsell coordinates for value 5 plotted in the a^*b^* and u^*v^* diagrams respectively. Loci of constant hue and of constant chroma are shown. If either diagram provided uniform spacing of the Munsell system, these loci would be straight, equally spaced radial lines and concentric, perfect circles.”[22]. It is clear that neither diagram is perfect in this respect, but the a^*b^* diagram is slightly better than the u^*v^* diagram.

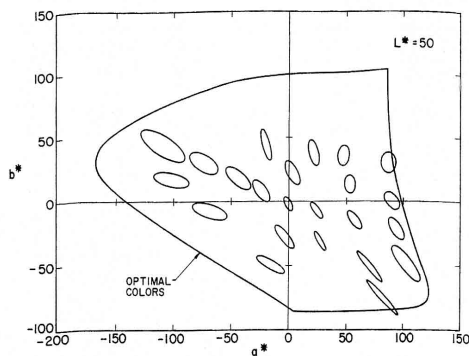


Figure 1.05: Mac Adam Ellipses plotted in the CIE 1976 a^*b^* diagram.

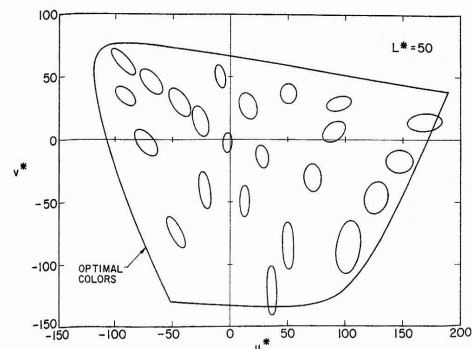


Figure 1.06: Mac Adam Ellipses plotted in the CIE 1976 u^*v^* diagram.

The MacAdam ellipses are also used to test colour-difference formulae. *“These are shown transformed to the a^*b^* and u^*v^* diagrams, respectively, in figure 1.05 and figure 1.06. The transformation was done in each case with the assumption that $L^*=50$. If either space were perfectly uniform, the corresponding diagram would represent the ellipses as equal-radius circles.”* [22] Here again neither diagram matches the conditions, but the u^*v^* diagram shows more ellipses that tend to circles than the a^*b^* diagram does [19].

So as the figures show, $L^*a^*b^*$ diagram performs slightly better when investigated with the Munsell Color System, which stands for bigger colour distance. Alternatively, the $L^*u^*v^*$ diagram shows more circle formed ellipses when investigated with the MacAdam ellipses, which stands for smaller, local distance.

The CIELab colour space may be appropriate to compare wide colour surfaces, but not to determine colour noise which is characterised in part by small and local structures. The CIEL $^*u^*v^*$ colour space, taken by itself, is not either capable to give a reliable physiological quantisation of colour noise difference. So a new approach for the aimed purpose must be found.

According to these results, the colour difference formula CIELabDE has been repeatedly modified by the CIE over the years: 1976, 1994, 2000. But in the previous diploma thesis dealing with the colour noise [11], it has been demonstrated that neither of the the improved CIELabDE formulae were practicable to use to quantify noise in a visual manner.

That is why a new approach has to be developed.

1.2 Description of the Experiment and Development of a new Approach

1.2.1 Shiraz Experiment

In order to determine how the eye reacts to noise for different frequency patterns and colours, experiments on over 30 individuals have been conducted with the help of the Shiraz program. This software written by Michael Bantel and Jan Fischer [10] and expanded by Christina Simon and Nicole Kidawa [11] can be used so that the viewing experiment takes place in front of the monitor.

Shiraz first permits the user to predefine images varying in colour, vertical square frequency patterns and contrast. Then a set of image is generated adding noise to the image. The digital noise input is a random pattern [10 p20 & 33] [11 p55] based on the theory of the statistical gauss function. However, the program always produces the same sequence of random numbers, so it is ensured that the noise input is the same for the same noise setting from one experiment to another. The eye identifies colours in terms of luminance, chroma and hue. Relying on this eye's behaviour, the noise input varies in amplitude of either the luminance, chroma or hue channel [10 p21-22] [11p26]. The noise input is then measured as a colour difference ΔE . The maximum noise input in the luminance channel is $\Delta E = \Delta L = 10$, in the chroma and hue channel it is $\Delta E = \Delta C = \Delta h = 15$ [11 p56].

For the specifically defined viewing conditions reported in the two former diploma thesis [11 p35], and [10 pp42-44] and in appendix A, the tested observers were asked to select the threshold image from the set of images with the just noticeable difference (JND) in terms of noise. This has been done for a variety of colours and for noise input in each channel: luminance, chroma and hue. A threshold image is calculated as the mean value of the slider's setting over the number of the tested persons. Consequently, the experiment has to be executed over many persons in order to exclude any errors due to psychological attributes (e.g. pressure, imagination...) or vision deficiency (although it is assumed that all persons have normal vision).

The experiment has been conducted in the context of the diploma work of Christina Simon and Nicole Kidawa for colour patches with frequency patterns, defined [11 pp40-44], and which results are reported [11 pp-103-110]. It has also been conducted for uniform colour patches, defined in the diploma thesis work of Michael Bantel and Jan Fischer [10 pp39-41], but in the context of this diploma work (results for the threshold images reported in appendix A).

These experiments are not a method to quantify noise, but permits the user to define threshold images, which are then used to investigate other approaches.

But from the results it can already be observed that for the noise input in the luminance channel, the measured colour difference ΔE of the threshold images is almost the same for the different colours. However, for noise input in the chroma or hue channel, the measured colour difference ΔE is varies greatly for the different tested colours.

Nevertheless, the ΔE from the Shiraz noise settings will just serve as a measure of how much noise had to be put in. It does not serve as a visual quantification unit.

1.2.2 Thesis: the Threshold Images should get the same Noise Value

The threshold images are defined for the just noticeable colour difference. So, because the eye perception is the same, a measuring method, which would quantify noise for matching the visual impression, would quantify these threshold images with the same values.

It has been demonstrated that neither the signal to noise ratio, nor the CIELabDE1976 [22], 1994 [10] or 2000 [11], are able to quantify physiologically noise as a ratio or as a colour difference. As a result, other approach methods have to be developed which would fulfil the assumption.

The two following models have been investigated:

- the model of visual noise measurement proposed by Hung et al (also as an annex in the *ISO 15739:2002(E)*) which simulates the processing of human vision by using the opponent space and contrast sensitivity functions [17]. This uses the CIELuv1976 colour space for the determination of a so called visual noise value.
- S-CIELabDE2000 colour difference model proposed by Fairchild et al [20] which simulates human vision approximately the same way as Hung but uses an image comparison afterwards based on CIELabDE2000.

Both are based on the cognition of the human visual system and both use a human visual algorithm, which tries to describe the visual recognition of colour by the human visual system. After the image data has been filtered with the algorithm, the visual noise measurement model uses a weighted sum of the standard deviation along the L^* , u^* and v^* axes of the CIELuv1976 colour space to evaluate the colour noise. The S-CIELabDE2000 model processes a colour difference between a noise free image and a noisy image.

1.2.3 Overview of the Thesis

In the second chapter the human visual system is presented in order to understand the human visual algorithm derived from it. The third chapter deals with the quantification of the threshold images with the visual noise measurement model, while the fourth chapter considers the S-CIELabDE2000 model. In the fifth chapter the precision of the algorithm used to describe the human visual system is evaluated by scaling the set of noisy images for different colours with the algorithm and comparing it to the threshold images. The comparison between the two models and a conclusion about their reliability are then presented in the sixth chapter.

2 .Chapter2: The Human Visual System and the Human Visual Model

Since both visual models: Visual Noise Measurement and S-CIELabDE2000, are derived from the human visual function, it is important to understand the basic anatomy, physiology, and performance of the visual system.

2.1 Definition of Colour

“Light is a term used to describe the range of wavelengths from 380nm to 780nm of the electromagnetic radiation spectrum to which the human visual system is sensitive” [26 p4].

“Colour is an attribute of visual sensation and is not a physical characteristic of an object.” [26 p4] The experience of colour occurs when light reflected from surfaces is observed, or when looking directly at the light sources. But colour does not occur only when focusing on the surface of the viewed object, but takes place as a mapping of the object on the brain.

Actually, the light coming through the lens' eye, falls on the retina and stimulates the light sensitive cells. Here the complex process of photo-transduction occurs: the energy of a photon is used to change the inherent membrane potential of the photoreceptor. This stimuli then travels through a series of neural relay cells via the nerves [4 p23]. The signal is then processed by neural mechanisms before being led further to the brain, which produces the sensation of colour. *“The term colour exists only relative to a living organism with light sensorial cell” [26 p5].*

2.2 Eye's Light Sensitivity System: the Photoreceptors

The light sensitive cells of the retina are the photoreceptors, *rods* and *cones*, that catch the photon of the light entering the eye and serve to transduce the information of the optical image into chemical and electrical signals [3 p4].

2.2.1 Sensitivity of the Photoreceptors

Rods are highly sensitive to low luminance levels (scotopic vision: e.g., less than 1 cd/m², moonlight, dark room), such that they can generate a detectable photocurrent response when they absorb just a single photon of light. Cones first respond to higher luminance levels (several cd/m²). At high luminance level (e.g., greater than 100 cd/m²), rods are saturated and only cones function (photopic vision). In the intermediate luminance levels, both rods and cones function and contribute to vision (mesopic vision) [3 p11] [4 p20].

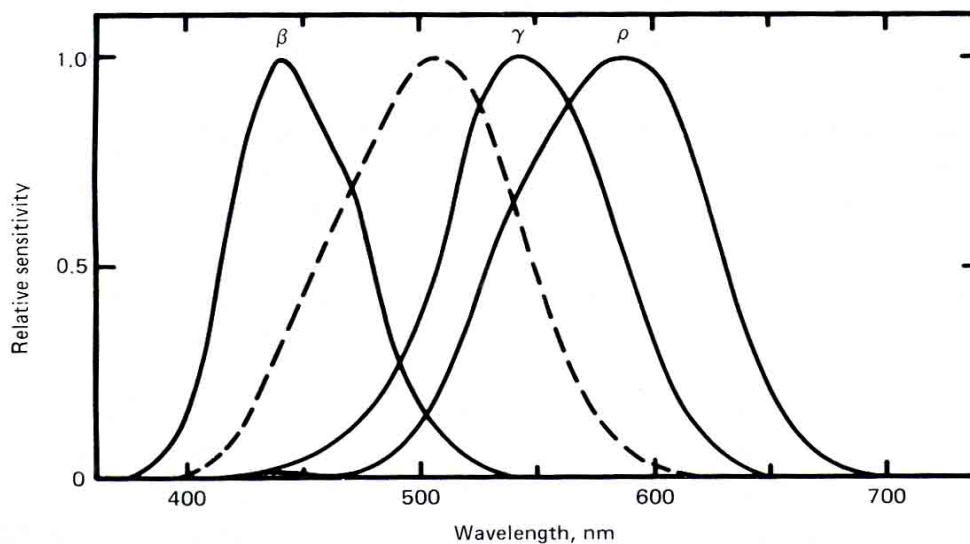


Figure 2.01: Broken line: the spectral sensitivity of the eye for scotopic (rod) vision. Full lines: spectral sensitivity curves of the three different types of cones: L = ρ , M = γ , and S = β , for photopic vision [4 p21].

Rods and cones differ in their spectral sensitivities. They both contain different photosensitive pigment. There is only one type of rod photosensitive pigment, rhodopsin, with a spectral responsivity peak at approximately 510nm [4 p21]. There are three types of cone photosensitive pigment with different peak spectral responsivities : 560nm, 530nm, and 420nm properly and respectively referred to as *L*, *M* and *S* cones [3 p11], and [26 p5].

Since there is only one type of rod cells, rod vision or scotopic vision, is sometimes referred to as "monochromatic" vision. But there are three types of cones, each responding to different wavelength ranges. The three signals are then processed with each other, generating the sensation of colour.

2.2.2 Chromatic Adaptation

Chromatic adaptation is observed by examining a white object, such as a piece of paper. Although observed under various light sources, the white paper keeps its white appearance. For instance, daylight is composed of more short-wavelength than fluorescent light, while incandescent light is made of more long-wavelength than fluorescent light. But the paper almost keeps its white appearance under the different light sources. This can be explained: the S-cones are less sensitive under daylight to balance the higher amount of short-wavelength. Conversely, the L-cones are less sensitive under incandescent light to balance the higher amount of long-wavelength [3 p28].

To resume, “*chromatic adaptation is the independent sensitivity control of the three cone spectral responsivity curves, that compensate changes in the spectral quality of illumination*”[5 p24].

2.2.3 Mosaic and Spatial Arrangement of the Photoreceptors

Another important feature of the photoreceptors is their distribution in the retina. In the *fovea*, which is the area of sharpest vision, the receptors are only cones. Outside of this, there are more rods. The fovea covers $1\frac{1}{2}^\circ$ diameter of the visual field, and lies 4° offset from one side of the optical axis. “*The ratio of cones to rods varies continuously from all cones and no rods in the fovea to nearly all rods and very few cones beyond 40° from the visual axis*” [4 p20]. About 10° to the other side of the optical axis is an area with no photoreceptors at all: the *blind spot* or *optical disk*. This area has no sensitivity to light since the nerve fibres connecting the retina to the brain pass through the surface of the eyeball at this point [4 p20].

Moreover, the distribution also differs among the three cone receptors. The S cones are absent in the most central area of the fovea. Instead, they are concentrated in a ring around the fovea and sparsely distributed on the retina. “*There are far more L and M cones than S cones and there are approximately twice as many L cones as M cones: the relative population of the L:M:S cones are of the ratio 40:20:1*” [3 p10]. In addition, the spacing between the S-cones is much larger than the spacing between the L and M cones.

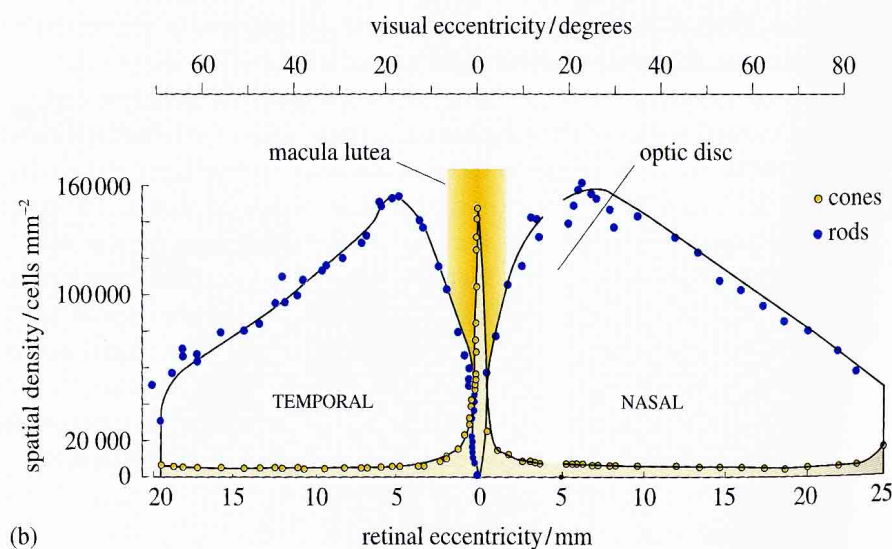


Figure 2.03: Density of rods and cones across the retina. Note the high density of cones in the central rod-free macular region and the high density of rods away from the fovea [9 p118].

The asymmetrical distribution among the cones and the larger spacing between S-cones can be explained. The eye is not corrected for chromatic aberration as *“it cannot simultaneously focus sharply on the three regions of the spectrum”* [4 p23]. The L and M peak wavelengths are closer together than M and S peaks are between one another. But still the eye best focuses light of around 560nm in wavelength. Both L and M-cones therefore detect images that are sharp. The S cones detects an image that is much more blurred, so it is not necessary to have a fine network of S cones. [4 p23].

Moreover the fovea is characterised by the *yellow spot* or *macula lutea*: pigments located on the cone axons that form a layer of fibres. Since light must pass through the fibres before reaching the cones, *“the fibres act as a short-wave filter, screening out the blue light”* [9 p117]. This improves visual acuity by decreasing the impact of the chromatic aberration of the optical image projected on the retina [9 p117].

2.3 Visual Signal Processing

2.3.1 Colour Sensation requires an Interaction between the Photoreceptors

“A given photoreceptor reacts to the intensity of a given wavelength” [26 p5]: an incandescent light of a certain intensity can have the same effect in a photoreceptor as a fluorescent light of a different intensity. This implies that a single photoreceptor can not detect the colour of a light source. *“Taken individually, each photoreceptor is colour blind”* [26 p5]. To be able to distinguish a colour, the colour vision requires interactions of the three types of cones [26 p5].

2.3.2 Structure of the Photoreceptors and Neurons Interconnections

The retina is made of several layers of neural cells. *“There is first a vertical signal processing taking place whereby photoreceptors are connected to bipolar cells, which are in turn connected to ganglion cells, which form the optic nerve”*.**[3 p6]**. But a horizontal signal processing also occurs, *“whereby the horizontal cells connect the photoreceptors and bipolar cells laterally to one another, and the amacrine cells, that connect bipolar cells and ganglion cells laterally to one another”* **[3 p6]**.

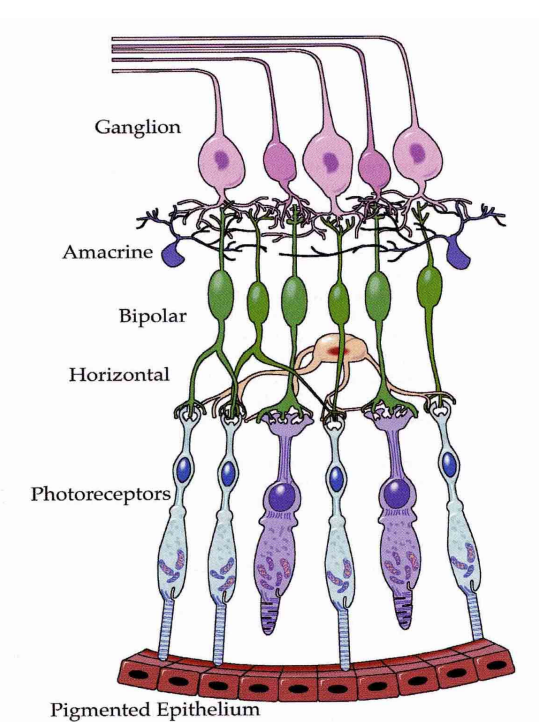


Figure 2.04: Schematic diagram of the “wiring” of cells in the human retina **[3 p7]**.

The retina transmitted to the brain thanks the nerve cells the receipted signals, *“which consist of sophisticated combinations of the receptor signals. Each synapse can perform a mathematical operation (add, subtract, multiply, divide) in addition to the amplification, gain control, and non-linearities that can occur within the neural cells”* **[3 p7]**. The signals collected from 100 million photoreceptors is compressed to signals in one million nerve cells *“without loss of visually meaningful data “***[3 p7]**.

2.3.3 Distribution of the Nerves' Fibres throughout the Photoreceptors

There are far more rods than cones. There are around 100 million rods for every 5 million cones. So it could be assumed that rods sample the retinal image very finely. Yet visual acuity under scotopic viewing conditions is very poor compared to visual acuity under photopic conditions [6].

This can be explained by the different kind of connections of the rods and cones with the nerve fibres. *“In the fovea, there are about the same number of nerve fibres as cones, but as the angle from the visual axis increases, the number of nerve fibres decreases continuously until as many as several hundred rods and cones may be served by a single nerve fibre”* [4 p20]. While this enhances sensitivity, this occurs at the expense of acuity.

2.3.4 Processing of the Signals: Opponent Colour Signals

Before reaching the brain (visual cortex) to be analysed in a more complex way (edge detection, movement...), the colour information provided from the ganglion cells is not of trichromatic type (red, green, blue) as it could be assumed from the cones sensitivities. The interaction that takes place, produces a colour information that contains three channels : an achromatic signal and two chromatic signals.

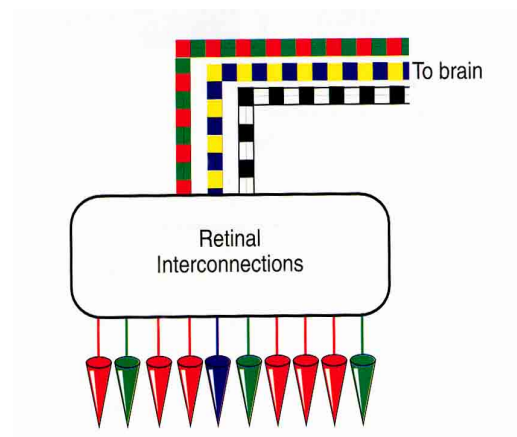


Figure 2.05: Cones interconnect in the retina leading to opponent – type signals [5 p16].

The neurons leading the achromatic signal, noted A, collect their inputs from both rods and all three types of cone [4 p24] and can be written as:

$$A = 2L + M + S + 720 + \text{Rods}.$$

The colour information from the input of the three types of cones can be compressed into two achromatic signals. This is because the information is not from the signals coming from each of the three cones but consists of the difference between them. So knowing the difference between L and M cones, and between S and M cones, the difference between S and L cones can be deduced. The two achromatic channels can also be referred to colour difference signal [4 p25]:

$$C1 = L - M$$

$$C2 = (S - L) - (M - S) = 2S - (L + M)$$

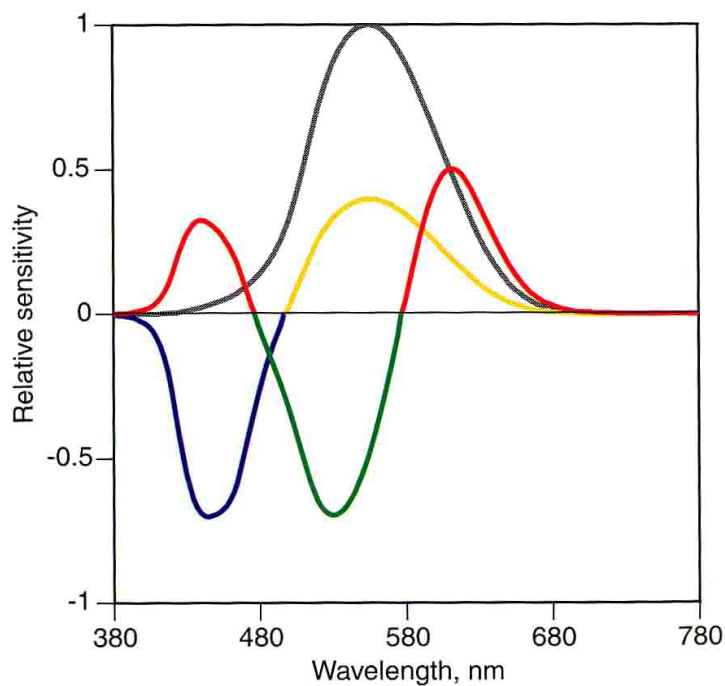


Figure 2.06: opponent space sensitivity response: the interaction of the cone responses[5 p16].

The colour information taking place in the neurons is hence often referred to opponent colour signals.

2.4 Spatial Properties of Colour Vision: the Contrast Sensitivity Function

Objects are better distinguished from each other, or from their background, if the difference in luminance or colour between them is large. Of these two factors, luminance plays the most important role. In practice, it appears that it is not the absolute difference in luminance that is important, but the relative difference. *“This relative difference can be expressed by the difference between two luminance values divided by the sum of them, which is simply called contrast.”* [3 p26] The reciprocal of the minimum contrast required for detection is called *contrast sensitivity* [35 p7].

2.4.1 Contrast Sensitivity Function and Spatial Frequency

A *contrast sensitivity function (CSF)* *“is defined by the threshold response to contrast (sensitivity is the inverse of threshold) as a function of spatial (or temporal) frequency”*. [3 p26] contrast sensitivity functions are usually *“measured with stimuli that vary sinusoidally across space (or time)”* [3 p26].

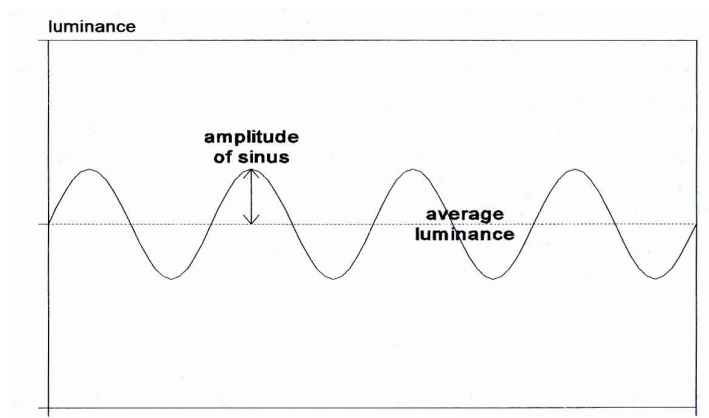


Figure 2.07: Example of a sinusoidal luminance variation. The modulation is defined by the amplitude of the sinusoidal variation divided by the average luminance. The contrast sensitivity is the reciprocal of the threshold value of the modulation for the detection of the variation. [35 p7].

2.4.2 Restrictions of the Model of the Contrast Sensitivity Function

Knowledge of the contrast sensitivity function is important for the understanding of the visual properties of the eye. Contrary to the colorimetric sensitivity curves of the eye adopted as a standard by the CIE (Commission International de l'Eclairage), a standard does not exist for the contrast sensitivity function of the eye. Defining such standard would be difficult because the contrast sensitivity of a luminance pattern depends, as seen on figure 2.08, on many parameters: Amplitude of the wave, the wave shape (sine, square,...), object luminance, surround luminance, border condition (frame, background), observing distance, field size, direction of the gratings (vertical, horizontal...).

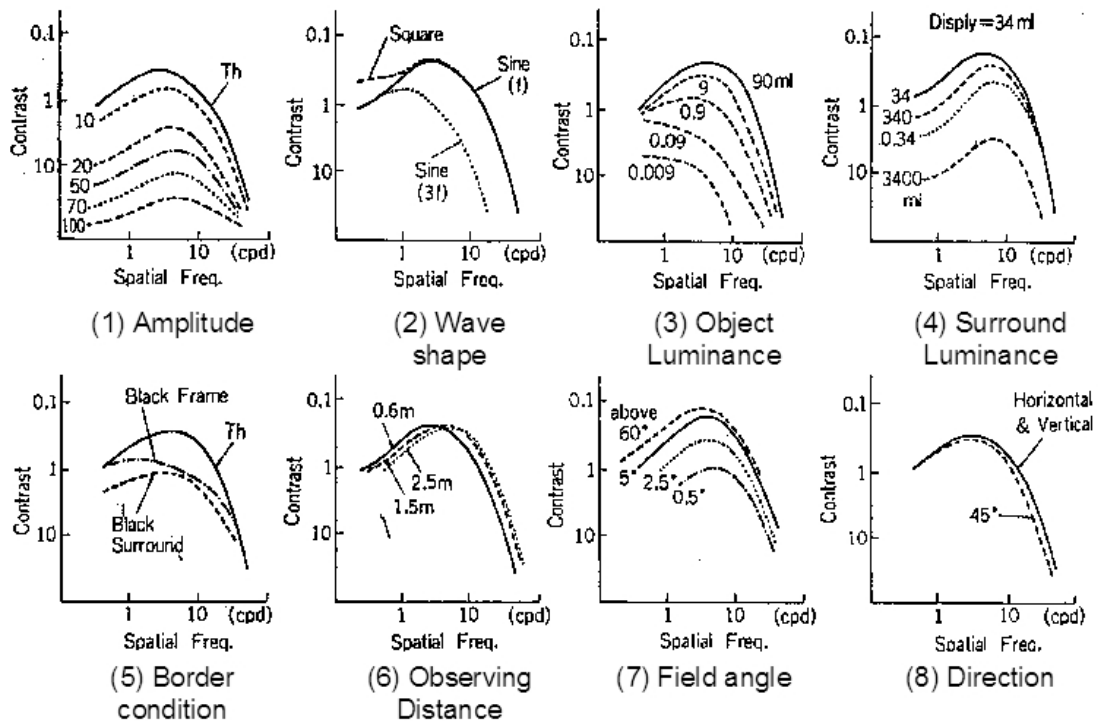


Figure 2.08: shape of the contrast sensitivity function depending on the changes in conditions [21].

The spatial contrast sensitivity model defined here is restricted to the normal situation of foveal vision and to photopic vision. Outside the fovea, the contrast sensitivity and the resolution of the eye is significantly reduced.

The contrast sensitivity function can be determined for each channel of the opponent colour space.

2.4.3 Achromatic or Luminance Contrast Sensitivity Function

“The luminance contrast sensitivity function is band-pass in nature, with peak sensitivity around 5 cycles per degree”[4 p26]. It draws near zero at zero cycles per degree, this is in accordance with the fact that the visual system is insensitive to uniform fields. It also converges toward zero at about 60 cycles per degree: after this limit the mosaic of the photoreceptors can not resolved details any more. [4 p26].

Indeed the photoreceptor mosaic is the limiting element for the sampling of the frequencies. Namely, since the achromatic signal is mostly made of L, M, S and few rods stimuli, the centre-to-centre foveal cones spacing is the smallest possible: 2,4 μm , which corresponds to 30 seconds of visual angle.

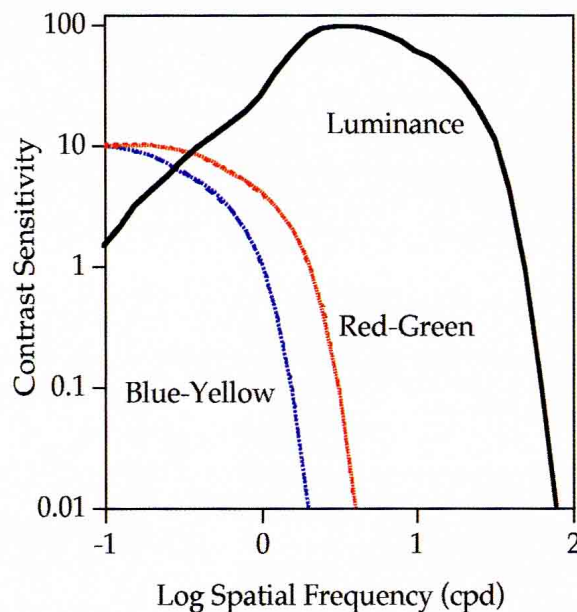


Figure 2.09: Spatial contrast sensitivity functions for luminance and chromatic contrast [3 p28].

2.4.4 Chromatic Contrast Sensitivity Function

“The chromatic mechanisms are of a low-pass nature and have significantly lower cut-off frequencies” [3p26], which are due to the photoreceptor mosaic, as explained previously. The red-green signal is made only from the L and M cones. Since there are only two types of cone, the centre-to-centre foveal cone spacing is greater than for the luminance contrast sensitivity function, and hence the sampling Nyquist frequency is smaller. Similarly, *“the blue-yellow chromatic contrast sensitivity function has a lower cut-off frequency than the red-green chromatic contrast sensitivity function due to the scarcity of S cones in the retina” [3p27]* and the larger S to S-cones spacing than the L to M-cones spacing.

This lower cut-off frequency indicates a reduced availability of chromatic information for fine details that is often taken advantage of in image coding and compression schemes (Jpeg compression [31]).

It is also important to point out that the contrast threshold of the luminance CSF is significantly higher than that of the chromatic contrast sensitivity function. In deed *“the visual system is more sensitive to small changes in luminance contrast compared with chromatic contrast” [3 p32]*. This could be explained by the summation of the cones and rods stimuli for the luminance signal, whereas the chromatic signal are made by inhibition between the cones' signals.

2.5 Human Visual Model and its Algorithm

Based on the cognition of the visual system, a human visual model has been developed [20] [17] and can be implemented as an algorithm [17] [16 annex C] [18].

2.5.1 Human Visual Model

In order to understand the visual noise measurement model, the human visual system, described in the four first paragraphs of this chapter, can be simplified in the followings steps: (the model is valid for photopic viewing conditions and normal vision):

- 1) An object is observed through the optical system of the eye (the spatial responses of the eye's optics is not taken account in the model because this reduction is not that important in comparison with the one taking place in the visual neural system).
- 2) The electromagnetic radiation coming from the object are detected by the photoreceptors: L, M and S cones for photopic vision [paragraph 2.2.1].

The detected signals are then processed by the visual neural system, which is complex [paragraph 23], but can be simplified into two steps although they both occur simultaneously during the neural processing:

- 3) First the detected signals are transferred into the opposite colour space, which consists of three sets of coordinates: white-black, A for achromatic, red-green, C1 for first chromatic channel, and yellow-blue C2 for second chromatic channel [paragraph 2.3.4].
- 4) Second, each image signal in the opposite colour space is filtered by each corresponding contrast sensitivity function [paragraph 2.4].
- 5) Finally, the processed signals reach the brain, where the actual sensation of colour occurs. This can be best described by the three coordinates: lightness, chroma and hue, which is the polar representation of the CIELab or CIELuv colour space.

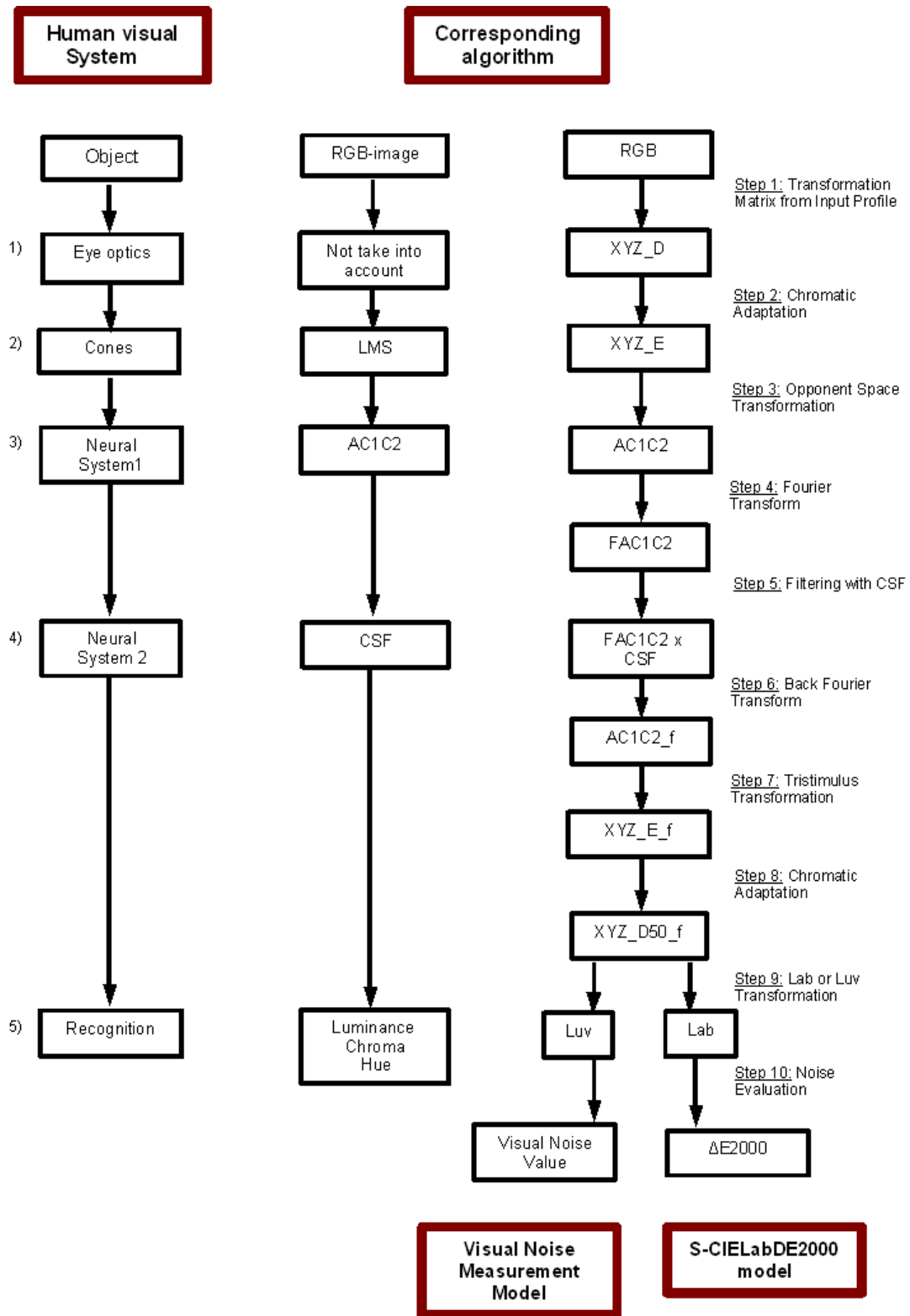


Figure 2.10: Representation of a Human Visual Model and its corresponding algorithm, used by the two models (partly inspired from [17]).

2.5.2 Algorithm of the Human Visual System

In order to simulate the human visual system for a visual noise evaluation, an algorithm following the steps described above [paragraph 2.5.1] has been implemented in Matlab® in the context of this diploma thesis. The algorithm is described in *Annex C* of the *ISO 15739:2002(E)* [16] as well as in the paper of Hung et al [17] and can be used in Photoshop® as a "Noise Measurement" Plug-in [18]. Still the Matlab® implementation differs slightly from the proposed algorithm since a different contrast sensitivity function and white point for the characterisation of the display are used.

The colour signal coordinates of the device (RGB for a display or for a digital still camera) must be first transformed into the colour signal coordinates of the eye (opponent colour space).

Step 1: since each device has its own colorimetric characteristics, device dependent colour space coordinates must be converted into device independent colour space coordinates (the profile connection space). Here, the RGB data of the image is transferred into the CIE tristimulus values X_d , Y_d , and Z_d by the matrix obtained from the ICC-profile describing the device. Depending on the manufacturer, the transformation can be a matrix or a Look up table [34 p18]. This has been taken into account in the implementation of the visual noise measurement in Chinon [mfile taggedRGBtoXYZ.m].

Each profile connection space has a specified white point given by the illuminant (in the praxis mainly illuminant D50 for displays) to which each coordinates of the space are then related to.

$$\begin{bmatrix} X_d \\ Y_d \\ Z_d \end{bmatrix} = M_{pcs} \cdot \begin{bmatrix} R \\ G \\ B \end{bmatrix} \quad (2.01)$$

with for example:

$$M_{pcs} = M_{sRGB} = \begin{bmatrix} 0,9907 & 0,075034 & -0,015343 \\ 0,0072788 & 0,99476 & -0,0015417 \\ 0 & 0 & 0,91827 \end{bmatrix} \quad (2.02)$$

The default parameters [18] of the Photoshop® Plug-in are set to the *sRGB IEC61966-2.1* profile. In this case the illuminant is D65 and the transformation matrix has been defined by the *sRGB standard IEC 61966* [36]. On the other hand, in the Matlab® implementation, the transformation matrix is read out of the used profiles.

Step 2: Before transforming the tristimulus values X_d , Y_d , and Z_d into the opponent colour space specific for the eye's processing of colour, the display tristimulus values are transformed into the X_e , Y_e and Z_e tristimulus values defined with the illuminant E.

The eye has a capacity of chromatic adaptation [paragraph 2.2.2], which means that the cones responsivity depends on the light illumination. Contrary to an illuminant, the eye does not have a predefined white point. Hence in order to model the eye (in analogy to a colour space), the eye needs to be characterised with a white point. For this purpose the illuminant E has been chosen because of its spectral distribution, which is equal over the whole spectrum.

$$\begin{bmatrix} X_e \\ Y_e \\ Z_e \end{bmatrix} = M_{adapt} \cdot \begin{bmatrix} X_d \\ Y_d \\ Z_d \end{bmatrix} \quad (2.03)$$

with:

$$M_{adapt} = \begin{bmatrix} \frac{L_{wpE}}{L_{wpIlluminant}} & 0 & 0 \\ 0 & \frac{M_{wpE}}{M_{wpIlluminant}} & 0 \\ 0 & 0 & \frac{S_{wpE}}{S_{wpIlluminant}} \end{bmatrix} \quad (2.04)$$

Given that the white point of the profile connection space can differ, the chromatic adaptation transformation can consequently also differ.

$$\begin{bmatrix} L_{wp} \\ M_{wp} \\ S_{wp} \end{bmatrix} = M_{vonKries} \cdot \begin{bmatrix} X_{wp} \\ Y_{wp} \\ Z_{wp} \end{bmatrix} \quad (2.05)$$

with

$$M_{vonKries} = \begin{bmatrix} 0,40024 & 0,70760 & -0,08081 \\ -0,22630 & 1,16532 & 0,04570 \\ 0,0 & 0,0 & 0,91822 \end{bmatrix} \quad (2.06)$$

In the technical literature, there are different primaries proposed for the chromatic adaptation via the cones' space. Since there is no recommendation, the matrices had to be tested with a uniform white image, and the tristimulus X_e , Y_e and Z_e responses compared [appendix D1]. The matrix that produces the tristimulus values closest to 1 has been chosen because illuminant E is spectrally equal. Here it is the von Kries transformation related by Berns [5], but which is very similar to the von Kries transformation proposed by Hunt [4 p71] (also found in the ICC.1:2001-12 specification [34 p87]).

Step3: These tristimulus values X_e , Y_e and Z_e are transferred into the opposite colour responses: white-black A, red-green C1, and yellow-blue C2. Here again the technical literature proposes different transformation matrices [**appendix D2**]. Since there is no recommendation, the matrices have been tested with a uniform white image, and the opponent responses compared. The matrix that seems to produce the most appropriate opponent coordinates for a white has then be chosen. In this case it was the matrix set in the default parameter text file of the Photoshop® plugin.

$$\begin{bmatrix} A \\ C1 \\ C2 \end{bmatrix} = M_{opposite} \cdot \begin{bmatrix} X_e \\ Y_e \\ Z_e \end{bmatrix} \quad (2.07) \quad \text{with:} \quad M_{opposite} = \begin{bmatrix} 0,0 & 1,0 & 0,0 \\ 1,0 & -1,0 & 0,0 \\ 0,0 & 0,4 & -0,4 \end{bmatrix} \quad (2.08)$$

The opponent colour signals are then processed with the contrast sensitivity function.

Step 4: Using the Discrete Fourier Transform, the set of the opponent responses is transferred from the spatial space into frequency space: FA, FC1 and FC2 respectively:

$$\begin{aligned} A &\xrightarrow{DFT} FA \\ C1 &\xrightarrow{DFT} FC1 \\ C2 &\xrightarrow{DFT} FC2 \end{aligned} \quad (2.09)$$

Step 5: In the frequency space, each response is filtered by the corresponding spatial responses of the contrast sensitivity function [paragraph 2.4]: this should simulate the decrease in sensitivity that occurs in the human visual system:

$$FA_f = FA \cdot CSF_{achromatic}$$

$$FC1_f = FC1 \cdot CSF_{chromatic} \quad (2.10)$$

$$FC2_f = FC2 \cdot CSF_{achromatic}$$

This blurring tends to increase as a function of cycles-per-degree of visual angle, so before filtering the opponent space coordinates in the frequency space, the contrast sensitivity function must previously be scaled depending on the eye's resolution of the image. This is dependant on a specific viewing angle (cycles per degree) which is defined through the image height or viewing distance.

In digital imaging applications, cycles-per-degree is a function of both addressability and viewing distance. In our Chinon program, we implemented two ways to calculate the cycles per degree:

Equation 2.11 proposed by Fairchild [20 p428]:

$$cycles/degree = \frac{ppi}{\frac{180}{\pi} \cdot \arctan\left(\frac{1 \text{ inch}}{viewing \text{ distance}}\right)} \quad (2.11)$$

For example, if a computer monitor is capable of displaying 72 pixels-per-inch (ppi) and is viewed at 18 inches then there are roughly 23 digital samples per degree of visual angle.

Equation. 2.16 developed in the context of this diploma thesis in order to match the experiment conditions.

B: Width of the monitor.

b: Width of the visual field as observed.

R: number of pixel presentable in the width of the monitor.

r: number of pixels seen in the visual field b.

α : angle of the visual field, per definition

$\alpha=1^\circ$.

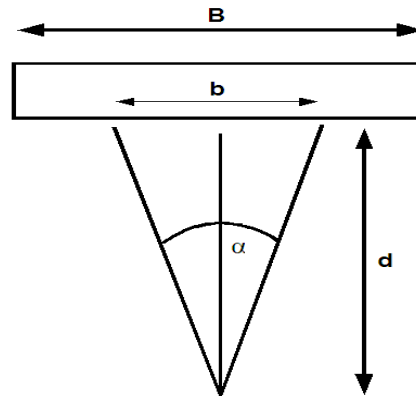


Figure 2.11: Representation visual field b in function of the viewing distance d and the angle of the visual field.

Relating to Figure 2.11:

$$\tan\left(\frac{\alpha}{2}\right) = \frac{(b/2)}{d} \quad (2.12)$$

\leftrightarrow

$$b = \tan\left(\frac{\alpha}{2}\right) \cdot 2 \cdot d \quad (2.13)$$

Calculation of how many pixels are in the visual field b:

$$r = \frac{b}{B} \cdot R \quad (2.14)$$

\leftrightarrow

$$r = \frac{2 \cdot R \cdot d \cdot \left(\frac{\alpha}{2}\right)}{B} \quad (2.15)$$

The Nyquist frequency is made out of two pixels:

$$\text{cycles / degree} = \frac{r}{2} = \frac{R \cdot d \cdot \tan\left(\frac{\alpha}{2}\right)}{B} \quad (2.16)$$

Often the monitor size is given by its diagonal size in inches. Moreover the format ratio of the monitor can vary depending on its kind (CRT or LCD etc...). So in the Chinon program, in addition to the diagonal monitor size, the user is asked to enter information about the horizontal and the vertical size. From this, the monitor width can then be determined with Pythagoras:

R_h : horizontal monitor resolution

R_v : vertical monitor resolution.

H: monitor height

Z: monitor diagonal.

$$H = ratio \cdot B \quad (2.17) \quad \text{with } ratio = \frac{R_v}{R_h} \quad (2.18)$$

From Pythagoras: $Z^2 = B^2 + H^2$ (2.19) it is obtained $B = Z \cdot \sqrt{1 + ratio^2}$ (2.20).

The contrast sensitivity function has not been standardized yet [paragraph 2.4.2]. The shape of the function is itself dependent of many parameters [figure 2.08] like the luminance of the object or its surrounding, the observing distance, the field angle... In reality a contrast sensitivity function should be used for carefully predefined settings.

In the Matlab® implementation, the used contrast sensitivity function is proposed by Fairchild [20 pp429-430] and there are three different functions to apply on the three opponent colour signals. While in the Photoshop® Plugin the contrast sensitivity function is defined as weights applied in a look up table [18]. Here, the same response curve for C1 and C2 are used, since chromatic contrast sensitivity function have nearly the same behaviour and magnitude compared to the achromatic contrast sensitivity function.

For both the luminance, the contrast sensitivity function has been scaled to unit 3 for the maximum value and to unit 1 for the chromatic contrast sensitivity function. This relies on the eye higher sensitivity for changes in luminance than for changes in colour [figure 2.09]. Since the contrast sensitivity function has not been standardized yet, this is an arbitrary choice which can still be discussed.

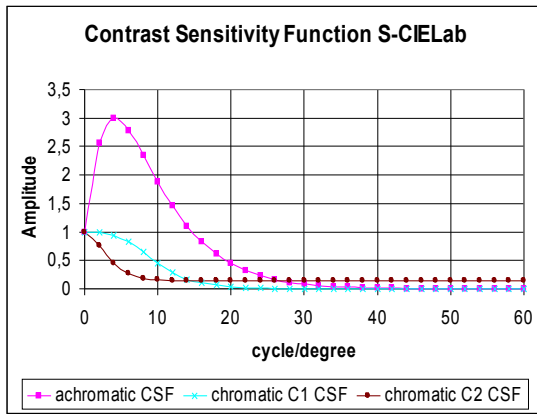


Figure 2.12: CSF proposed by Fairchild [20]

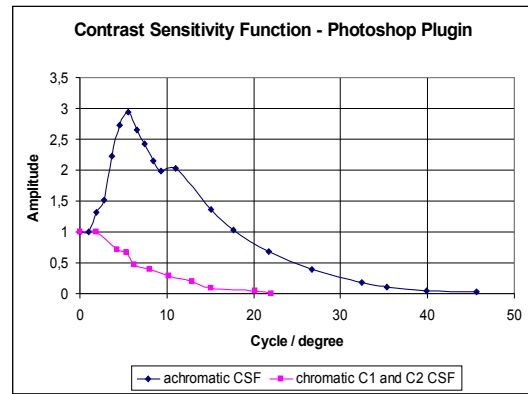


Figure 2.13: CSF proposed by Hung et al [18]

In order to be able to evaluate a noise value, the now filtered eye-adapted coordinates must be converted into a colour space where a noise value can be determined. So firstly, all previously transformation steps must be reversed.

Step 6: Corresponding to step 4, Inverse Discrete Fourier Transform is used, and each filtered response is now transferred back into real space.

$$\begin{aligned}
 FA_f &\xrightarrow{\text{inverse DFT}} A_f \\
 FC1_f &\xrightarrow{\text{inverse DFT}} C1_f \\
 FC2_f &\xrightarrow{\text{inverse DFT}} C2_f
 \end{aligned}
 \tag{2.21}$$

Step 7: Corresponding to step3, the three opposite colour responses A_f , $C1_f$ and $C2_f$ are transferred into tristimulus values, X_{ef} , Y_{ef} and Z_{ef} with the inverse opposite matrix.

$$\begin{bmatrix} X_{ef} \\ Y_{ef} \\ Z_{ef} \end{bmatrix} = M_{\text{inverse opposite}} \cdot \begin{bmatrix} A_f \\ C1_f \\ C2_f \end{bmatrix}
 \tag{2.22}$$

Step 8: Corresponding to step 2, the inverse matrix of the von Kries adaptation model is applied, and each tristimulus value X_{ef} , Y_{ef} and Z_{ef} should be transferred back into the former tristimulus values white-point settings of the display: X_{df} , Y_{df} and Z_{df} . For ease of comparison for practical applications, the filtered tristimulus values X_{ef} , Y_{ef} and Z_{ef} are not obligatory transferred back into the former illuminant display settings, but back into the tristimulus values of the standard illuminant D50.

$$\begin{bmatrix} X_{ef} \\ Y_{ef} \\ Z_{ef} \end{bmatrix} = M_{adapt\ inverse} \cdot \begin{bmatrix} X_{df} \\ Y_{df} \\ Z_{df} \end{bmatrix} \quad (2.23)$$

Now that the actual tristimulus values X_{df} , Y_{df} and Z_{df} have been filtered with the human visual algorithm the quantification of noise can now be determined. To do so, the two following approaches are going to be investigated:

First the determination of a visual noise value with the visual noise measurement model, which will be dealt with in the chapter 3.

Second, the determination of a noise value as a colour difference with the S-CIELabDE2000 model, which will be dealt with in the chapter 4.

3 .Chapter 3: Visual Noise Measurements Model

3.1 Visual Noise Value Formula

3.1.1 The Formula

3.1.1.1 The Formula from the CIELuv1976 Colour Space

After having filtered the image data with the human visual model algorithm, corresponding to step 8, the tristimulus values X_{d_f} , Y_{d_f} and Z_{d_f} have been filtered, from which the visual noise value can now be determined.

Step 9: First the tristimulus values X_{d_f} , Y_{d_f} and Z_{d_f} are being converted into the uniform CIELuv 1976 colour space [8 p165]:

$$L^* = 116 \cdot \sqrt[3]{\left(\frac{Y}{Y_w}\right)} - 16 \quad (3.01) \quad \text{for} \quad \frac{Y}{Y_w} \geq 0,008856 \quad \text{otherwise} \quad L^* = 903,3 \cdot \left(\frac{Y}{Y_w}\right) \quad (3.02)$$

$$u^* = 13 \cdot L \cdot (u' - u'_w) \quad (3.03) \quad \text{with} \quad u' = \frac{4X}{(X + 15Y + 3Z)} \quad u'_w = \frac{4X_w}{(X_w + 15Y_w + 3Z_w)} \quad (3.04)$$

$$v^* = 13 \cdot L \cdot (v' - v'_w) \quad (3.05) \quad \text{with} \quad v' = \frac{9X}{(X + 15Y + 3Z)} \quad v'_w = \frac{9X_w}{(X_w + 15Y_w + 3Z_w)} \quad (3.06)$$

Step 10: Here, the visual noise value can be determined, and is defined as the weighted sum of three standard deviations of the colour noises along the L^* , u^* and v^* axes from the CIELuv 1976 colour space [16] [17] [18]:

$$\text{Visual Noise Value} = 1 \cdot \text{std}_{L^*} + 0,852 \cdot \text{std}_{u^*} + 0,323 \cdot \text{std}_{v^*} \quad (3.07)$$

The weights for each axes has been determined with an empirical approach to fit the visual experiences by giving some coefficients [21]. These coefficients seem to match the human visual colour discrimination behaviour. Namely, the eye recognises better differences in luminance than in chroma, as well as differences in the red-green channel than in the yellow-blue channel.

3.1.1.2 The Formula from the CIELab1976 Colour Space.

Although it was not recommended in the *ISO 15739:2002(E)* [16], in the Matlab® implementation the visual noise value is also determined as the weighted sum of three standard deviations of the colour noises along the L*, a* and b* axes from the CIELab1976 colour space:

The luminance coordinate L* is calculated with the equations 3.01 and 3.02 used before for the CIELuv1976 colour space.

The a* and b* coordinates are calculated as following [8 p167]:

$$a^* = 500 \cdot \left(f\left(\frac{X}{X_w}\right) - f\left(\frac{Y}{Y_w}\right) \right) \quad (3.09)$$

$$b^* = 200 \cdot \left(f\left(\frac{Y}{Y_w}\right) - f\left(\frac{Z}{Z_w}\right) \right) \quad (3.10)$$

with:

$$f\left(\frac{X}{X_w}\right) = \begin{cases} \sqrt[3]{\left(\frac{X}{X_w}\right)} & \text{for } \frac{X}{X_w} > 0,008856 \\ 7,787 \cdot \left(\frac{X}{X_w}\right) + \frac{16}{116} & \text{otherwise} \end{cases}$$

$$f\left(\frac{Y}{Y_w}\right) = \begin{cases} \sqrt[3]{\left(\frac{Y}{Y_w}\right)} & \text{for } \frac{Y}{Y_w} > 0,008856 \\ 7,787 \cdot \left(\frac{Y}{Y_w}\right) + \frac{16}{116} & \text{otherwise} \end{cases}$$

$$f\left(\frac{Z}{Z_w}\right) = \begin{cases} \sqrt[3]{\left(\frac{Z}{Z_w}\right)} & \text{for } \frac{Z}{Z_w} > 0,008856 \\ 7,787 \cdot \left(\frac{Z}{Z_w}\right) + \frac{16}{116} & \text{otherwise} \end{cases}$$

In analogy to equation 3.07, the visual noise value is obtained:

$$\text{Visual Noise Value} = 1 \cdot \text{std}_L + 0,852 \cdot \text{std}_a + 0,323 \cdot \text{std}_b \quad (3.11)$$

3.1.1.3 CIELuv1976 vs. CIELab1976

As it has already been discussed in paragraph 1132, both colour spaces are supposed to be approximately uniform according to the CIE, and the two formulae are almost equal in their degree of agreement with visual judgements of colour difference [19].

They actually differ in their orientation and the CIELuv1976 has the advantage of being a linear chromaticity diagram, in which additive colour mixture is represented by straight lines. This means that “*when two coloured lights, C1 and C2, are mixed additively*” [19] and plotted in the diagram, “*the colour C3 produced will be on the straight line joining C1 and C2, at a position that can be calculated from the relative amounts of*” [19] the two mixed colours. Consequently the CIELuv1976 formula is mostly used by people dealing with self-luminous colours. But it must be kept in mind that it has not been recommended by the CIE because, from the point of view of uniform spacing of colours, there is no evidence to support this.

The CIELab1976 diagram is derived from an already in the industry commonly used formula and is used mainly by surface colour industries. So the choice of which formula to use in a particular situation will often depend, not so much on scientific merit, but on other factors such as familiarity, convenience of use in particular industrial applications and conformance to the practice [22] [19].

But according to the Robertson's investigations [19], which have been already presented briefly in the paragraph 1132, the CIELab1976 colour space should be more appropriate to measure wide colour surfaces, while the CIELuv1976 colour space should perform better to measure local colour differences. Because noise is more characteristic of local structures, the CIELuv 1976 colour space have been preferred and proposed in the *ISO*

15739:2002(E) [16]. But regarding these observations, the CIE has not made any recommendations since it could find no evidence to support one more than the other and the formulae are considered to have equal merit as far as uniformity of spacing of colours is concerned. That is why, in addition in this diploma thesis, it has been decided to investigate also the noise value with the weighted sum of the standard deviations along the L^* , a^* and b^* axes.

3.2 Results of the Visual Noise Measurement Model

The threshold images [paragraph 1.2.1], have been tested on their visual noise value with the Photoshop® plugin and the implementation of the noise measurement algorithm in Matlab®, Chinon. If the visual noise measurement model is valid, i.e., if it describes correctly the human visual perception, it is expected that the same visual noise value will be measured for the threshold images regardless of the noise input channel (luminance, chroma or hue) [paragraph 1.2.2]. The challenge is maybe to get any idea for what the visual noise (VN) values stand for as it should quantify visually how much noise the eye can see.

How to use the plugin: refer to: *Operating instructions of the Photoshop Plugin: Noise Measurements Plug-in ver.1.20 User's Guide, November 8th, 1999, Konica Corporation.* [18]. (In the measurements in this work, the self-made Test Chart: ISO_chart_pos_shiraz.txt has been used (refer to the diploma thesis' CD).

How to use Chinon: refer to appendix C.

Table 3.01: Setting of Chinon for the followings evaluation (parameters and viewing conditions of our experiment):

viewing distance	60cm
horizontal monitor resolution	1280
vertical monitor resolution	1024
monitor diagonal	19 (LCD)
calculated cycles per degree	17,78
monitor profile	Monitor_25012006_1.icc

The following tables 3.02, 3.03, and 3.04 and respectively corresponding graphs 3.02, 3.03 and 3.04 report the visual noise value results for the investigations of the noise measurement model with the threshold images. This is for the uniform patches with colour blue, brown, cyan, dark grey, dark violet, yellow, skin1, skin2, light grey, magenta, mid-blue, mid-green, orange, pastel, and red defined by Jan Fischer and Michael Bantel [10 p40].

First the noise input for the threshold image as a colour difference and its corresponding variance are reported. Then the visual noise value for each threshold image is determined by the Photoshop® Plug-in's filter and then with Chinon with the visual noise value as standard deviation from Luv and at last from Lab. Then for each noise input channel (luminance, chroma, hue), the mean value of the visual noise values of all the tested colours is calculated. Each visual noise value of the threshold images are compared to the mean value and this is reported as deviation.

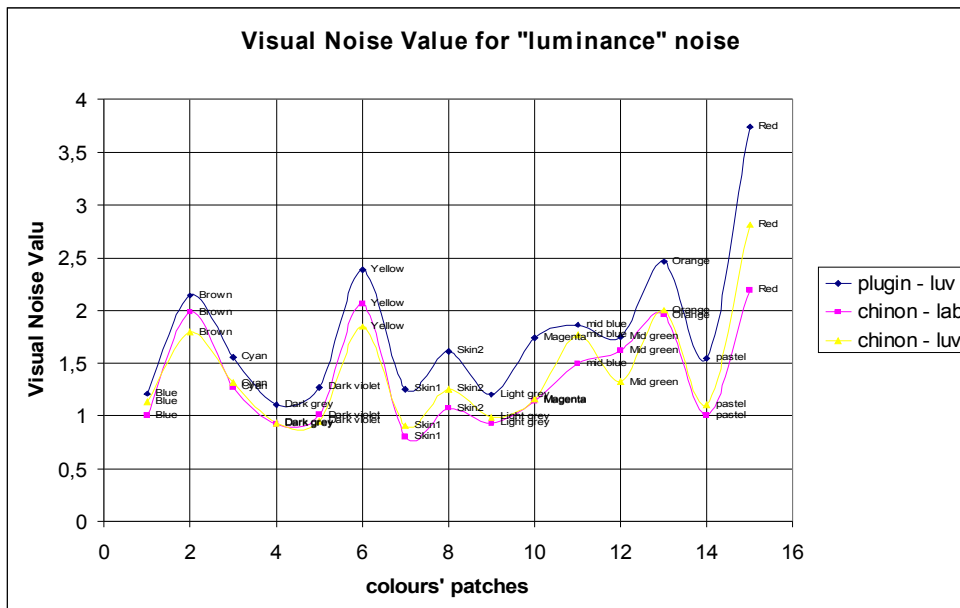
3.2.1 Noise Evaluation for Colour Difference in the Luminance Channel

Table 3.02: visual noise value of the threshold images with noise input in the luminance channel.

Colour patch	Shiraz		Visual noise Value			deviation to mean value		
	ΔL	variance	Plugin luv	chinon luv	lab	plugin luv	chinon luv	lab
Blue	0,4	0,03	1,21	1,13	1,00	-0,58	-0,29	-0,36
Brown	0,5	0,04	2,14	1,79	1,99	0,35	0,37	0,62
Cyan	0,5	0,04	1,56	1,31	1,27	-0,23	-0,10	-0,09
Dark grey	0,5	0,02	1,1	0,93	0,92	-0,69	-0,49	-0,44
Dark violet	0,4	0,03	1,27	0,95	1,00	-0,52	-0,47	-0,36
Yellow	0,6	0,04	2,38	1,85	2,06	0,59	0,43	0,70
Skin1	0,4	0,03	1,25	0,91	0,80	-0,54	-0,51	-0,56
Skin2	0,4	0,04	1,61	1,25	1,07	-0,18	-0,17	-0,29
Light grey	0,5	0,05	1,2	0,98	0,93	-0,59	-0,43	-0,44
Magenta	0,4	0,02	1,74	1,16	1,14	-0,05	-0,26	-0,23
mid blue	0,6	0,05	1,86	1,76	1,50	0,07	0,35	0,13
Mid green	0,4	0,03	1,75	1,32	1,62	-0,04	-0,10	0,26
Orange	0,5	0,03	2,46	2,00	1,96	0,67	0,59	0,59
pastel	0,5	0,03	1,55	1,10	1,00	-0,24	-0,32	-0,36
Red	0,6	0,1	3,74	2,81	2,19	1,95	1,40	0,83
mean value			1,79	1,42	1,36			
variance			0,47	0,28	0,23			
st deviation			0,69	0,53	0,48			

The luminance differences ΔL for detecting the noise threshold are small. This may be due to either simply the uniformity of the noise input values for the threshold images for the luminance channel, or a too coarse scaling of the noise input in the luminance channel in Shiraz. Indeed the maximum noisy image is associated with a colour difference $\Delta E = \Delta L = 10$, and the threshold is always smaller than $\Delta E = \Delta L = 1$. But this may be a precipitous assumption, since the variance for determining the threshold images are very low. This means that all the tested observers almost agree on the same noisy image, and that there are no doubts about the reliability of the measurements.

Graph 3.02: plots of the visual noise value for the threshold images with noise input in the luminance channel.



The visual noise values are very similar in that the deviation of the visual noise values stays low, except for the red, which visual noise value lays 2 count higher than the mean value (bold font in the table 3.02). Consequently all the reddish colours like brown, yellow and orange have the highest visual noise values. This exceptional behaviour can be partly explained later thanks to further investigation [paragraph 3.3.1.1].

Related to the graphical representation of the visual noise value of the threshold images, graph 3.02, the Matlab® implementation of the visual noise algorithm seems to achieve better results than the Photoshop® plugin (smaller standard deviation for the mean value of the threshold images). In addition, there are no real differences between the visual noise value calculated from the CIELuv 1976 than from the CIELab 1976. Actually it can be noticed that the curves have the same shape.

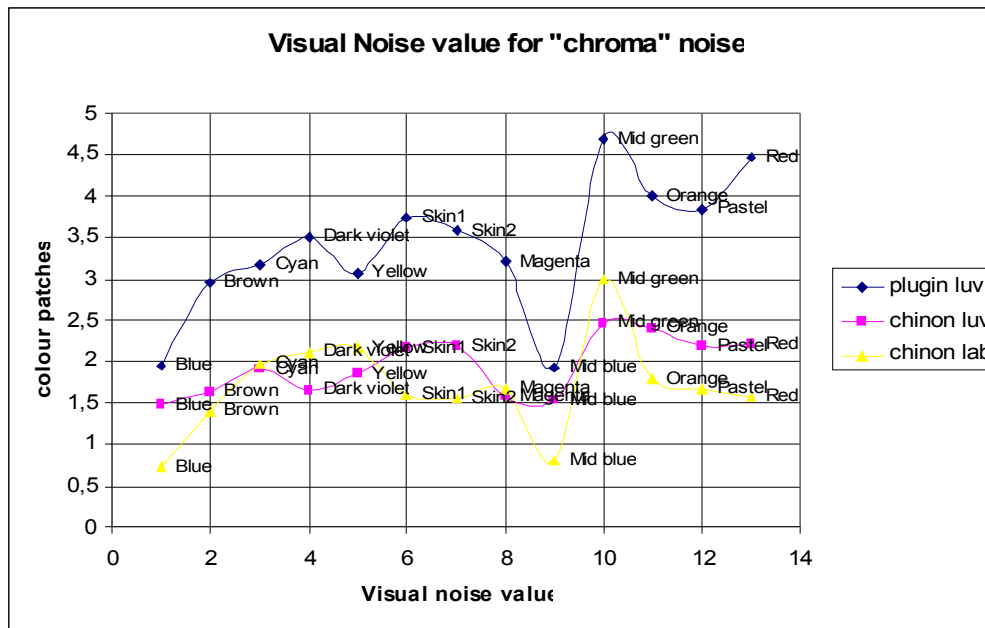
But in general, as it is expected, the threshold images achieve similar visual noise values. Still this first conclusion must be taken with care since this first result only applies to one kind of noise, and the noise input seems to be already uniform in itself ($\Delta E = \Delta L$ colour differences of the noise input are similar).

3.2.2 Noise Evaluation for Colour Difference in the Chroma Channel

Table 3.03: visual noise value of the threshold images with noise input in the chroma channel.

Colour patch	Shiraz		Visual noise Value			deviation to mean value		
	ΔC	variance	Plugin luv	chinon luv	chinon lab	plugin luv	chinon luv	chinon lab
Blue	4,1	1,8	1,94	1,47	0,72	-1,43	-0,48	-0,96
Brown	4,4	1,84	2,95	1,64	1,39	-0,42	-0,31	-0,30
Cyan	5,2	3,68	3,17	1,92	1,98	-0,20	-0,03	0,29
Dark violet	6,8	6,99	3,51	1,64	2,10	0,14	-0,31	0,41
Yellow	15	15,15	3,08	1,84	2,17	-0,29	-0,11	0,49
Skin1	3,9	1,5	3,74	2,17	1,59	0,37	0,21	-0,10
Skin2	3,5	1,95	3,59	2,18	1,55	0,22	0,22	-0,14
Magenta	5,6	6,49	3,21	1,58	1,67	-0,16	-0,38	-0,02
Mid blue	5	5,08	1,93	1,54	0,80	-1,44	-0,41	-0,88
Mid green	10,5	13,58	4,68	2,45	3,00	1,31	0,50	1,31
Orange	7	6,14	3,99	2,41	1,79	0,62	0,46	0,10
Pastel	3,9	2,15	3,84	2,18	1,68	0,47	0,23	-0,01
Red	4,3	2,14	4,47	2,20	1,58	1,10	0,25	-0,11
Mean Value			3,39	1,94	1,69			
variance			0,60	0,10	0,29			
std deviation			0,77	0,32	0,54			

Graph 3.02: plots of the visual noise value for the threshold images with noise input in the chroma channel.



Here the dark grey and light grey colour are not evaluated because, by definition, it is not possible to put any chroma deviation in a grey sample ($\Delta E = \Delta C = 0$).

While the luminance difference as noise input is quiet constant (luminance difference stays in a range of $\Delta L = \Delta E$ between 0,4 and 0,6), the chroma difference varies a lot for different colours. This is more than $\Delta E = \Delta C = 10$ for yellow and mid-green while, for the others colours, the noise input stays in a range of ΔC between 4 and 7 (red and blue colours get the smallest values). This can be explained with the eye's sensitivity behaviour which is more sensible for luminance than for colour. So relating only to the colour discriminations, this would mean that the eye would see chroma's differences more clearly for red and blue, while it would less clear for yellow and mid-green.

It can also be noticed that the higher the colour difference, $\Delta E = \Delta C$ as noise input, the higher the variances are. This means that the higher the colour difference gets, the more difficult it is to determine an exact threshold image.

But despite these large chroma differences in the noise input, the visual noise values are similar. Relating to the standard deviation of the mean value over the threshold images, the Matlab® implementation of the algorithm seems to be more homogeneous (smaller variance) - in particular, the visual noise formula calculated along the Luv axes rather than the formula calculated along the Lab axes.

Here it can be noticed that the curves do not have the same shape, they all differ from each other depending on the colour. In the case of the Matlab® implementation, this is probably due to the difference in orientation between the colour space CIELab1976 and CIELuv1976 [**paragraph 3.1.1.3**]. In the case comparing the visual noise value from the formula along the Luv axes between the Photoshop® plugin and our Matlab® implementation, this can be due to the different contrast sensitivity functions used [**paragraph 2.5.2**].

In analogy, the same shape of the curves for noise input in the luminance channel [paragraph 3.2.1] can be explained. Regarding the two curves of the Matlab® implementation (Luv and Lab formulae), the luminance coordinate is calculated as the same for the CIELab1976 and CIELuv1976 colour space [formula 3.01 and 3.02]. Regarding the curves of the Matlab® implementation and the Photoshop® Plug-in, the tools used two different contrast sensitivity functions in the algorithm, but the luminance contrast sensitivity functions seem to have a similar shape [paragraph 2.5.2], while the chromatic contrast sensitivity functions differ from each other [paragraph 2.5.2]. This explains the similarity in the shape of the two curves for noise input in the luminance channel and the difference of shape of the two curves for noise input in the chroma channel.

It can be noticed that the highest deviation from the mean value of the visual noise value over the threshold images occurs this time for blue and green (bold font in the table). No relevant explanations could be found for this.

For yellow, but also for green, the observers were reluctant to tell if there were noise input at all (for these colours the colour variation is very high, over 13, and the chroma's difference is in a range of a $\Delta E = \Delta C$ over 10). Out of the measurements, the noise input of yellow was first averaged to 12,1, with the highest variance of 15,15. So it is possible that the threshold is for a noise input higher than $\Delta C = 15$ (maximum value of noise input in the chroma channel set by Shiraz) and it could actually not be determined.

For the results, it has been assumed that the setting of Shiraz did not allow any noise perception in yellow and the noise input was set to $\Delta C = 15$. For the formula calculated from the Luv axes, the value is still smaller than the mean value of the threshold image, while for the formula calculated from the Lab axes, the value is quite higher than the mean value. However, this remains within an acceptable range (deviation of 0,5 to the mean value).

This agrees with the assumption that the noise threshold could have actually been out of range of the possible noise input. Moreover, it agrees with the assumption that the tested person in the demand of seeing noise tried to see noise in yellow where it could actually not be seen. Perhaps increasing the maximum setting of Shiraz to $\Delta E = \Delta C = 20$ could avoid this uncertainty.

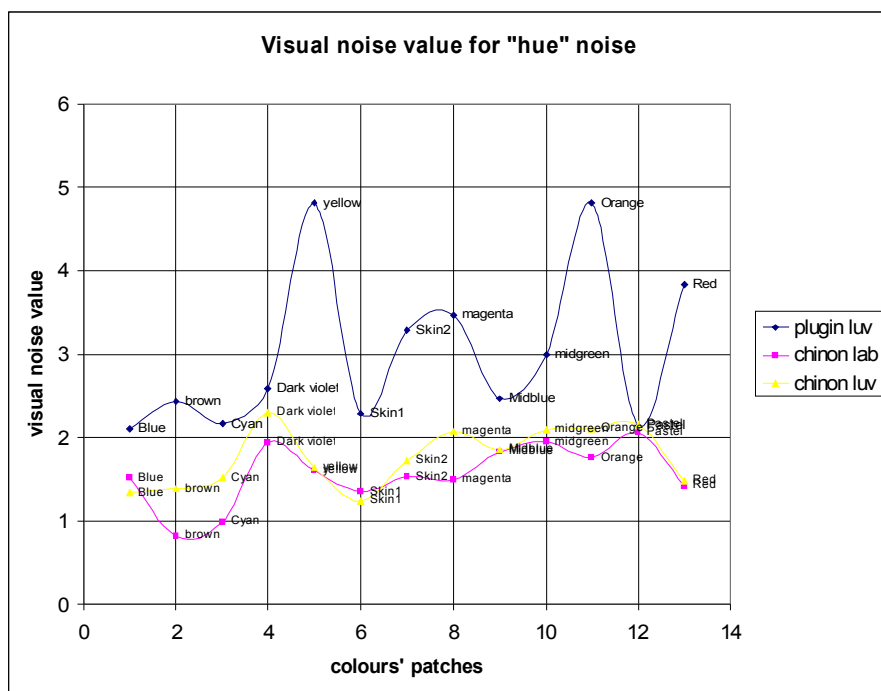
Despite this uncertainty, the variance and the standard deviation for the visual noise value over the threshold images stay under an acceptable range. Thus, the visual noise measurement model shows satisfying result by quantify the threshold images for noise input in chroma.

3.2.3 Noise Evaluation for Colour Difference in the Hue Channel

Table 3.04: visual noise value of the threshold images with noise input in the hue channel.

Colour patch	Shiraz		Visual noise Value			deviation to mean value		
	$\Delta\Phi$	variance	Plugin	chinon		plugin	chinon	
			luv	luv	lab	luv	luv	lab
Blue	6,2	5,07	2,1	1,34	1,51	-0,93	-0,42	-0,04
brown	6,6	4,6	2,43	1,38	0,81	-0,60	-0,38	-0,74
Cyan	11,2	12,71	2,17	1,51	0,99	-0,86	-0,25	-0,56
Dark violet	6,2	5,54	2,59	2,30	1,94	-0,44	0,54	0,39
yellow	5,9	2,72	4,81	1,64	1,60	1,78	-0,12	0,04
Skin1	12,4	12,72	2,29	1,24	1,35	-0,74	-0,52	-0,21
Skin2	11,2	16,7	3,28	1,72	1,52	0,25	-0,04	-0,03
magenta	2,8	1,57	3,46	2,07	1,49	0,43	0,31	-0,07
Midblue	3,9	1,85	2,46	1,85	1,83	-0,57	0,09	0,27
midgreen	5,8	3,26	2,99	2,10	1,94	-0,04	0,34	0,39
Orange	6,1	4,64	4,81	2,11	1,76	-1,78	0,35	0,20
Pastel	15	7,37	2,14	2,16	2,06	-0,89	0,40	0,50
Red	7,9	8,47	3,84	1,48	1,42	0,81	0,28	-0,14
mean value			3,03	1,76	1,56			
variance			0,92	0,13	0,13			
st deviation			0,96	0,36	0,37			

Graph 3.04: plots of the visual noise value for the threshold images with noise input in the hue channel.



Here the dark grey and light grey colours are not evaluated because by definition it is not possible to put any hue deviation in a grey sample ($\Delta h = 0$).

The hue colour difference also shows big differences among the colours. This concerns a range of Δh between 2,8 for the magenta colour and 11,2 for cyan. This would mean that the eye is most sensitive to changes of hue in magenta and is worst in cyan.

The visual noise values are, similar for all the threshold images. Again the Matlab® implementation gets more homogeneous visual noise value than the Photoshop® Plug-in.

The shape of the curves are also quite similar and do not show big differences between the use of the formula calculated along the Lab axes or the Luv axes. The shape of the curve of the Photoshop® Plug-in are showing more deviations with the yellow, red and orange colours getting the highest visual noise value, and blue and cyan getting the smallest. This may show an inadequate filtering of the opponent colours with the chromatic contrast sensitivity function.

3.2.4 First Conclusions

Because of the high standard deviation (from 1,5 to 15) [Table 3.02 and 3.03] to determine through experiments the threshold images for noise input in the chroma and hue channel, the precision of the measurements could have been doubted. But still the visual noise measurement model fulfils the expected thesis. In other words, for the threshold images the visual perception is the same so the visual noise value should also be the same.

Table 3.04: Mean value of the visual noise value of the threshold images

Noise Input	Plugin Luv	Chinon Luv	Chinon Lab
ΔL	1,79	1,42	1,36
ΔC	3,37	1,95	1,69
Δh	3,03	1,76	1,56
Mean value	2,73	1,71	1,54
Standard deviation	0,83	0,27	0,17

Table 3.05: Standard deviation of the mean value of the visual noise value of the threshold images

Noise Input	Plugin Luv	Chinon Luv	Chinon Lab
ΔL	0,69	0,53	0,48
ΔC	0,77	0,32	0,54
Δh	0,96	0,36	0,37

The Matlab® implementation of the algorithm of the model is achieving the best results (similar values of the visual noise value for the different noise input channel, with the smallest and acceptable standard deviations). However, the Photoshop® plugin is already less homogeneous inside the noise input channels themselves (higher standard deviations). Moreover, the visual noise value for luminance noise input is 1 noise-count value smaller than the visual noise value of the colour's channels, which are the same. This could match with the observation that noise in the luminance was easier to detect than the noise in chroma and hue.

But this may be due to a too weak weighting of the chromatic contrast sensitivity function. Since the threshold images stands for the same visual perception (JND) regardless of the kind of noise, it is expected that the visual noise value is not only the same over the different colours of a set with same kind of noise input, but that the visual noise value is also the same for the different kind of noise. While the Matlab® implementation fulfils the thesis expectations, the Photoshop® Plug-in does not, that is why it would be assumed that the weighting of the used chromatic contrast sensitivity function are not accurate enough.

This assumption can match with the former observations. Namely that for the hue and chroma noise input, the shape of the curves between the Matlab® implementation and the Photoshop® Plug-in the **[graph 3.02, 3.03, 3.04]**, describing the dispersion of the visual noise value for each colour referring to the mean value, are different. This is probably due to the use of a different chromatic contrast sensitivity function **[paragraph 2.5.2]**.

From table 3.04 and 3.05, comparing the results of the Matlab® implementation between the Luv and Lab formulae, there are no noticeable differences. They both have similar mean value over the three kinds of noise input and have relatively low and similar standard deviations.

It is taken for granted that the smaller the noise input, the more sensitive the eye. The noise input in the luminance channel is far lower than in the chroma and hue channel. This observation matches with the eyes higher sensitivity to changes in luminance than to colour.

So according to the colour difference of the noise input for each channel, the following assumption could be made: the eye would discriminate chroma's differences better for red and blue, while it would discriminate the worst for yellow and mid-green. This is because the colour difference, in order to detect the just noticeable noise, would be the smallest for red and blue and the highest for yellow and mid-green.

In analogy it can be assumed that the eye is most sensible for hue difference in magenta and the worst in cyan. Since the colour difference for the noise input in the luminance channel were almost the same for all colours, no assumption could be made about the eye's sensitivity in this case.

In order to verify the assumptions made about the eye's colour sensitivity, further investigations have been made by scaling the noise input out of the human visual model algorithm in chapter 5.

But first, since the Matlab® implementation of the visual noise measurement is getting satisfying results, it is going to be tested for practical uses. The two grey patches (from the example of chapter 1) are tested with it, as well as all the patches of the OECF-20 chart.

3.3 Praxis oriented Tests of the Visual Noise Measurement Model

3.3.1 Test of the two Grey Patches

Relying now only on the results of the Matlab® implementation of the visual noise value formula of the CIE Luv1976 colour space, the visual noise value of the two grey patches, already measured with the signal to noise ratio method [paragraph 1.2], has been evaluated. For the grey patch taken at a sensitivity of 100ISO, the visual noise value is 2,65 and for the one taken at sensitivity of 400ISO the visual noise value is 3,70, despite both being evaluated with the same value when measured with the signal to noise ratio. Here the visual noise values were calculated for a contrast sensitivity function scaled on 26 cycles per degree, for a 100% viewing on a 72dpi monitor.

According to the former investigation [paragraph 3.2.4], the threshold visual noise value is on average 1,71. This means that, for all visual noise values smaller than 1,71, noise can not be seen while, for all values greater, noise can be seen. So the two visual noise values of the two grey patches are in accordance with this, since noise can easily be seen on the patches. Moreover it could be observed that the patch taken at sensitivity of 400ISO had a more disturbing noise perception. Its higher visual noise value also matches with this observation.

Because of its satisfying results, the visual noise measurement from the Matlab® implementation of the CIE Luv1976 formula has been integrated as part of the new version of the IE-Analyser®, software of the company *Image Engineering*, for measurement of digital cameras. In the following paragraph, the visual noise measurements of the patches of the OECF20-test charts photographed for two different ISO-sensitivity settings of the camera *Canon® Ixus65* are reported.

3.3.2 Example of the Visual Noise Measurement Model used in the Image Engineering Analyser®

As had been done before for the two grey patches, the patches of the OECF20-chart have been tested with the visual noise measurement model. The chart has been photographed with the camera *Canon® Ixus65* once at sensitivity of 100ISO and once at sensitivity of 400ISO. Then it was run through the visual noise measurement tool of the Image Engineering Analyser®. The two different formula evaluation of the visual noise value, Luv or Lab, were used and with three different settings, which corresponded to different resolution of the eye:

Setting 1: for a 100% viewing of the image on a monitor with 72 dpi seen at a distance of about 60cm (but at a minimum distance of 40cm), corresponding in this case to 26,39 cycles per degree.

Setting 2: for a 10x15 cm print of the image with 300dpi seen at a maximum distance of 25 cm, corresponding in this case to 48,68 cycles per degree.

Setting 3: for a 30x40 cm print of the image with 300dpi seen at a minimum distance of 25 cm, corresponding in this case to 31,62 cycles per degree.

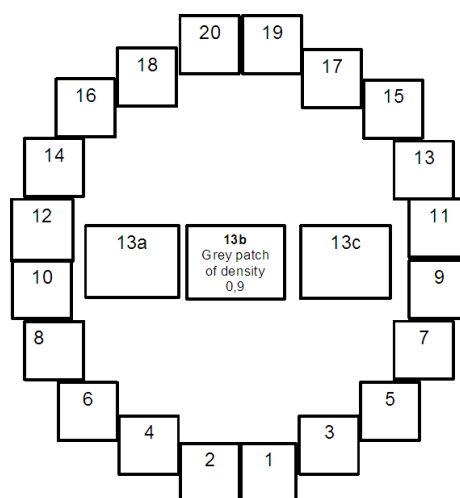


Figure 3.01: Representation of the OECF20 chart patches with corresponding referring number.

3.3.2.1 OECF20-Chart photographed with the Camera *Canon ix65* at sensitivity of 100ISO and 400ISO

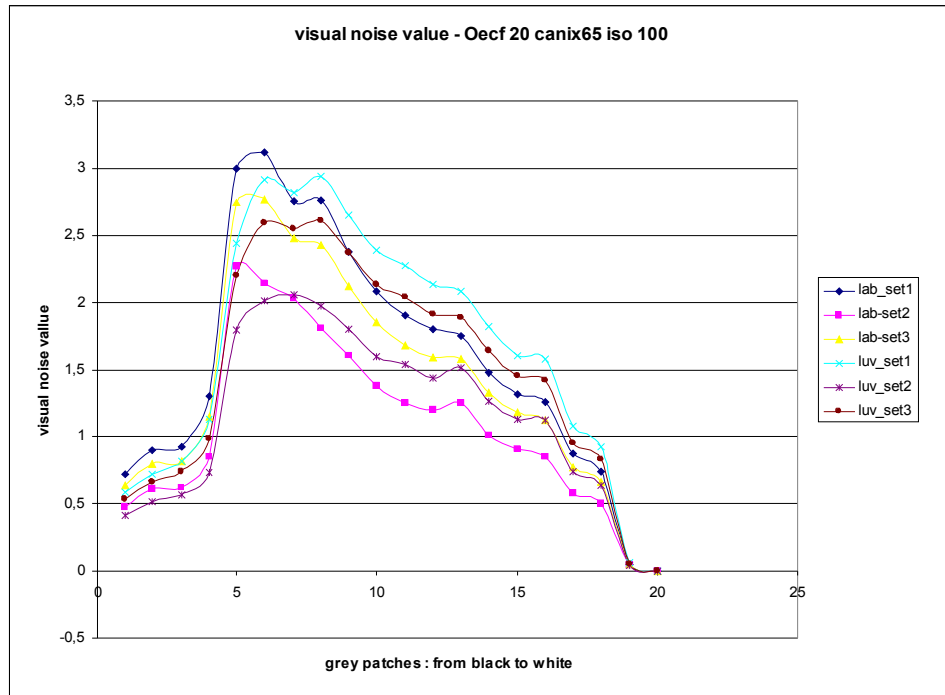
Table 3.06: Visual noise of the 20 grey patches of the OECF20-chart.

patch	Sensitivity of 100ISO						Sensitivity of 400ISO					
	Chinon Lab Formula			Chinon Luv Formula			Chinon Lab Formula			Chinon Luv Formula		
	Set 1	Set2	Set3	Set1	Set2	Set3	Set 1	Set2	Set3	Set1	Set2	Set3
1	0,59	0,42	0,54	0,72	0,48	0,64	1,91	1,36	1,73	2,52	1,69	2,26
2	0,72	0,52	0,66	0,9	0,61	0,8	2,08	1,51	1,91	2,73	1,86	2,47
3	0,82	0,57	0,74	0,93	0,62	0,82	2,69	2	2,49	3,47	2,45	3,16
4	1,13	0,73	0,99	1,3	0,85	1,15	3,73	2,66	3,41	4,6	3,21	4,17
5	2,44	1,79	2,2	3	2,27	2,74	6,14	4,23	5,53	7,33	5,07	6,59
6	2,91	2,01	2,59	3,12	2,14	2,77	7,05	4,29	6,07	7,97	4,56	6,73
7	2,82	2,06	2,55	2,75	2,03	2,48	6,96	4,7	6,15	7,51	4,69	6,38
8	2,94	1,97	2,61	2,76	1,81	2,43	5,95	3,89	5,23	5,74	3,79	5,05
9	2,65	1,8	2,37	2,38	1,61	2,12	5	3,32	4,43	4,63	2,98	4,06
10	2,39	1,6	2,13	2,08	1,38	1,85	4,81	3,17	4,27	4,25	2,76	3,74
11	2,28	1,54	2,04	1,9	1,25	1,68	4,2	2,78	3,73	3,71	2,4	3,26
12	2,13	1,44	1,91	1,8	1,2	1,59	3,41	2,3	3,04	3,08	2,1	2,75
13	2,08	1,51	1,89	1,75	1,25	1,58	3,43	2,34	3,07	2,95	1,95	2,62
14	1,82	1,27	1,64	1,48	1,01	1,33	2,89	1,9	2,56	2,44	1,59	2,15
15	1,61	1,13	1,45	1,32	0,91	1,18	2,48	1,69	2,22	2,03	1,35	1,81
16	1,58	1,12	1,42	1,26	0,85	1,12	2,19	1,53	1,97	1,8	1,23	1,61
17	1,08	0,74	0,95	0,88	0,58	0,77	1,63	1,03	1,43	1,37	0,86	1,19
18	0,93	0,64	0,83	0,74	0,5	0,66	1	0,63	0,86	0,83	0,5	0,71
19	0,06	0,04	0,05	0,05	0,04	0,05	0,42	0,29	0,38	0,39	0,27	0,35
20	0	0	0	0	0	0	0	0	0	0	0	0

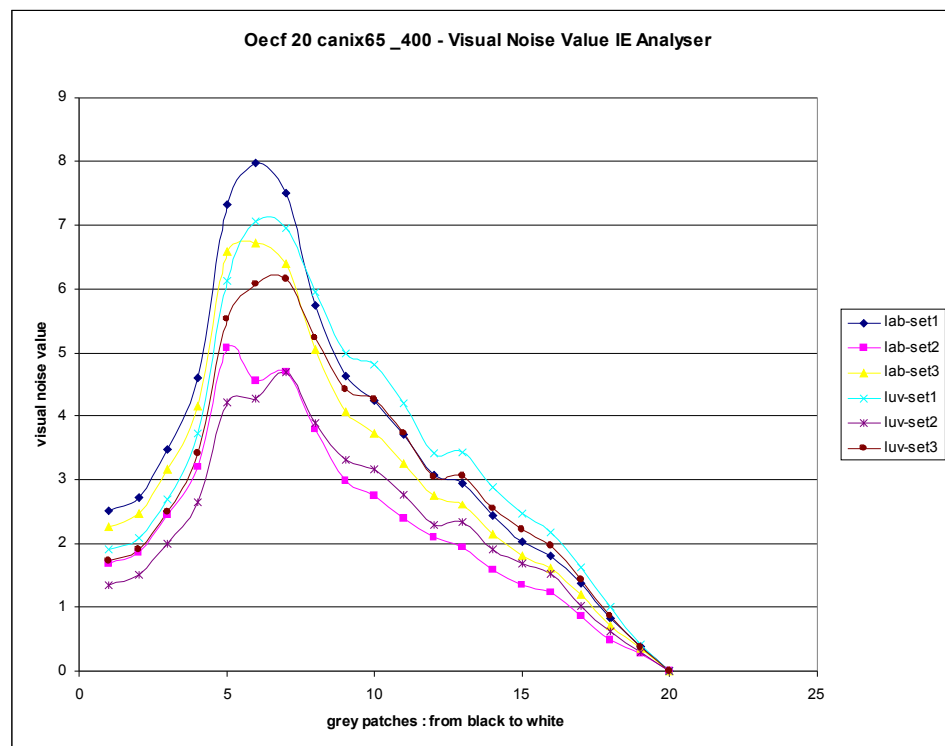
Table 3.07: Visual noise of the 3 mid-grey patches of the OECF20 chart.

patch	Sensitivity of 100ISO						Sensitivity of 400ISO					
	Chinon Lab Formula			Chinon Luv Formula			Chinon Lab Formula			Chinon Luv Formula		
	Set 1	Set2	Set3	Set1	Set2	Set3	Set 1	Set2	Set3	Set1	Set2	Set3
1	2,47	1,67	2,21	2,18	1,45	1,94	4,84	3,25	4,3	4,43	2,98	3,92
2	2,47	1,7	2,22	2,14	1,43	1,9	4,48	2,99	3,98	3,98	2,59	3,51
3	2,27	1,53	2,02	1,99	1,34	1,77	4,06	2,63	3,57	3,61	2,31	3,15

Graph 3.04: graphical representation of the visual noise value in function of the 20 patches



Graph 3.05: graphical representation of the visual noise value in function of the 20 patches



3.3.2.2 Brief analysis

Referring to chapter 3 at paragraph 3.2.4, after testing the threshold images through all three kind of noise, the mean value is 1,71 for the visual noise value calculated from the Luv formula, or 1,54 calculated from the Lab formula. This means that for visual noise values under 1,71 or 1,54, any incidence of noise should not be perceptible to the eye. Over these values, the noise becomes perceptible and, relating to the two sample grey patches, the noise is already visually unacceptable when it is above 2,5.

Figure 3.02 and 3.03 (showed following page) are prints, corresponding to setting 2, of the OECF20 chart photographed with the camera *Canon® Ixus65* at an sensitivity of 100ISO and of 400ISO.

In observing the printed images, and comparing the visual noise impression with the visual noise value for each patch (in bold font in table 3.06), and relying on the known reference values of the threshold images, it can be concluded that the visual noise value matches with the visual noise impression:

For the OECF20 chart photographed at a sensitivity of 100ISO, there are only four patches (patch 5 to 8) with a visual noise value above the threshold value set to 1,71, with the maximum visual noise value of 2,27 for the patch 5, which corresponds to a dark grey. This is actually the patch, which is the most disturbing for the eye, the three other patches show a slight just perceptible inhomogeneity of surface. Observing the other patches, no noise can be seen.

For the OECF20-chart photographed at a sensitivity of 400ISO, expect for the four last patches (patch 17 to 20), all the patches have a visual noise value above the threshold value. The most disturbing noise is seen on patch 5, 6, 7 and 8, which get the highest visual noise value (5,07; 4,56; 4,69; 3,79).

To conclude, the visual noise measurement has been validated as a physiologically quantification of the colour noise and performs good results when applied in the praxis. Though it can only measure the noise for uniform patches, the evaluation of a complex scene is not possible. That is why the S-CIELabDE2000 model has also been investigated, since it can measure the colour difference for a complex spatial frequency pattern.

4 .Chapter 4: S-CIELabDE2000 Model

4.1 S-CIELabDE2000 Formula: Comparison of a "Noisy" Image with a "Noise-free" Image

Since the former model is only valid for uniform patches or images, the S-CIELabDE2000 model [20] has been investigated with threshold images, which contain rectangle spatial patterns with different contrast.

The S-CIELabDE2000 model is also based on the human visual model, so by the implementation in Matlab®, the first eighth steps are the same as in the Noise Measurements but the last steps are different:

Step 9: the filtered tristimulus values are transformed into the CIELab1976 [8 p167] colour space according to the equations 3.01, 3.02, 3.09, and 3.10. This takes place for the "noisy" threshold image and its corresponding "noise free" image.

$$\begin{bmatrix} L^*_{free} \\ a^*_{free} \\ b^*_{free} \end{bmatrix} = CIELab\ 1976_{formula} \cdot \begin{bmatrix} X_{Dfree} \\ Y_{Dfree} \\ Z_{Dfree} \end{bmatrix} \quad (4.01)$$

$$\begin{bmatrix} L^*_{noise} \\ a^*_{noise} \\ b^*_{noise} \end{bmatrix} = CIELab1976_{formula} \cdot \begin{bmatrix} X_{Dnoise} \\ Y_{Dnoise} \\ Z_{Dnoise} \end{bmatrix} \quad (4.02)$$

Step 10: Then for each corresponding pixel, the colour difference ΔE between the "noisy" threshold image and the "noise-free" image is processed according to the CIEDE2000 [23] [20].

Compared to CIEDE1976, the CIEDE1994 formula includes lightness, chroma and hue weighting functions. The CIEDE2000 formula has been derived from the CIEDE1994 formula and “includes an interactive term between chroma and hue differences to improve performance of the blue region” [20 p431]. It also “includes a hue dependent function that corrects perceived hue differences” [20 p431], and a scaling factor for the a* axes for improving the performance of grey colours [20 p431].

The adjustment of the colour difference is made separately for each pixel, i.e., on a pixel-by-pixel basis for the image pair. In each equation, the subscript [x,y] refers to x-y coordinates of each pixel of the image. When being processed together, the image pairs are referred to as the "free" noise image and the "noise" image [20 p431].

- First step: “is an adjustment of the a* axis to correct for the colour difference perception of low chroma colours” [20 p431]. This is done by “using a modified Gaussian curve on the mean chroma difference” [20 p431].

In order to calculate the Gaussian function, the arithmetic mean chroma between the "free" noise image and the "noise" image must first be calculated:

$$C^* = \sqrt{a^{*2}_{[x,y]} + b^{*2}_{[x,y]}} \quad (4.03)$$

$$\bar{C}^*_{[x,y]} = \frac{C^*_{free[x,y]} + C^*_{noise[x,y]}}{2} \quad (4.04)$$

Gaussian function:

$$G_{[x,y]} = 0,5 \cdot \left(1 - \sqrt{\frac{(\bar{C}^*_{[x,y]})^7}{(\bar{C}^*_{[x,y]})^7 + 25^7}} \right) \quad (4.05)$$

Equation 4.05 is then used to scale the a* axis:

$$a' = (1 + G_{[x,y]}) \cdot a^*_{[x,y]} \quad (4.06)$$

- **Second step:** the polar coordinates LCh are then calculated from the Lab cartesian coordinates:

$$L'_{[x,y]} = L^*_{[x,y]} \quad (4.07)$$

$$C'_{[x,y]} = \sqrt{a'^2_{[x,y]} + b'^2_{[x,y]}} \quad (4.08)$$

$$h'_{[x,y]} = \arctan\left(\frac{b'^*_{[x,y]}}{a'_{[x,y]}}\right) \quad (4.09)$$

- **Third step:** the colour difference between the "free" noise image and the "noise" image for each polar coordinate are then calculated:

$$\Delta L' = L'_{free[x,y]} - L'_{noise[x,y]} \quad (4.10)$$

$$\Delta C' = C'_{free[x,y]} - C'_{noise[x,y]} \quad (4.11)$$

$$\Delta h' = h'_{free[x,y]} - h'_{noise[x,y]} \quad (4.12)$$

“Care must be taken when calculating hue angle differences between the "noise free" image and the "noisy" image if the hue angles reside in different hue quadrants. If the absolute difference between the two hue angles is greater than 180 degrees, then it is important to add 360 to the smaller of the hue angles” [20 p432]:

$$\text{if } |\Delta h'_{[x,y]}| > 180 \quad \text{then} \quad \min(h'_{free[x,y]}, h'_{noise[x,y]}) + 360 \quad (4.13)$$

$$\Delta H = 2 \cdot \sqrt{C'_{free[x,y]} \cdot C'_{noise[x,y]}} \cdot \sin\left(\Delta h' \frac{[x,y]}{2}\right) \quad (4.14)$$

- **Fourth step:** In order to calculate the other weighting functions, the arithmetic mean lightness, chroma and hue-angle between the sample and batch images must first be calculated:

$$\bar{L}'_{[x,y]} = \frac{L'_{free[x,y]} + L'_{noise[x,y]}}{2} \quad (4.15)$$

$$\bar{C}'_{[x,y]} = \frac{C'_{free[x,y]} + C'_{noise[x,y]}}{2} \quad (4.16)$$

$$\bar{h}'_{[x,y]} = \frac{h'_{free[x,y]} + h'_{noise[x,y]}}{2} \quad (4.17)$$

“Again, care must be taken when determining the mean hue angle if the hue values for the pixel reside in different quadrants. {Equation 4.13} should be applied when calculating mean hue as well” [20 p432].

- **Fifth step:** “Weighting functions are then calculated to adjust for the perceived colour differences between lightness, chroma, and hue in the CIELAB space. These weighting functions are also calculated on a pixel-by-pixel basis” [20p432].

Lightness weighting function:

$$S_{L[x,y]} = 1 + \frac{0.015 \cdot (\bar{L}'_{[x,y]} - 50)^2}{\sqrt{20 + (\bar{L}'_{[x,y]} - 50)^2}} \quad (4.18)$$

Chroma weighting function:

$$S_{C[x,y]} = 1 + 0,045 \cdot \bar{C}'_{[x,y]} \quad (4.19)$$

“The hue weighting is a function of both hue angle and chroma. First, the hue angle dependency is determined, using {Eq 4.20}. This is then combined with the chroma dependency in {Eq 4.21}” [20p432].

Hue angle dependency function:

$$T_{[x,y]} = 1 - 0,17 \cdot \cos(h'_{[x,y]} - 30) + 0,24 \cdot \cos(2h'_{[x,y]}) + 0,32 \cdot \cos(3h'_{[x,y]} + 6) - 0,20 \cdot \cos(4h'_{[x,y]} - 63) \quad (4.20)$$

Chroma dependency function:

$$S_{H[x,y]} = 1 + 0,015 \cdot C_{[x,y]}^- \cdot T_{[x,y]} \quad (4.21)$$

-Sixth step: “The blue region of CIELAB is known to be highly non-linear in regards to hue angle and chroma interaction. A rotation function has been created to compensate for this interaction” [20 p432]:

First a chromatic dependent term is determined:

$$R_{C[x,y]} = 2,0 \cdot \sqrt{\frac{C_{[x,y]}^{*7}}{C_{[x,y]}^{*7} + 25^7}} \quad (4.22)$$

This is followed by a hue angle dependency:

$$\Delta \theta_{[x,y]} = 30 \cdot e^{-(h'_{[x,y]} - 275^\circ / 25)^2} \quad (4.23)$$

Then the rotation function is applied:

$$R_{T[x,y]} = -\sin(2 \Delta \theta_{[x,y]}) \cdot R_{C[x,y]} \quad (4.24)$$

- Seventh step: Finally, the total colour difference for each pixel can be calculated:

$$\Delta E_{[x,y]} = \sqrt{\left(\frac{\Delta L'_{[x,y]}}{K_L \cdot S_{L[x,y]}}\right)^2 + \left(\frac{\Delta C'_{[x,y]}}{K_C \cdot S_{C[x,y]}}\right)^2 + \left(\frac{\Delta H'_{[x,y]}}{K_H \cdot S_{H[x,y]}}\right)^2 + R_{T[x,y]} \cdot \left(\frac{\Delta C'_{[x,y]}}{K_C \cdot S_{C[x,y]}} \cdot \frac{\Delta H'_{[x,y]}}{K_H \cdot S_{H[x,y]}}\right)} \quad (4.25)$$

To resume the colour difference formula:

- The last term of the sum is the interactive term between chroma and hue differences [23].

- S_L , S_C , S_H are the weighting functions for lightness, chroma and hue components respectively. The values calculated for these functions vary according to the position of the sample pair being considered in the space [23].

- R_T : allows chromatic ellipses in some regions of the a^*b^* plane to be rotated [23].

- The parametric weights K_L , K_C , K_H can be adjusted to different viewing parameters such as textures, backgrounds, separations, etc. for the lightness, chroma, and hue components. In this case and “*for most imaging applications, these weights are unknown, and should be all set to 1,0*” [20 p432].

In fact, the colour difference ΔE obtained between the noise-free image and the noisy image, is an error image: the "image of the noise pattern".

In order to simplify the evaluation, the obtained error image is reduced to a single number representing the overall perceived difference. “*A common practice is to take the mean CIEDE2000 of the image's pixels. While useful in providing an overall idea, this can lead to error*” [20 p433] evaluation. For example, it is possible that an image with smooth uniform noise can have the equal mean error to an image with less noise, but which has a higher noise amplitude deviation. This would actually be more perceptibly noticeable. The spatial filtering itself should give greater weight to the lower frequency large shifts and less weight to the individual pixels, “*although it is still possible to have identical mean errors*” [20 p433]. “*This can be in some ways avoided when comparing additional statistics such as the error variance, standard deviation or median (...)*” [20p433]. For example, Fairchild recommend the error maximum for detecting threshold image differences [20 p433].

Going back to the algorithm.

Step 11: Finally the mean value of the colour difference ΔE of all the pixels is calculated.

$$S \bar{\Delta E} = \frac{\sum_1^n \Delta E_n}{n} \quad \text{with} \quad n = \text{number of pixels} \quad (4.27)$$

The mean value of the colour difference ΔE is taken as a quantification of noise, since noise can also be considered as a colour difference. Following the hypothesis, the mean value of the colour difference $S \bar{\Delta E}$ of all the pixels of the image should be the same for each threshold image.

The median, standard deviation, variance and maximum error of the colour difference have also been calculated.

4.2 Investigation of the S-CIELabDE2000 Model

4.2.1 Investigation with Threshold Images with rectangular spatial Patterns with different Contrast

A set of threshold images of different colours have been evaluated with the S-CIELabDE2000. The calculations were for mean value, median, standard deviation, variance, and maximum pixel value of the difference image – the difference between the noisy image and the noise free image. The set of colours were purple, blue, brown, yellow, green, skin, light-blue, magenta, mid-blue, olive-green, violet, and have a rectangular frequency pattern of 4 pixels per cycles and different contrast model

Table 4.01: Setting of Chinon for the following evaluations (parameters and viewing conditions from the former diploma thesis work of Nicole Kidawa and Christina Simon [11 pp38-39]):

viewing distance	90cm
horizontal monitor resolution	640
vertical monitor resolution	480
monitor diagonal	21 inch set to 20 inch (used monitor is CRT)
calculated cycles per degree	12,37
monitor profile	Monitorprofil080403.icc

In the three following tables (4.02, 4.03, and 4.04), the noise input as colour difference has been reported for the threshold images and their corresponding variance, as well as the colour difference ΔE calculated in a former experiment [11] with the CIELabDE2000 formula. Finally, the S- ΔE mean, median and standard deviation value of the pixel of the difference image have been reported, because they seem to match the expectations of having homogeneous values for the different threshold images.

But the S- ΔE variance and maximum error value have not been reported (though according to Fairchild the error maximum should be appropriate for detecting threshold image differences [paragraph 4.1]). This is because these values for the different threshold images did not seem relevant as they varied too greatly. For these two values the standard deviation is over 3,57 and the variance is over 12,75.

4.2.1.1 Noise Input as a Colour difference in the Luminance Channel

Table 4.01: mean value of the CIELabDE2000 and the mean, median and standard deviation value of the S-CIELabDE2000 colour difference of the threshold images with noise input as a luminance difference.

Purple 1 has a contrast of 22%, while purple2 has a contrast of 35%. All the other colours have a contrast of 10%.

colour difference	noise input ΔL	variance	ΔE_{2000}	S- ΔE_{2000} mean	S- ΔE_{2000} median	S- ΔE_{2000} std dev
purple1	1,11	0,28	1,09	3,22	1,92	3,28
purple2	1,26	0,22	1,24	2,03	1,51	1,69
blue	0,78	0,14	0,75	1,72	1,39	1,26
brown	0,94	0,13	0,73	2,98	1,60	3,36
yellow	1,05	0,32	0,69	2,52	1,51	2,50
green	0,9	0,13	0,71	2,77	1,50	2,96
skin	0,83	0,12	0,66	1,88	1,19	1,84
light blue	0,81	0,15	0,75	2,03	1,29	2,09
magenta	0,81	0,15	0,75	1,66	1,25	1,39
mid-blue	0,89	0,26	0,78	1,58	1,35	1,04
olivegreen	0,9	0,22	0,69	2,36	1,35	2,51
violet	0,85	0,15	0,81	1,71	1,17	1,57
mean value	0,93	0,19	0,80	2,20	1,42	2,12
variance	0,02	0,00	0,03	0,31	0,04	0,63
std deviation	0,14	0,7	0,18	0,56	0,21	0,79

The variance and the standard deviation of the ΔE_{2000} value and the S- ΔE_{2000} median remain low, while the ones of the S- ΔE_{2000} mean value and the S- ΔE_{2000} standard deviation are much higher. The ΔE_{2000} value and the S- ΔE_{2000} median obtain similar levels of accuracy for the threshold images. and perform the best.

But investigating noise input as chroma difference and as hue difference as well, helps to get a better overview of the noise evaluation depending on the kind of noise input.

4.2.1.2 Noise Input as Colour Difference in the Chroma Channel

Table 4.02: mean value of the CIELabDE2000 and the mean, median and standard deviation of the S-CIELabDE2000 colour difference of the threshold images with noise input as a chroma difference.

colour difference	noise input ΔC	variance	ΔE_{2000}	S- ΔE_{2000} mean	S- ΔE_{2000} median	S- ΔE_{2000} std dev
purple1	8,98	8,4	2,61	2,55	1,76	2,42
purple2	11,2	10,53	3,2	4,02	2,42	4,18
blue	7,57	8,05	2,57	1,44	1,20	0,94
brown	6,07	7,7	2,74	1,95	1,70	1,31
yellow	11,8	7,09	3,12	1,19	1,02	0,81
green	9,9	11,25	3,76	3,08	2,60	2,18
skin	5,28	5,63	3,72	1,79	1,52	1,27
light blue	6,39	13,16	2,09	1,80	1,47	1,32
magenta	7,74	6,54	2,09	1,28	1,07	0,85
mid-blue	7,18	7,77	2,57	1,18	1,02	0,68
olivegreen	9,54	11,69	4,15	3,17	2,69	2,21
violet	8,46	10,35	2,87	2,48	1,95	1,98
mean value	8,34	9,01	2,96	2,16	1,70	1,68
variance	4,06	5,39	0,43	0,83	0,61	0,99
std deviation	2,02	2,32	0,65	0,91	0,95	0,99

The S- ΔE_{2000} mean and standard deviation value have the highest variance and standard deviation, while the S- ΔE_{2000} median value and the ΔE_{2000} value have the lowest (but in comparison to their values in the luminance channel, there are greatly higher).

Although the S- ΔE_{2000} median value and the ΔE_{2000} value still achieve the most similar values over their threshold images, their higher standard deviation and variance shows that a homogeneous quantification of the threshold images is in this case not as good achieved as for noise input in the luminance channel.

4.2.1.3 Noise Input as Colour Difference in the Hue Channel

Table 4.03: mean value of the CIELabDE2000 and the mean, median and standard deviation values of the S-CIELabDE2000 colour difference of the threshold images with noise input as a hue difference.

colour difference	noise input Δh	variance	ΔE_{2000}	S- ΔE_{2000} mean	S- ΔE_{2000} median	S- ΔE_{2000} std dev
purple1	4,79	2,81	2,24	1,23	0,95	0,99
purple2	6,17	9,21	2,87	2,63	1,48	2,81
blue	6,01	5,62	3,25	1,86	1,54	1,31
brown	13,39	4,24	4,55	2,79	2,10	2,29
yellow	6,82	12,02	3,93	2,05	1,74	1,44
green	8,55	10,94	2,83	2,14	1,54	1,84
skin	13,6	2,47	2,57	2,09	1,57	1,74
light blue	14,22	1,48	1,84	2,01	1,62	1,53
magenta	3,84	2,69	1,84	0,78	0,69	0,47
mid-blue	4,32	5,45	3,25	1,54	1,31	1,00
olive green	9,88	9,35	2,77	1,89	1,52	1,39
violet	8,29	8,99	3,80	1,44	1,14	1,09
mean value	8,32	6,27	2,98	1,87	1,43	1,49
variance	13,78	13,44	0,69	0,32	0,14	0,39
std deviation	3,71	3,67	0,83	0,57	0,37	0,63

Here the variance and standard deviation are, in general, smaller than the one from the chroma noise input, but still much higher than the one from the luminance noise input.

While the S- ΔE_{2000} median value gets the lowest variance and standard deviation, the ΔE_{2000} value has the highest variance and standard deviation. In this case only the S- ΔE_{2000} median value performs the best by getting the most similar values over the threshold images.

To resume, for each noise input channel taken individually, the S- ΔE_{2000} median value performs the best in the luminance, chroma and hue channel. The ΔE_{2000} value performs better than S- ΔE_{2000} mean and standard deviation value only for the luminance and chroma noise input channel.

But in order to compare the evaluation of noise over the different kind of input, the mean values of the colour differences of the threshold images have been reported in the following table.

Table 4.04: Mean value of the colour difference for all the threshold images.

noise input	ΔE_{2000}	S- ΔE_{2000} mean	S- ΔE_{2000} median	S- ΔE_{2000} std dev
ΔL	0,80	2,20	1,42	2,12
ΔC	2,96	2,16	1,70	1,68
Δh	2,98	1,87	1,43	1,49
mean value	2,25	2,08	1,52	1,76
variance	1,57	0,03	0,02	0,10
std deviation	1,25	0,18	0,16	0,32

For the threshold images over the three kind of noise input, the S-CIELabDE2000 values have similar values. This is not the case for the ΔE_{2000} value, where the mean value of the threshold images in the luminance channel is 2 unit counts smaller than the mean value in the chroma and hue channel.

For the different kind of noise the S- ΔE_{2000} mean, median and standard deviation values are performing better than the ΔE_{2000} value. The S- ΔE_{2000} median value is performing better overall because it has the lowest variances and standard deviations in each noise channel with also the lowest variance and standard deviation for the mean values of the threshold images over the three different kind of noise.

As a first conclusion, the S- ΔE_{2000} median value performs the best by quantifying the threshold images with the similar values. So it is assumed that the S- ΔE_{2000} median value would be the best appropriate to quantify noise as a colour difference in a physiological manner.

In order to have a more accurate approach to the first evaluations, further investigation has been made into the S-CIELabDE2000 colour difference, with a focus on its dependence on frequency pattern and contrast.

4.2.2 Further Investigation: Colour Difference in function of the Contrast and the Frequency Patterns

An extended experiment has been conducted with the colours: cyan, red, mid-blue, light grey, and mid-green, each colour getting a rectangular frequency pattern of either 4, 6 or 10 pixels and each a contrast of either 3, 10 or 22%. So there are 9 different patterns of contrast and frequency for each colour. In table 4.05, for the colour mid-blue, the median value of the colour difference of the difference image over the 9 patterns has been calculated. The behaviour of the other tested colours is similar; their results have been reported in appendix F. A similar value between the 9 different patterns is expected, if the S-CIELabDE2000 can fulfil the thesis' assumption.

Table 4.05: median value of the colour difference over the pixels for mid-blue for noise input in the luminance, chroma, and hue channel for each of the 9 patterns of contrast and frequency.

frequency in pixels pro cycles	contrast in %	noise input ΔL	S- ΔE_{200} median	noise input ΔC	S- ΔE_{200} median	noise input Δh	S- ΔE_{200} median
4	3	0,78	1,14	8,32	0,92	4,28	1,08
6	3	0,78	1,14	8,95	0,98	4,60	1,15
10	3	0,72	1,14	8,07	0,89	4,13	1,08
4	10	0,9	1,24	9,68	1,11	4,87	1,29
6	10	0,97	1,55	10,39	1,21	5,14	1,37
10	10	0,82	1,23	8,79	1,00	4,48	1,20
4	22	1,22	2,17	11,58	1,79	5,68	2,03
6	22	1,11	2,14	11,19	1,63	5,13	1,78
10	22	0,95	1,85	10,18	1,51	5,33	1,91

For all three kind of noise, the median value of colour difference is actually increasing with increasing contrast. Namely, it is increasing to 1 unit count from 3% contrast to 22% contrast and remains almost constant depending on the frequency pattern (decreasing with

increasing frequency patterns, with sometimes a maximum at 6 pixels pro cycle, while the highest variation occurs for higher contrast).

If the S-CIELabDE2000 model has adapted perfectly to the human visual system, it would be expected that all the colour difference S- ΔE_{2000} median values remain constant, but this is not the case. The S-CIELabDE2000 model can evaluate visual colour noise of images with spatial frequency contents as colour difference, but it shows some limitations.

Since the S-CIELabDE2000 model seems, for the expectations, to perform the best for low contrast frequency pattern, uniform patches have been run through it.

4.3 Investigation of the Colour Difference for Uniform Patches

4.3.1 Investigation with Threshold Images

Here the threshold images are the same as in chapter 3 [paragraph 3.2] as well as the setting of Chinon (table 3.01).

Table 4.06: mean value, variance and standard deviation of the threshold images for the ΔE_{2000} value and the S- ΔE_{2000} mean value, variance, standard deviation, median and maximum error.

noise input	for all threshold images	ΔE_{2000}	S- ΔE_{2000}				
			mean value	variance	std deviation	median	maximum error
ΔL	mean value	0,58	0,71	0,20	0,42	0,61	3,05
	variance	0,02	0,03	0,02	0,02	0,02	0,91
	std dev	0,14	0,17	0,13	0,13	0,15	0,95
ΔC	mean value	1,86	0,77	0,22	0,44	0,67	3,39
	variance	0,53	0,06	0,04	0,04	0,04	1,97
	std dev	0,73	0,25	0,20	0,19	0,20	1,40
Δh	mean value	2,72	0,94	0,41	0,62	0,80	4,47
	variance	0,48	0,06	0,04	0,03	0,04	1,02
	std dev	0,69	0,24	0,20	0,17	0,20	1,01

Looking first at the mean value of the colour difference values over the three kind of noise input, the S- ΔE_{2000} mean, variance, standard deviation and median value have relative similar values with low variance and standard deviation. However, this is not the case for the S- ΔE_{2000} maximum error value and the ΔE_{2000} value (this has already been investigated in the former diploma thesis, here they just have been reported for comparison).

These results match the thesis of similar noise value for the threshold images. To conclude, except for the S- ΔE_{2000} maximum error value, the S-CIELabDE2000 can quantify noise as a colour difference in a visual manner for uniform colour patches.

4.3.2 Brief conclusion

The colour difference of the S-CIELabDE2000 model is used as a quantification of the noise. For threshold images with frequency pattern, the S-CIELabDE2000 shows a tendency to get similar values only for the S- ΔE_{2000} median value, but further investigation shows that it has some limitations though. The quantification of threshold images as uniform patches is getting similar values for the S- ΔE_{2000} mean, variance, standard deviation and median values, and not, as it has been suggested, for the S- ΔE_{2000} maximum error.

In order to better compare the two models and have an overview of our investigations, the results from chapter 3 and 4 have been summed up in chapter 6. But first in chapter 5, by means of the two models, it is investigated if the algorithm can depict the eye sensitivity and colour discrimination in some way.

5.Chapter 5: Noise Scaling as a Description of the Eye Sensitivity

The investigation of the visual noise measurement and the S-CIELabDE2000 models, in chapter 3 and 4, shows that the algorithm of the human visual system is performing quite good for noise evaluation of uniform patches. In order to get a more accurate idea of how well the algorithm describes the human visual system, the quantification of noise is scaled as a function of noise input as a colour difference for the colours red, green, blue, cyan, magenta, and yellow, and for each kind of noise input.

5.1 Visual Noise as a Function of the Noise Input

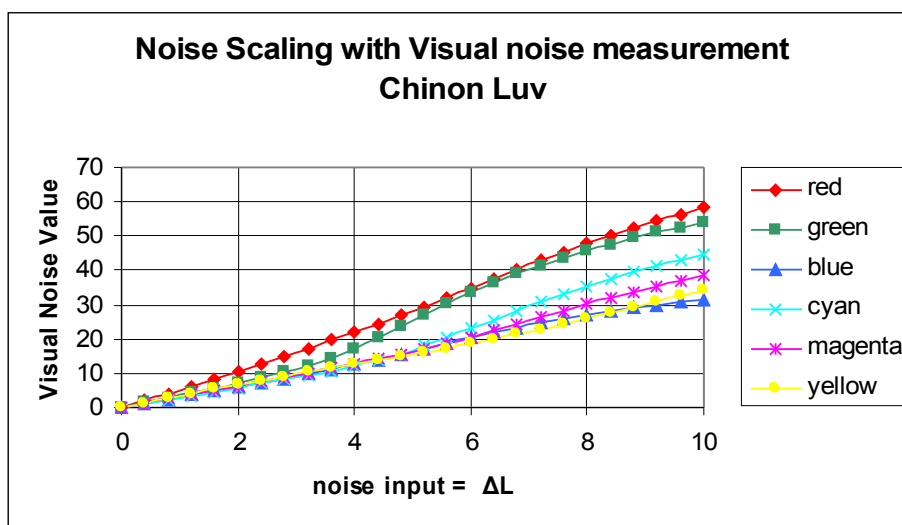
Here, not only are the threshold images evaluated with the models, but also the entire noisy images generated by Shiraz with steps of $\Delta E = \Delta L = 0,4$ for noise input in the luminance channel and steps of $\Delta E = \Delta C = \Delta h = 0,6$ for noise input in the chroma and hue channel. Because both models perform well for uniform patches, the following colours have been chosen: red, green, blue, cyan, magenta and yellow. So these noisy images have been evaluated with the Photoshop® plugin and with Chinon for both formulae (Lab and Luv), as well as with the S-CIELabDE2000 formula.

Here only the Chinon's graphs are shown and only the results for the visual noise formula along the Luv axes for several reasons. First because the Matlab® implementation performed better than the Photoshop® Plug-in. Second because the visual noise formula was actually developed for the CIELuv1976 colour space, although it has also been investigated with a visual noise formula based on the CIELab1976, which also performs quite well. Finally, although the S-CIELabDe2000 model performs well for uniform patches, it was actually developed to be able to deal with complex spatial frequency patterns.

But note that the noise scaling graphs for the Photoshop® Plug-in, the Matlab® implementation with the formula CIELab1976 and the S-CIELabDE2000 model have been reported in the appendix E.

5.1.1 Visual Noise Scaling along the Luminance Channel

Graph 5.01: Scaling of the visual noise value in function of the noise input along the luminance channel.



The noise input is from $\Delta E = \Delta L = 0$ to $\Delta E = \Delta L = 10$ and is added in steps of $\Delta E = \Delta L = 0,4$. The scaling of the visual noise values depends on the colours: from 0 (for no noise input) to 30 for blue to 60 for red and green. The other four colours have their maximum noise values (for a $\Delta E = 10$) in a range from 30 to 45.

The fact that the modulation of the visual noise values is different for the colours could reflect the eye's sensitivity and its discrimination's behaviour. The eye seems to be the most sensitive for red and green, and the least for blue and yellow. This means that the eye would better discriminate luminance differences for red colours than for yellow colours.

The graph 5.01 can also explain the singular behaviour for the determination of the visual

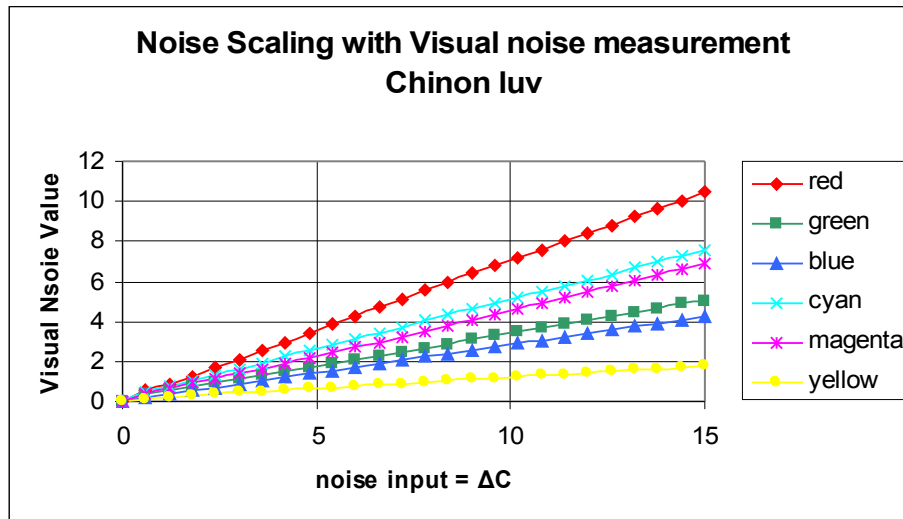
noise value of the threshold image of red, which had a very high visual noise value in comparison to the mean visual noise value over the other threshold images (over 1 unit count) [paragraph 3.2.1]. The function for red shows the biggest slope: a small luminance difference as noise input implies a big difference of the visual noise value.

As it has already be noticed, the noise input of the luminance channel is almost the same for all the threshold images, from 0,4 to 0,5, and 0,6 for red. Putting the Shiraz's slider above the setting of 1,5 unit is already showing a clear noise pattern. The slider steps of luminance noise input are perhaps too coarse: $\Delta E = \Delta L = 0,2$ with a maximum value of $\Delta E = 10$, which is significantly too high. Although the variance for the determination of the threshold images for the luminance noise input is very low, the scaling of the noise input $\Delta E = \Delta L$ could be more precise. This would allow a more precise determination of the threshold and consequently of the visual noise value. Doing so could maybe avoid a too high visual noise value for red, as mentioned in the previous paragraph.

It could be assumed that the different modulation of the scaling of the different colours could depict the eye's sensitivity. However, the noise input determined for the threshold images are similar, so no conclusion can be made about this assumption yet.

5.1.2 Visual Noise Scaling along the Chroma Channel

Graph 5.02: Visual noise value in function of the noise input in the chroma channel



The chroma noise input is scaled from $\Delta E = \Delta C = 0$ to $\Delta E = \Delta C = 15$ and is added in steps of $\Delta E = \Delta C = 0,6$. Although the colour's difference is higher for chroma than for luminance, the scaling of the visual noise is smaller (11 for the maximum value of red – which is less than the half of the smallest scaling in luminance for blue with 30 - and only 3 for the maximum values of yellow). This matches with the behaviour of the eye, which discriminates the chroma's differences a lot worse than the luminance's differences. This is in accordance with the high variances for the determination of the threshold images and the higher values of colour difference for the threshold images for the chroma channel than for the luminance channel. This observation is also made by Nicole Kidawa and Christina Simon [11].

According to the graph 5.02, the red, cyan, magenta and green colours have the highest visual noise scaling. This means that the eye would better discriminate chroma differences for these colours, than for blue and yellow. In order to check if this a reliable statement, the required noise input for the threshold images is compared with the slope of the curves.

Table 5.01 shows the setting of the Shiraz slider for noise input for the threshold images: the smaller the colour difference input the more sensitive the eye is for the specific colour. For each colour, the noise input is ranked from most sensitive to least sensitive. The noise scaling curves is also ranked from most sensitive (having the highest slope) to least sensitive (having the lowest slope) for the three variants of the visual noise measurement model and the S-CIELabDE2000 model.

Table 5.01: noise input in the chroma channel for the threshold images and corresponding ranking from the smallest noise input to the highest, as well as ranking of the slope of the curves for the tested colours from the highest to the lowest.

Colour	Noise input ΔC	Ranking of the noise input	Visual noise model			S-CIELabDE 2000
			Photoshop	Chinon Luv	Chinon Lab	
red	4,3	2	1	1	1	2
green	10,5	5	4	4	3	4
blue	4,1	1	3	5	5	3
cyan	5,2	3	5	2	1	1
magenta	5,6	4	2	3	3	5
yellow	15	6	6	6	5	6

For the ranking of Chinon with the formula Lab, red and cyan were having the same slope as well as green and magenta, and yellow and blue, that's why they are ranked with same number.

According to the noise input for the threshold images, which is considered as reference for the comparison, the eye is actually the most sensitive for red, blue, cyan and magenta and less for green and yellow. There is no graph which would match this ranking. For the red, blue, cyan and magenta colour, this may be explained, that the noise input is very similar for the threshold images, so some imprecisions could be tolerable. Moreover the graphs all have their own ranking with the tendency that yellow has the lowest slope and red the highest, which matches with the noise input ranking.

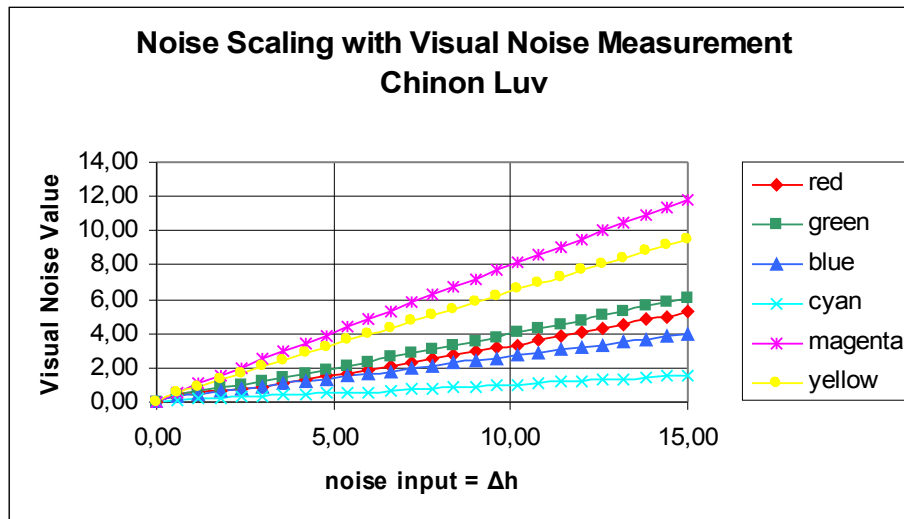
The fact that the maximum scaling of the visual noise values of yellow reaches only 1,75 (which is smaller than the mean visual noise value for chroma of 1,95) is in accordance with the fact that the tested persons doubted to see noise at all. Indeed the visual noise values have the tendency to grow very slowly and eventually become constant. Consequently whatever the noise input, it is difficult to tell if there was some change in the colour difference or not. This explains the difficulty of the tested person to tell exactly when the noise threshold appears (bigger variance for the setting of the noise input for the yellow colour for example 15,15).

To conclude, no scaling of the noise with both model and variants of the visual noise measurement model matches totally with the ranking of the noise input for the threshold images. However, there are some similarities. This shows that the noise scaling with the human visual algorithm tends to be only a coarse description of eye discrimination for chroma.

5.1.3 Visual Noise Scaling along the Hue Channel

Analogue observations done in the precedent paragraph can be made for noise input in the hue channel.

Graph 5.03: Visual noise value in function of the noise input along the hue channel



Here also the hue's difference goes until $\Delta E = \Delta h = 15$ and is added in steps of $\Delta E = \Delta L = 0,6$. The visual noise scaling is twice smaller for the highest hue scaling (magenta) than the smallest luminance scaling (blue). This observation matches with the fact that the eye is more sensitive to luminance variations than colour ones and, in this case, hue differences.

According to the curves' slopes, for variations in hue, the eye would have the best discrimination in magenta, followed by yellow, then by green, red and blue, and at last by cyan. In table 5.02 the same ranking as in table 5.01 has been done, but this time for noise input in the hue channel.

Table 5.02: noise input in the hue channel for the threshold images and corresponding ranking from the smallest noise input to the highest, as well as ranking of the slope of the curves for the tested colours from the highest to the lowest.

Colour	Noise input Δh	Ranking of the noise input	Visual noise model			S-CIELabDE 2000
			Photoshop	Chinon Luv	Chinon Lab	
red	7,9	5	4	4	4	2
green	5,8	2	3	3	3	4
blue	6,2	4	5	5	5	5
cyan	11,2	6	6	6	6	6
magenta	2,8	1	1	1	1	3
yellow	5,9	3	2	2	2	1

According to the noise input for the threshold images, which is considered as reference for the comparison, the eye is actually the most sensitive for magenta, then green, yellow and blue and at last for red and cyan. Here the three variants of the visual noise measurement model are all having the same ranking of the slopes. And it can be assumed that it matches the ranking of the noise input. Indeed green and yellow are inverted as well as red and blue, but in both case the noise input value Δh between the two pairs of colours are very similar, which can lie in the measurement of the noise input threshold and which is tolerable.

That is why the visual noise scaling with the visual noise measurement model can represent, to some extent, the eye's sensitivity and colour discrimination for hue.

5.1.4 Comparing Noise Scaling and Facility to determine Threshold Images

As it has already been noticed for chroma, the higher the colour difference $\Delta E = \Delta C$ as noise input, the higher the variances are by determining the threshold image. This means that the higher the colour difference gets, the more difficult it is to determine an exact threshold image.

The following table shows the values of the graph 5.03 - the visual noise values in function of the noise input in the hue channel. The cell filled with colour corresponds to the determined threshold image.

Table 5.03 contains the data corresponding to the graph 5.03 for the scaling of noise input in the hue channel.

Δh	VN red	VN green	VN blue	VN cyan	VN magenta	VN yellow
0,00	0,00	0,00	0,00	0,00	0,00	0,00
0,60	0,47	0,43	0,29	0,13	0,56	0,54
1,20	0,52	0,61	0,46	0,19	1,05	0,93
1,80	0,62	0,83	0,61	0,25	1,54	1,32
2,40	0,75	1,04	0,76	0,32	2,01	1,70
3,00	0,89	1,25	0,92	0,38	2,48	2,08
3,60	1,13	1,46	1,08	0,43	2,97	2,46
4,20	1,31	1,68	1,24	0,48	3,43	2,85
4,80	1,50	1,90	1,38	0,52	3,91	3,21
5,40	1,70	2,13	1,52	0,56	4,39	3,59
6,00	1,92	2,36	1,68	0,61	4,86	3,96
6,60	2,11	2,61	1,81	0,65	5,34	4,33
7,20	2,30	2,84	1,98	0,72	5,81	4,71
7,80	2,53	3,07	2,11	0,78	6,27	5,08
8,40	2,73	3,31	2,27	0,84	6,74	5,45
9,00	2,98	3,55	2,41	0,90	7,22	5,82
9,60	3,15	3,80	2,57	0,96	7,67	6,20
10,20	3,36	4,05	2,72	1,03	8,15	6,58
10,80	3,61	4,29	2,88	1,08	8,61	6,92
11,40	3,83	4,53	3,04	1,16	9,06	7,30
12,00	4,04	4,78	3,17	1,24	9,53	7,67
12,60	4,30	5,02	3,33	1,29	9,99	8,04
13,20	4,54	5,31	3,50	1,36	10,45	8,40
13,80	4,80	5,57	3,64	1,44	10,92	8,78
14,40	5,01	5,83	3,81	1,52	11,36	9,14
15,00	5,28	6,09	3,95	1,60	11,79	9,50

Relying on the table 3.04, the noise input $\Delta E = \Delta h$ was 5,9 for yellow and 11,2 for cyan. The hue difference here is obviously more difficult to detect for cyan than for yellow. As a matter of fact, the variance to determine the noise image threshold is 2,71 for yellow and 12,72 for cyan. This relation between high variance for determining the threshold images with the difficulty to detect it can be highlighted thanks to the analysis of the table 5.03.

Here relying on table 5.03, it can be noticed that because of the different scaling of the visual noise value for the different colours, an error on the determination of the threshold images (ΔE value) does not have the same impact on the visual noise value. An error of a $\Delta E = 1,2$ would lead to a ΔVN of 1 for yellow while for cyan only to a ΔVN of 0,2. But as it has been just reported before, the image threshold for the cyan was more difficult to determine with accuracy. So the imprecision is, in this case, higher but has a smaller impact.

The same observations can be made for the noise input in chroma.

5.2 Noise Scaling between the Chroma and Hue Noise Input

The former investigations show that the noise scaling with the human visual algorithm is not always able to precisely describe the eye's sensitivity over the different colours for each noise input channel: luminance and chroma are coarse description, hue matches more precisely the eye sensitivity. Here the noise scaling is not compared between the colour for one noise input channel, but for each colour the noise scaling is compared between the luminance, chroma and hue channel.

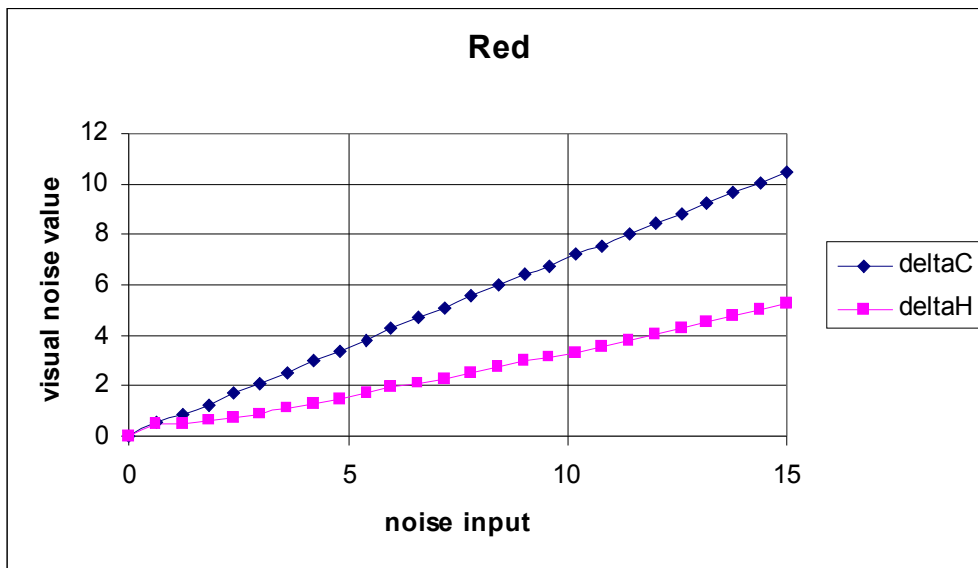
When comparing the visual noise scaling with the graph 3.01. 3.02 and 3.03, the luminance channel had a higher scaling for the visual noise value (5 to 10 times higher), although the maximum luminance noise input is $\Delta L=10$, while for chroma and hue it is $\Delta C=\Delta h=15$. Moreover the noise input of luminance for threshold images is smaller (in the range of 0,5) than the noise input of the chroma and hue (between 3 and 15).

Both observations contribute to the statement that the eye is more sensitive for differences in the luminance channel than in the colours channel, and this matches with the human eye sensitivity characteristics.

Since the visual noise scaling of the chroma and hue are more similar, it is more difficult to tell in which case the eye is more sensible in hue or chroma depending on the colour. The slopes of the visual noise scaling are compared between chroma and hue for each colour. For example, the graph 5.04 shows the noise scaling with Chinon with the Luv formula between the chroma and hue noise input for the colour red.

The same graphs have been done for the five other colours: green, blue, cyan, magenta and yellow. They have also been done for each variant of the visual noise measurement model (Photoshop® Plug-in, Chinon with the Luv and Lab formula) and for the S-CIELabDE2000 model.

Graph 5.04: Visual noise value from Luv Chinon in function of the noise input for chroma and hue difference for the colour red.



The graph 5.04 shows that for red the eye should be more sensible for colour difference in chroma than in hue, since the slope of the noise scaling is higher for chroma than for hue.

In table 5.04, for each colour, the noise input for the threshold is reported as a colour difference for chroma and hue. The comparison between both channels for each colour tells if the eye is more sensitive for chroma or for hue. The smaller the noise input, the more sensitive the eye is. The comparison between the slope of chroma and hue for each colour and each model has been reported. The higher the slope of the visual noise scaling, the more sensitive should be the eye.

Table 5.04: Comparison of the noise input in chroma and in hue for the threshold images for the colour red, green, blue, cyan, magenta and yellow, and comparison between the slope of chroma and hue for each colour for the three variants of the visual noise measurement model and the S-CIELabDE2000 model.

Colour	Noise input		Comparison of the noise input	visual noise measurement			S-CIELabDE 2000
	ΔC	Δh		Photoshop Plug-in	Chinon Luv	Chinon Lab	
red	4,3	7,9	C > H	C > H	C > H	C > H	H > C
green	10,5	5,8	H > C	H > C	H > C	H > C	H > C
blue	4,1	6,2	C > H	C > H	equal	H > C	H > C
cyan	5,2	11,2	C > H	equal	C > H	C > H	C > H
magenta	5,6	2,8	H > C	H > C	H > C	H > C	H > C
yellow	15	5,9	H > C	H > C	H > C	H > C	H > C

According to the experimental results of the noise input, the eye is more sensitive in chroma than in hue for the colour: green, magenta and yellow. At the same time, it is more sensitive in hue than in chroma for the colour: red, blue and cyan

The noise input for the threshold images, which is taken as reference, is compared with the ranking of the slope of the noise scaling between the chroma and hue for each colour (in this case: red, green, blue, cyan, magenta, yellow):

The Chinon Lab variant performs the best, matching exactly with the comparison order of the noise input. The Chinon Luv variant assumes the eye sensitivity between chroma and hue for blue as equal, while the noise input differs with 2 ΔE units. This can still be regarded as an acceptable range, and that is why the Chinon Luv variant could also perform quite well. The Photoshop® Plug-in assumes that the sensitivity between hue and chroma for cyan is equal, although the noise input differs by 6 ΔE units, and the S-CIELabDE2000 model inverts the sensitivities for red, although the noise input differs by 4 ΔE units.

To conclude, the used human visual algorithm performs good in describing the eye's sensitivity between the luminance, chroma and hue channel for each colour. It shows only slight imprecisions depending with which variants of the model the algorithm has been implemented.

5.3 Brief conclusion

In order to evaluate how good the used human visual algorithm describes and matches with the eye sensitivity, the ranking of the noise input as colour difference for the threshold images is compared with the ranking of the slopes of the visual noise scaling with the human visual scaling. This is firstly done for each kind of noise input (luminance, chroma, and hue) over the colours, and then done for each colours over the three kind of noise input.

Firstly it has been noticed that the ranking of the slopes between the colours for each noise input channel varies depending on the model, sometimes showing some similarities for the slopes' ranking. But comparing it to the ranking of the noise input for the threshold images, there was no significant match for chroma and no real conclusion for luminance could be done. For hue, the visual noise measurement model showed a satisfying matching, and the visual noise scaling with the used human visual algorithm could be regarded as a good description of the eyes sensitivity for hue differences.

Secondly it has be noticed that the magnitude of the slope of the noise scaled with luminance noise input were far higher (5 to 10 times higher) than the one scaled with the chroma or hue noise input. This is fulfilled by the two models. This matches with the fact that the eye is more sensitive for luminance differences than for colour differences. Then the eye's sensitivity between the hue and chroma was compared for each colour. Comparing the ranking of the slopes with the ranking of the noise input values for the threshold, the rankings were matching in almost every case, especially the best for the Matlab® implementation of the visual noise with the Lab formula.

To conclude, the algorithm is not accurate enough in order to describe the eye's sensitivity between the colours in each noise input channel: luminance, chroma and hue. But it is already describing precisely the eye's sensitivity between the noise input channel for each colour. These imprecisions may still lie in an inaccurate weighting of the chromatic contrast sensitivity function.

6 .Chapter 6: Conclusion

6.1 Quantification of noise: The Stand of the Research and the new Approach: an Algorithm describing the Human Visual System

6.1.1 Stand of the Research

Since noise is a prevalent phenomena in digital imaging, a method to quantify colour noise in order to make reliable statement about the seen image quality has to be found and developed.

The signal to noise ratio method proposed in the normative part of the *ISO 15739:2002(E)* paper [16] is not giving acceptable results. In looking at the example of the two grey patches from chapter 1, for two different kind of noise, one being more disturbing than the other, the signal to noise ratio method evaluates them with the same value. This does not match the visual impression, so the signal to noise ratio can not be considered as reliable and other methods have to be investigated.

In the diploma thesis of Michael Bantel and Jan Fischer, as well as of Nicole Kidawa and Christina Simon, with the self java® implemented software, Shiraz, the colour noise has been investigated, being quantified as a colour difference from the CIELabDE1976, 1994 and 2000. This approach relies on the assumption that the CIELab colour space should be a visually uniform space to describe colour. Actually, as mentioned by some technical papers [19] [22], this is not the case, and as the results of these diploma thesis have shown, the quantification of colour noise matching the eye impression using the CIELab colour space has not been successful.

6.1.2 The new Approach: an Algorithm describing the Human Visual System

The new method investigated in this diploma thesis relies on the implementation of an algorithm trying to describe the human visual system. After doing a chromatic adaptation, the tristimulus values of a the image pixels are transferred into the opponent colour space, which are then spatially filtered with the contrast sensitivity function. This describes how the human visual system processes the colour signals. The filtered opponent colour signals are then transferred back to filtered tristimulus values, which can then be transformed in colour space that describes the way in which the eye recognises colour .Since the eye interprets colour in terms of luminance, chroma and hue,; CIELuv1976 or CIELab1976 (CIELCh1976 is the polar representation) are used and, from here the colour noise can finally be quantified.

Two models are based on this algorithm to quantify the colour noise:

- Firstly the visual noise measurement model, which as it is proposed in the appendix C of the *ISO 15739:2002(E)* [16] and the Hung Paper [17], which then evaluates the noise as a so called visual noise value, is the weighted sum of the standard deviations along the L^* , u^* and v^* axes from the CIELuv1976 colour space for all the image pixels of a uniform colour patch.
- Secondly the S-CIELabDE2000 model, which then evaluate the noise as a colour difference pixel by pixel between a noisy image and its corresponding noise free image.

6.2 Results of the Noise Quantification with the two Models

Experiments performed on many observers with the Shiraz software have permitted to define threshold images. These have been determined as images containing a just noticeable noise impression for different kind of noise input as colour difference in the luminance, chroma and hue channel. The assumption is that the threshold images stand for the same noise impression, so a reliable method quantifying the colour noise in a visual manner should evaluate the threshold image with the same value. The threshold images have been run through both models.

6.2.1 Quantification of Noise with the Visual Noise Measurement Model

6.2.1.1 Tools of the Visual Noise Measurement Model

The visual noise measurement model can be run as a Plug-in in Photoshop®, but has also been implemented in Matlab® as the weighted sum of the standard deviations along the L^* , u^* and v^* axes from the CIELuv1976 colour space. It has also been evaluated along the L^* , a^* and b^* axes of the CIELab1976 colour space. The formula for the visual noise value has actually been developed for the CIELuv1976 colour space, because noise can be seen as local colour difference. In addition some technical papers recommend the use of the CIELuv1976 rather than the CIELab1976 for micro colour differences [paragraph 1.1.3.2].

The differences in the algorithm between the Photoshop® Plug-in and the Matlab® implementation of the visual noise measurement model are due to the use of a different contrast sensitivity function and the chromatic adaptation matrix [paragraph 2.5.2].

The threshold images have been run through the three variant tools of the visual noise measurement model.

6.2.1.2 Evaluation of the Threshold Images with the Visual Noise Measurement Model.

Testing the algorithm with two different tools, the Matlab® implementation gives better results by getting similar visual noise value for the threshold images. This may be due to the use of a different contrast sensitivity function, with the one used in Matlab®, proposed by Fairchild [20], being more accurate.

There are no real differences between the implementation of visual noise value formula from the CIELuv1976 or CIELab1976 colour space. Both give satisfying results [paragraph 3.2]. The differences between both spaces have been discussed previously [paragraph 3.1.1.3], each having their own characteristics, but none perform better than

the other. The choice of the CIELuv1976 colour space can be preferred, since the visual noise formula has been implemented for the use of this colour space.

The limitation of the model is that it only evaluates the noise for uniform colour patches. That is why the S-CIELabDE2000 model has also been investigated for quantification of noise as a colour difference.

6.2.2 Noise Quantification with the S-CIELabDE2000 Model

The model can evaluate spatially complex images. In this case, the threshold images are rectangular vertical frequency patterns from a predefined colour with different contrast levels. But since the evaluation is based on a colour difference, it needs a noise free image and a noisy image for comparison. In fact, the colour difference ΔE obtained between the noise-free image and the noisy image, is an error image. This stands for the "image of the noise pattern", and is then used to quantify the noise.

6.2.2.1 Tool of the S-CIELabDE2000 Model

The S-CIELabDE2000 model has been implemented in Matlab®.

6.2.2.2 Evaluation of the Threshold images with the S-CIELabDE200 Model

According to the results, the S-CIELabDE2000 model seems at first to perform quite well in evaluating the spatially complex patterned threshold images with similar colour difference values. But investigating further the colour difference in terms of the magnitude of the spatial patterns, and of the contrast, it can be noticed that the colour difference value is getting 1 ΔE unit higher when the contrast is increased to 20%.

So this is not matching the expectations, and this shows the limitations of the accuracy of the model to quantify colour difference in a visual way for complex images. But it is interesting to notice that investigating the colour difference of the uniform colour patches, the model achieves similar colour difference values.

6.2.3 Conclusion for both Models

To conclude, both models perform well in quantify the threshold images as uniform colour patches with similar values. Though it is limited to uniform colour surfaces, the algorithm used to simulate the processing of colours in the human visual system seems to be valid. If it is the case, this algorithm should be able to describe that the eye is more sensitive to luminance differences than for colour differences, chroma or hue.

6.3 Does the human visual Algorithm used match the Eye's Sensitivity?

The noise quantification, with the human visual algorithm, has been scaled in terms of the noise input in luminance, chroma and hue (for the colours: red, green, blue, cyan, magenta and yellow).

6.3.1 Eye's Sensitivity between Colours in term of Luminance, Chroma, and Hue

The ranking of the required noise input for the threshold image is compared to the ranking of the slope of the curves of the noise scaling. This is done for each kind of noise input channel between the colours. The ranking of the required noise input is considered as the reference.

For luminance, the ranking of the required noise input is too similar to make any significant conclusions. For chroma, the ranking of the curves' slope does not always match the ranking of the required noise input of the threshold images. In this case, the

algorithm can only be seen as a coarse description of the eye's sensitivity. For hue, the ranking of the curves' slope for the visual noise measurement almost matches the ranking of the required noise input for threshold images for all models. In this case the algorithm used in the visual noise measurement can describe the eye sensitivity for hue differences between the colours.

6.3.2 Eye's Sensitivity between Luminance, Chroma and Hue in term of Colour

The ranking of the required noise input for the threshold images is compared to the ranking of the slope of the curves of the noise scaling. This is done between the three kinds of noise input, for each colour. The ranking of the noise input is considered as the reference.

The ranking of the slope of the noise scaling matches the ranking of the required noise input. This is the case for both models with only small imprecisions, the Matlab® implementation of the visual noise measurement with the visual noise formula derived from Lab having the best results. It can be concluded that the algorithm can describe the sensitivity of the eye to interpret colour difference in terms of luminance, chroma and hue, for each specific colour depending on the hue of the colour.

6.3.3 Brief conclusion

The eye's sensitivity depends on the hue of the colour. Although they are not being precise enough, these analyses show that the algorithm describing the human visual system is valid, although it is still imprecise and can be improved.

6.4 Improvement of the Measurements and of the Method

6.4.1 Improvement of the Measurements

Working with Shiraz in doing the experiments, it can be concluded that the scaling of the ΔE could still be improved [paragraph 3.2]. It has been noticed that, for noise input in the luminance channel the threshold image are never more than $\Delta E = \Delta L = 1$ and that the required noise input for the threshold images are all very similar in the range of $\Delta E = \Delta L = 0,4$ to $0,6$. So a maximum value of 2 for $\Delta E = \Delta L$ would be sufficient and would allow the measurements to be more accurate, though the variance are already very small (up to $0,03$).

While for the noise input in the chroma and hue channel, for few colours (for yellow and skin respectively), the slider has been set to the maximum value of $\Delta E = 15$. However, noise could not be perceptible yet, so we conclude that the maximum value could be set higher (set to $\Delta E = \Delta C = \Delta h = 20$ or 25).

The way the experiments were conducted could be handled differently. This implies the question of the definition of the noise threshold. In this experiment, the observers were asked to choose the image in which they think the noise appears. They were free to shift the slider back and forth. Doing this they could get an impression of what the noise could look like. Other approaches could lead to different results.

One idea would be to build two viewing field in the program: one showing the noise input, and another showing a corresponding noise free image. Doing this the tested-persons could have a direct comparison and detect noise perhaps more easily. They would not have to rely on their memory, and should not have to shift the slider back and forth. Another idea would be that the slider should not be allowed to move back on an image with less noise. Doing so may not lead to determine threshold images describing the just noticeable difference, but maybe threshold images describing the just disturbing difference.

6.4.2 Improvement of the Human Visual Algorithm

For both models, the quantification of noise in a visual manner is only valid for uniform colour patches. And still there are some variations over the quantification of noise for the threshold images: they do not get exactly the same noise quantification. This can be due that the used human visual algorithm can not perfectly describe the human visual system, which is quiet complex and always adapting itself to its environment. There are many factors, that are still uncertain:

Uncertainties for the used human visual algorithm itself:

- The contrast sensitivity function has not be standardized yet. As shown in figure 2.08 [paragraph 2.4.2], the contrast sensitivity function changes its shape in terms of many parameters. So the contrast sensitivity function should be used and defined for specific parameters depending on the environment and the context.
- The contrast sensitivity function should be zero for the zero cycles-per-degree component. This corresponds to the DC-component since there is no spatial pattern and consequently no contrast. The DC-component contains essentially the mean value of the image channel and, for simple patches, this mean value is the value of the patch itself [20 p430]. So in order to keep the main information of the image contained in the DC-component, the contrast sensitivity function has been normalized to 1 for zero cycle-per-degree. But this may not match the actual filtering occurring in the eye since there is no filtering occurring for zero cycles-per-degree. It could be suggested to apply the filtering in a different way [37]: being in the frequency domain of the opponent colour signals, first the DC-component could be substracted, so it is set to zero. It can be then filtered with the contrast sensitivity function having an amplitude set to zero for the component zero cycles-per-degree. The DC-component could be added back afterwards.
- As shown in appendix D, there are different proposed transform matrices for chromatic adaptation which differ slightly from one another. Which one to use depends on ones own purpose, because although the von Kries and the Bradford are recommended, there is no standardisation.

- The same observation can be made for the use of the transformation matrix from the tristimulus values to the opponent colour space coordinates. There are several proposed matrices [**paragraph 2.5.2**] and [**Appendix D2**], some seem to be invalid (see results [**Appendix D25**]). But there are also no standardised recommendations for which one to use.

Uncertainties of the visual noise measurement model:

- the weights of the standard deviation of the $L^*u^*v^*$ visual noise formula: These have been determined with an empirical approach [**paragraph 3.1.1**] for the purpose of the visual noise measurement model. The settings of the experiments are unknown. So, like the contrast sensitivity function, these weightings may be defined for a specific environmental setting and may actually vary with the lighting environment characteristic. So, depending on the context, the weighting may change and always be readjusted depending on the environment.

Uncertainties of the S-CIELabDE2000 model:

- According to the Luo et al's paper [**23**] the CIE has been improving the uniformity of the $CIE L^*a^*b^*DE$ formula. The stand of the research has been reached with the CIELabDE2000 formula until now.
- The CIELabDE formula contains the parametric weights K_L, K_C, K_H [**paragraph 4.1, formula 4.25**], which can be adjusted to different viewing parameters such as textures, backgrounds, separations, etc... for the lightness, chroma, and hue components [**23**]. For most imaging applications, these weights are unknown, and like in the present case, they should be all set to 1,0. Developing a better understanding of how to choose the right weights would maybe improve the accuracy of the quantification.
- The median value seems the most appropriate value in order to describe the observed visual noise. However, this may be only in this present case and for the same specific Gaussian pattern of noise. For another kind of noise, maybe another statistic would perform better.

There is no doubt that a better and more precise cognition of the human visual system would improve the human visual algorithm. Consequently, this could improve the quantification of noise matching the visual impression. However, until now, this new approach has been the most successful when compared to the former methods used.

Still, the two models are giving satisfactory results only for the evaluation of uniform patches. The quantification of perception of noise in complex images is not yet suitable with the human visual algorithm used.

7 .Bibliography

- [1] Loos, H. 1989: Farbmessung Grundlagen der Farbmetrik und ihre Anwendungsbereiche in der Druckindustrie, Bielefeld.
- [2] Sève, R. 1996: Physique de la couleur, de l'apparence colorée à la technique colorimétrique, Masson, Paris.
- [3] Fairchild, Mark D. 2005: Color Appearance Models, second edition, John Wiley & Sons, Chichester, West Sussex.
- [4] Hunt, RWG. 1987: Measuring Colour, John Wiley and Sons, Chichester, West Sussex. Measuring Colour, R.W.G. Hunt, Ellis Horwood, Series, Applied Science and Industrial Technology, 1989 p71
- [5] Berns, Roy S. 2000: Billmeyer and Saltzman's Principles of Color Technology, third edition, John Wiley & Sons.
- [6] Wandell, A. Brian. 1995: Foundations of Vision, Sinauer Associates, Inc. Publishers, Sunderland, Massachusetts.
- [7] Hunt, RWG, 2004: The Reproduction of Colour, sixth Edition, John Wiley & Sons, Chichester, West Sussex.
- [8] Wyszecki, G and Stiles, W.S., 1967 Color Science: Concepts and Methods, Quantitative Data and Formulae, first edition, John Wiley & Sons. pp
- [9] Roberts, David, 2002: Signals and Perception, The Fundamentals of Human Sensation, Palgrave MacMillan, Hampshire and New York.
- [10] Untersuchung der Farbabstandsformeln des CIELAB Farbraums auf ihre Eignung, Farbrauschen quantitativ und physiologisch richtig zu beschreiben, Fischer. J, Bantel. M, Fachbereich Photoingenieurwesen an der Fachhochschule Köln, Juli 2002
- [11] Perception of noise depending on spatial frequency and contrast with the aid of the CIE-Lab color space, Kidawa. N, Simon. K, Image Science and Media Technology University of Applied Sciences Cologne, July 2003.
- [12] Wikipedia, the free encyclopedia: http://en.wikipedia.org/wiki/Standard_deviation
12.07.06
- [13] Human Color Vision, 2nd Edition, Peter K. Kaiser and Robert M. Boyton, Optical Society of America

- [14] Java 2 Grundlagen und Einführung, RRZN Regionales Rechenzentrum für Niedersachsen / Universität Hannover, erste Auflage, April 2001.
- [15] Sun Microsystems, Sun Developer Network (SDN), Java Technology, <http://java.sun.com/>, 12.12.05 – 30.06.06
- [16] ISO Norm: ISO/FDIS 15739:2002(E), Secretariat ISO/TC42, International Imaging Industry (I3A), 550 Mamoroneck Avenue, Harrison, NY 10528-1615 USA
- [17] Kozo Aoyama, Hirochimi Enomoto, Po-Chieh Hung, An evaluation of scanner noise based upon a human visual model, Konica Corporation, R&D Center, Tokyo, Japan
- [18] Operating instructions of the Photoshop Plugin: Noise Measurements Plug-in ver.1.20 User's Guide, November 8th, 1999, Konica Corporation.
- [19] The CIE 1976 color-difference formulae, Robertson A.R., Color Research and application/Inter Society Color Council; Colour Group, New York; Wiley; 1997; 2,1; pp.7-11.
- [20] A Top Down Description of S-CIELAB and CIEDE2000, Garrett M. Johnson, Mark D. Fairchild. Munsell Color Science Laboratory, Chester F. Carlson Center for Imaging Science, Rochester Institute of Technology. Rochester, NY, 14623, Volume 28, Number 6, December 2003.
- [21] Toyohiko Hatada, O Plus E, 63, pp. 78-85 (1985) in Japanese [Email Dr. Hung]
- [22] Historical development of CIE recommended color difference equations, Robertson, A. R., Color research and application, Wiley, New York, 1990, 15, 167-170.
- [23] The development of the CIE2000 colour difference formula: CIEDE2000, Luo, M.R., Cui, G., Rigg, B, Color research and application, Wiley, New York, 2001, 26, 340-350.
- [24] November 2002, Release 13 : Learning MATLAB 6.5, Student Version with Simulink, The MathWorks.
- [26] Wiley, 2004 : Computational Colour Science Using Matlab, Stephen Westland, University of Leeds UK, Caterina Ripamonti, University of Pennsylvania USA, Wiley.
- [27] Alasdair McAndrew, 2004: Introduction to digital Image Processing with Matlab®, Thomson Course Technology, Boston, Massachusetts.
- [28] Gonzalez, Rafael C.; Woods, Richard E.; Eddins, Steven L, 2004 : Digital Image

- Processing using Matlab®, Pearson Prentice Hall, Upper Saddle River, New Jersey.
- [29] The Mathworks Deutschland, MATLAB and Simulink for Technical Computing
<http://www.mathworks.de/>, 15.0206 – 30.06.06
 - [30] Stanford Vision and Imaging Science and Technologie S-CIELAB, Xuemei Zhang, A Spatial Extension to the CIE L*a*b* DeltaE Color Difference Metric Introduction to ScieLab: <http://white.stanford.edu/~brian/scielab/introduction.html>, 02.12.05
 - [31] Stanford Vision and Imaging Science and Technologie S-CIELAB: Zhang & Wandell, 1997: A spatial extension of CIELAB for digital color image reproduction, in: *SID Journal*. <http://white.stanford.edu/~brian/scielab/scielab3/scielab3.pdf>, 02.12.05
 - [32] Boynton-MacLeod Colour Space , Westland's Email.
 - [33] Imaging Science at RIT:
http://www.cis.rit.edu/people/faculty/johnson/pub/ciede_scielab.pdf, 02.12.05
 - [34] ICC.1:2001-04 :http://www.color.org/ICC_Minor_Revision_for_Web.pdf
 - [35] International Color Consortium Specification ICC.1:2004-10 (Profile version 4.2.0.0) [revision of ICC.1:2003-09]: <http://www.color.org/ICC1V42.pdf>
 - [36] Die JPEG Kompression, Sebastian Wickenburg, Aeneas Roach, Johannes Gross
http://www.mathematik.de/spudema/spudema_beaetraege/beitraege/rooch/nkap04.html
 - [37] The JPEG Still Picture Compression Standard, Gregory K. Wallace, Multimedia Engineering, Digital Equipment Corporation, Maynard, Massachusetts, Submitted in December 1991 for publication in the IEEE Transactions on Consumer Electronics.

8 .Declaration

Eidesstattliche Erklärung

Ich versichere hiermit, die vorgelegte Arbeit in dem gemeldeten Zeitraum ohne fremde Hilfe verfasst und mich keiner anderen als angegebenen Hilfsmittel und Quellen bedient zu haben.

Köln, den 15ten August 2006,

Johanna Kleinmann

Sperrvermerk

Die vorgelegte Arbeit unterliegt keinem Sperrvermerk.

Weitergabeerklärung

Ich erkläre hiermit mein Einverständnis, dass das vorliegende Exemplar meiner Diplomarbeit oder eine Kopie hiervon für wissenschaftliche Zwecke verwendet werden darf.

Köln, den 15ten August 2006,

Johanna Kleinmann

Danksagung

Ing. Svenja Schulz

Ing. Uwe Artmann

Msc. Lee Rankin

Prof. Dr. Po Chieh Hung

Dr. Dipl. Ing. Jean-Christophe Rioual

Dipl. Ing. Ronan Creach

Appendix, Table of Content

Appendix A: Shiraz, Settings and Results for the Determination of the Threshold Images.....	1
A1. Shiraz, a Java® Application.....	1
A11. How to Install Shiraz.....	1
A12. How to use Shiraz.....	2
A2. Settings of the Shiraz Experiments.....	3
A3. Results of the Threshold Images measured with Shiraz.....	3
Appendix B: Settings of the Photoshop® Plugin, Visual Noise Measurement.....	7
B1. How to install the Plugin.....	7
B2. How to run the Plugin.....	7
Appendix C: User Guide Chinon.....	11
C1. How to run Chinon, a Matlab® Application.....	11
C11. If you have a Matlab® Version with the Image Processing Toolbox.....	11
C12. If you do not have a Matlab® version.....	11
C121. First copy the Chinon Folder anywhere on your Computer.....	11
C122. Installation.....	11
C2. How to use Chinon.....	12
C21. Settings of Chinon.....	12
C22. How Chinon returns the Results.....	14
C23. Notice to avoid any Problems while running Chinon.....	15

Appendix D: Colour Transformation Matrices.....16

D1. Chromatic Adaptation Matrices to transfer the Tristimulus Values, X, Y and Z into the Cone Space L, M, and S..... 16

D11. von Kries Matrix..... 16

D12. Smith-Porkony cone space matrix..... 17

D13. Bradford Transformation..... 17

D14. The Hunt-Pointer-Estevéz Transformation..... 18

D15. the CIECAM02 Matrix..... 18

D16. Evaluation of the Matrices..... 19

D2. Matrix Transforms from the Tristimulus Values to the Opponent Colour Space Coordinates..... 20

D21. Matrix from the Photoshop® Plugin..... 20

D22. Matrix from the Konica® paper..... 20

D23. Matrix from the Photoshop® Plugin User Guide..... 21

D24. Matrix from the S-CIELabDE2000 Paper..... 21

D25. Evaluation of the Matrices..... 22

Appendix E: Visual Noise Scaling with the Human Visual Algorithm.... 23

E1. Results for the Visual Noise Measurement Model with the Photoshop® Plugin and Chinon with the Lab formula, and for the S-CIELabDE2000 model..... 23

E11.Noise Scaling along the Noise Input LCh for the Colours: Red, Green, Blue, Cyan and Blue..... 24

E111. Noise Input in the Luminance Channel..... 24

E112. Noise Input in the Chroma Channel..... 25

E113. Noise input in the Hue Channel..... 27

Appendix F: Investigation of the S-CIELabDE2000 Model.....29

F1. Cyan.....29

F2. Red.....30

F3. Mid-green.....30

F4. Light grey.....31

F5. Mid-green.....31

Appendix A: Shiraz, Settings and Results for the Determination of the Threshold Images

A1. Shiraz, a Java® Application

A11. How to Install Shiraz

Refer to the diploma thesis work of and to Nicole Kidawa and Christina Simon [11 pp46-49] in order to know how to install Shiraz

Shiraz has been written in the Java® programming language. To be able to run Shiraz, following Java® kits have to be installed first [11]:

- jdk1.3.1_01 or j2sdk1.4.10_06
- java3D

which can be downloaded from the website: Sun Microsystems, Sun Developer Network (SDN), Java Technology: <http://java.sun.com>. [15]

Shiraz can be installed anywhere on the computer.

Since the new version of Shiraz3, by doing the experiment of noise, the actual viewed image with noise can be saved directly as tiff by clicking the button "save as tiff". There is no menu that opens to let the user choose the folder where it would like the images to be saved. That's why before doing the test, the user must ensure to set the folder where the images are going to be saved. This can be done as followed:

- go to the Shiraz3 folder, do a right click on the data "run.bat", then at the 7th line, type in the path of the folder where you would like the images to be saved, for example:

```
set dir="Z:\Shiraz39\images"
```

Moreover the first time you want to run Shiraz3, you will maybe need to compile it once (but if you did not change anything in the code, you should not have to do it). First right click on the data "build.bat", at the 6th line type in the path where the commando "javac" should be find, this should be in the "bin" folder of your jdk_* folder that you have previously installed:

```
c:\Programme\Java\jdk1.3.1_01\bin\javac ... (the rest of the commando should stay unchanged).
```

At last in order to be able to run Shiraz3, you need to set the path where the commando "java" can be found: right click on the data "run.bat", at the 8th line, type in the path where the commando can be found, this should also be in the "bin" folder of your jdk_* folder that you have previously installed:

```
C:\Programme\Java\jdk1.3.1_01\bin\java ... (the rest of the commando should stay unchanged).
```

To start Shiraz3, you can just double click on the data "run.bat" or with the command window go in the folder where Shiraz is installed, and then just type the order „run“. The window of the Shiraz program should open.

A12. How to use Shiraz

Refer to the diploma thesis work of Michael Bantel and Jan Fischer [10 pp-32-37 and pp71-78] and to the diploma thesis of Nicole Kidawa and Christina Simon [11 pp-50-58] in order to know how to use Shiraz.

A2. Settings of the Shiraz Experiments

In order to determine a set of threshold images for uniform patches, an experiment has been run with Shiraz in the context of this diploma thesis.

The experiment conditions are based on the work of the diploma thesis of Michael Bantel and Jan Fischer [10 pp15-17 and pp42-45] and of the diploma thesis of Christina Simon and Nicole Kidawa [11 pp34-39]:

- dark room
- monitor : LCD from Eizo ColorEdge CG19 (highest ΔE over the monitor surface has been measured to be 2,4).
- calibration of the monitor : attention has been paid on the brightness, the value was set to 140cd/m^2 , because higher value are much to bright for normal perception, $T_c = 5000\text{K}$, $\gamma = 2,2$.
- Viewing distance: 60 cm
- Monitor resolution: 1280x 1024 pixels
- 16 persons have been asked to take part to the test
- threshold has been defined as a detection threshold (when the noise was just seen), the tested-persons were allowed to shift the slider back and forth before choosing their image threshold.

A3. Results of the Threshold Images measured with Shiraz

Blue stands for impossible ΔE -values like 15 or 0, when noise was visible (it can be due to a mouse-click error). These values have just been thrown out of the analyse.

Red stands for a ΔE -value of 0 that has been replaced by a ΔE -value of 15, when no noise has been visible and the test person forgot to put the slider to the value for no noise $\Delta E=15$.

Yellow stands for noise, that has been visible very soon, but the slider was left to a ΔE -value of 0, so as default value $\Delta E=0,2$ has been set.

To generate the tiff threshold images in Shiraz3, the threshold values have been rounded to the first decimal.

Blue

ΔL :	0,4	0,6	0,2	0,2	0,8	0,2	0,4	0,2	0,6	0,4	0,4	0,4	0,4	0,4	0,2	0,4
Mean value:	0,39															
Variance:	0,03															
ΔC :	5,70	3,3	7,2	3,3	5,1	5,7	3,6	2,7	4,5	3,3	3,6	2,7	3	3	3	4,8
Mean value:	4,10															
Variance:	1,80															
Δh :	9,00	6	6	3,9	9	3,6	7,2	8,7	4,2	5,1	4,5	3,6	10,8	7,2	4,2	6
Mean Value:	6,19															
Variance:	5,07															

Brown

ΔL :	0,60	0,8	0,4	0,6	0,8	0,2	0,4	0,6	0,4	0,8	0,6	0,4	0,6	0,4	0,2	0,2
Mean value:	0,50															
Variance:	0,04															
ΔC :	4,20	6,3	4,5	2,7	5,4	1,8	4,5	6,6	3,9	4,2	3,6	5,4	5,7	4,8	2,7	2,7
Mean Value:	4,42															
Variance:	1,84															
Δh :	5,70	5,7	6	3,3	8,4	3,9	9,3	10,2	6,9	7,8	5,7	6,9	9,3	6,3	3,3	3,3
Mean value:	6,58															
Variance:	4,60															

Cyan

ΔL :	0,60	0,8	0,2	0,6	0,8	0,2	0,4	0,6	0,2	0,6	0,6	0,4	0,6	0,4	0,4	0,6
Mean value:	0,50															
Variance:	0,04															
ΔC :	5,70	6	4,8	7,2	5,4	3	7,2	7,8	2,4	1,2	4,8	6	6,6	4,5	4,5	4,5
Mean value:	5,19															
Variance:	3,68															
Δh :	7,80	15	7,2	8,4	11	15	14	13,2	11,1	15	9,9	13,2	11,1	15	2,7	9
Mean value:	11,16															
Variance:	12,71															

Dark grey

ΔL :	0,60	0,8	0,4	0,6	0,6	0,2	0,6	0,4	0,6	0,6	0,6	0,4	0,4	0,6	0,4	0,4
Mean Value:	0,51															
Variance:	0,02															
ΔC :	5,40	6	6	4,5	4,8	1,2	4,5	6,3	4,8	5,4	5,4	5,1	3,3	3,9	1,8	3,3
Mean Value:	4,48															
Variance:	2,14															
Delta Phi:	14,70	15	15	15	14	15	15	15	12,3	15	11,1	15	15	15	15	15
Mean value:	14,48															
Variance:	1,36															

Dark violet

ΔL :	0,60	0,6	0,2	0,4	0,6	0,2	0,4	0,4	0,6	0,6	0,4	0,2	0,4	0,6	0,2	0,2
Mean value:	0,41															
Variance:	0,03															
ΔC :	9,30	7,5	6	6	4,5	3	7,5	11,4	10,2	11,7	6,6	4,8	6,9	3,9	4,2	6
Mean value:	6,84															
Variance:	6,99															

Appendix A: Shiraz, Settings and Results for the Determination of the Threshold Images

Δh :	9,60	7,8	3	4,2	6,9	2,1	6,3	8,4	9,9	7,5	6	6,3	6,3	5,7	2,1	6,6
Mean value:	6,17															
Variance:	5,54															
Yellow																
ΔL :	0,60	0,6	0,2	0,6	0,4	0,2	0,6	0,6	0,4	0,8	0,6	0,6	1	0,6	0,4	0,6
Mean Value:	0,55															
Variance:	0,04															
ΔC :	15,00	15	15	15	8,4	15	15	15	3,9	15	9,6	6	6,9	12,3	12	15
Mean value:	12,11															
Variance:	15,15															
Δh :	6,90	6,9		4,2	4,2	3	6,3	7,8	5,4	6	7,5	6,6	6,9	7,8	2,7	5,7
Mean value:	5,86															
Variance:	2,72															
Skin1																
ΔL :	0,60	0,6	0,2	0,6	0,6	0,2	0,4	0,6	0,4	0,4	0,2	0,4	0,6	0,4	0,2	0,4
Mean value:	0,43															
Variance:	0,03															
ΔC :	4,50	3,6		2,1	3,3		4,5	6,9	4,8	3,9	5,4	3,3	3	3,3	2,7	3,6
Mean value:	3,92															
Variance:	1,50															
Δh :	15,00	15	15	8,1	7,8	6	15	15	15	15	8,7	15	7,5	15	10	15
Mean value:	12,39															
Variance:	12,72															
Skin2																
ΔL :	0,40	0,6	0,2	0,6	0,4	0,2	0,6	0,4	0,2	0,6	0,6	0,2	0,8	0,4	0,4	0,2
Mean value:	0,43															
Variance:	0,04															
ΔC :	5,70	4,2		2,4	1,5	1,2	4,2	5,4	3,6	5,4	4,2	2,7	3,9	2,4	2,7	2,7
Mean value:	3,48															
Variance:	1,95															
Δh :	15,00	7,8	6	7,8	6	5,7	15	15	15	15	7,2	15	15	15	7,8	11
Mean value:	11,21															
Variance:	16,70															
Light grey																
ΔL :	0,60	0,8	0,2	0,4	0,4	0,2	0,6	0,6	0,4	0,6	0,6	0,4	1	0,4	0,2	0,4
Mean value:	0,49															
Variance:	0,05															
ΔC :	6,00	4,8		4,5	4,5	0,9	2,7	4,8	3,6	4,5	4,5	1,8	5,4	5,1	5,1	2,4
Mean value:	4,04															
Variance:	2,11															
Δh :	15,00	15	15	15	9,3	15	15	15	15	15	9	15	15	15	14	13
Mean value:	14,04															
Variance:	4,07															
Magenta																
ΔL :	0,60	0,4	0,2	0,4	0,4	0,2	0,4	0,6	0,2	0,6	0,4	0,2	0,6	0,4	0,2	0,4
Mean value:	0,39															
Variance:	0,02															
ΔC :	6,90	4,8	4,8	2,1	5,7	3	8,4	10,8	9	8,1	4,8	5,4	5,4	4,2	1,2	4,8
Mean value:	5,59															
Variance:	6,49															
Δh :	4,80	3,6	3	0,9	1,8	1,2	3,9	5,1	2,7	3,9	1,8	3,6	2,7	2,4	1,5	2,1
Mean value:	2,81															
Variance:	1,57															

Appendix A: Shiraz, Settings and Results for the Determination of the Threshold Images

Mid-blue																
ΔL	1,00	0,8	0,2	0,4	0,6	0,2	0,6	0,8	0,6	0,6	0,6	0,8	0,4	0,6	0,6	0,4
Mean value:	0,58															
Variance:	0,05															
ΔC :	8,40	5,1	7,5	2,7	3,3	1,5	6,6	5,7	4,2	6	4,8	4,8	2,4	9	2,7	
Mean value:	4,98															
Variance:	5,08															
Δh :	5,40	4,5	5,4	2,1	3	1,2	3,9	4,8	5,4	5,1	3,3	2,7	5,1	4,8	3	2,4
Mean value:	3,88															
Variance:	1,85															
Mid-green																
ΔL :	0,60	0,4	0,2	0,4	0,4	0,2	0,6	0,8	0,4	0,4	0,6	0,4	0,6	0,4	0,2	0,2
Mean value:	0,43															
Variance:	0,03															
ΔC :	7,80	15	15	15	10	5,7	9,6	12,6	15	15	5,7	6,6	10,8	11,1	6,9	6,6
Mean value:	10,54															
Variance:	13,58															
Δh :	7,20	6,3	7,5	7,5	7,5	1,5	7,5	7,5	6,3	5,4	4,8	4,2	6,3	4,5	3	5,7
Mean value:	5,79															
Variance:	3,26															
Orange																
ΔL :	0,60	0,4	0,2	0,4	0,6	0,2	0,6	0,6	0,4	0,6	0,6	0,4	0,6	0,4	0,2	0,2
Mean value:	0,44															
Variance:	0,03															
ΔC :	8,10	9	6,6	8,1	7,5	3	10	12,6	6	8,4	5,4	4,8	6,6	6,6	3	6
Mean value:	6,99															
Variance:	6,14															
Δh :	6,00	7,8	7,2	3,6	7,5	2,7	8,1	10,2	3,9	7,8	6,6	5,1	7,5	5,7	2,4	5,7
Mean value:	6,11															
Variance:	4,64															
Pastel																
ΔL :	0,60	0,6	0,4	0,4	0,2	0,2	0,6	0,6	0,4	0,6	0,6	0,4	0,6	0,2	0,2	0,4
Mean value:	0,44															
Variance:	0,03															
ΔC :	5,40	4,5	4,8	2,4	3,3	1,2	3,9	5,7	2,7	6,3	3,9	5,1	4,8	4,5	2,7	1,8
Mean value:	3,94															
Variance:	2,15															
Δh :	12,90	15	15	15	8,4	15	15	15	15	15	9,3	15	15	15	7,2	15
Mean value:	13,61															
Variance:	7,37															
Red																
ΔL :	0,80	1	0,4	0,6	0,2	0,2	0,6	0,8	0,8	0,6	0,4	1,2	1,2	0,4	0,4	0,4
Mean value:	0,63															
Variance:	0,10															
ΔC :	4,20	7,2	3	3	2,7	1,5	5,7	6,3	4,8	4,8	4,8	4,8	4,2	4,8	3,9	2,7
Mean value:	4,28															
Variance:	2,14															
Δh :	10,80	4,5	7,5	4,8	9,3	3,9	13	11,4	9,3	7,2	6,3	12,6	5,7	6,9	6	
Mean value:	7,92															
Variance:	8,47															

Appendix B: Settings of the Photoshop® Plugin, Visual Noise Measurement

A description of how to use the Photoshop® plugin Noise Measurement is explained in the following literature: *Noise Measurements Plug-in, ver. 1.20 User's Guide, November 8th, 1999, Konica Corporation [16]*.

Here it is just describe how to install and use the plugin for the purpose of this diploma work:

B1. How to install the Plugin

The noise-measurements.8BF data has to be installed, copied, in the following folder of the computer:

C:\Programme\Adobe\PhotoshopCS\Plugin-Ins\noise_measurements

B2. How to run the Plugin

The plugin runs as follow in Photoshop®:

- open the tiff image, that is in an RGB Mode (otherwise the filter will not work)

Although there is no need to care about the actual monitor-colormangement, attention has to paid on the colour settings of the software Photoshop®, the tiff files, generated in Shiraz, are untagged, so first a profile has to be assigned: the monitor calibration profile, *Monitor_25.01.2006_1.icc*, this profile sets RGB colour values that the test-subjects saw.

The Photoshop® noise measurement plugin algorithm has been defined for the sRGB profile (see more about filter settings) *sRGB-IEC61966-2.1.icc*. So we assume, that although the filter algorithm has been calculated for the specific colour profile *sRGB IEC61966-2.1.icc*, the monitor profile, which is also an RGB profile could be equivalent to *sRGB IEC61966-2.1.icc*. That the two profiles are similar can be checked with the Macintosh® tool ColorSync®.

The transparent space corresponds to the sRGBprofile and the colour-filled one to the *Monitor_25.01.2006_1.icc* profile. On the 3D representation of the two colour profiles, it can be seen that the white and black points are on the same spots.

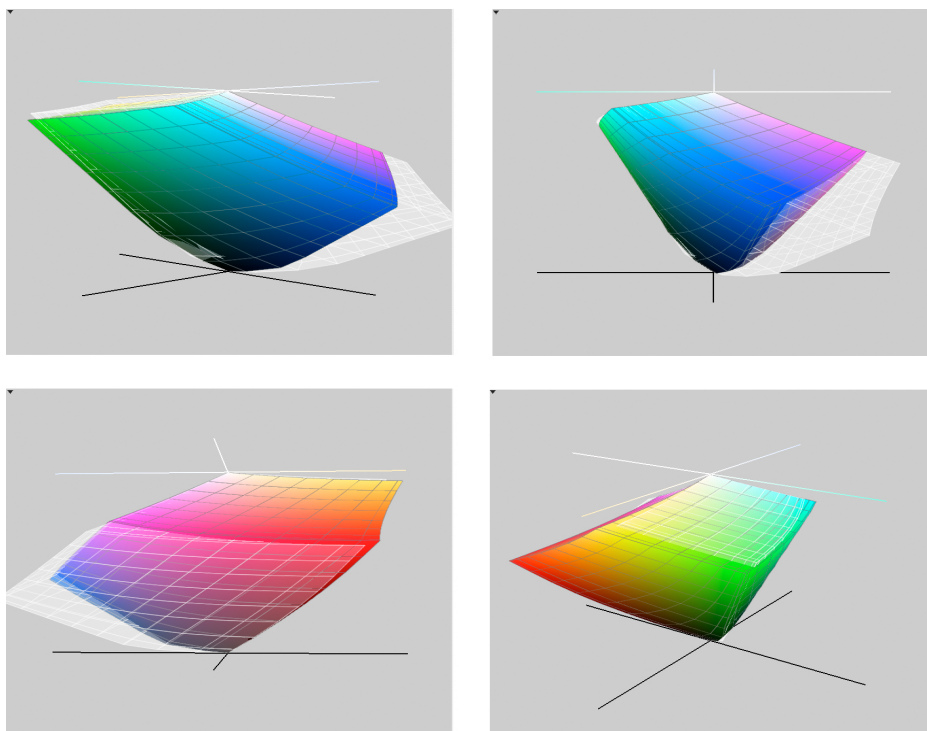


Figure B.01: Representation in ColorSync® of the gamut of the profile *sRGB IEC61966-2.1.icc* (transparent) and *Monitor_25.01.2006_1.icc* (full colour).

They also have the same shape, the only differences are that the *Monitor_25-01-06_1.icc* is a little bigger in the greens and much smaller in the blues and magentas.

The tagged RGB images with the monitor profile *Monitor_25.01.2006_1.icc* are filtered with the algorithm defined for the sRGB profile.

- select with the rectangle tool the area, which has to be measured.
- go to the menu [Filter][Iso Standards][Noise Measurements]
- Settings of the Noise Measurements Filter : the following window appears:

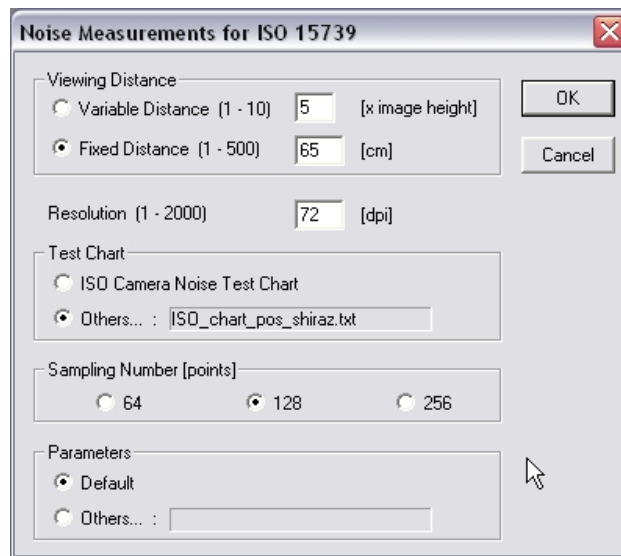


Figure B.02: Window of the settings of the Photoshop® plugin, Noise measurements for ISO 15739.

- The viewing distance is taken from the Michael Bantel and Jan Fischer's [10 p44] test conditions: the minimal distance was calculated to 60 cm and the maximum distance to 100cm. So first an average fixed distance of 82cm has been chosen. But after a few pretest it was noticed that the test persons has the tendency to come nearer to the screen during the test, so that why the persons were then setted at 65 cm.
- The resolution is based on the monitor resolution: 72dpi.

- The test chart had to be defined here, the defaults settings of the plug-in are defined for an OECF charts. So according to the instructions in the User's Guide [16], the test Chart's reference has to be defined as a text file (Text Editor®), which defined the position of the fields, that must be measured. Here the noise measurement takes place only for one colour field per image, so there is only one field to define in the text file. Refer to the text file *ISO_chart_pos_Shiraz.txt* to find the position syntax of the field for the measurement of the Shiraz images:

```
50.0<TAB>50.0<CR>
```

- Sampling Number: 64 stands for a measurement over 64x64 pixels field. The tiff images generated in Shiraz are 300x200 pixels. So 128 is chosen to get a measure for the larger pixel field possible in order to average any possible pixel errors in comparison to the smaller sampling number 64, and because a field of 256x 256 pixels would have been too wide in the height.
- The settings of the parameter describe the filter [16 pp11-13]. The algorithms of the noise-measurement filter are defined in a text file. It sets the white point (depending on the profile), the colour transformation for the adaptive colour space, the colour transformation for the opponent colour space, the code for the uniform colour space (Lab or Luv) and their corresponding noise weighting values, and at last the colour based spatial filtering. These parameters aim to describe the colour perception of the eye. They can be changed in a new text file. Here the default text-file parameter is used, because its white point is defined for the sRGB profile.
- After the filter setting, the image is filtered, the results can be saved in a text file or an Xcel® file.

Appendix C: User Guide Chinon

C1. How to run Chinon, a Matlab® Application

C11. If you have a Matlab® Version with the Image Processing Toolbox

You can directly run Chinon:

- install the `chinon` folder on your computer.
- add first the `chinon` folder to the path: [File] [Set Path] [Add with subfolders] and browse.
- Then just type the order „`chinon`“ in the command line.
- Then just follow the instructions.

C12. If you do not have a Matlab® version

C121. First copy the Chinon Folder anywhere on your Computer

The `chinon` folder contains following data:

- `MCRInstaller.exe` data
- `chinon.exe` data
- `chinon.ctf` data
- `source` folder

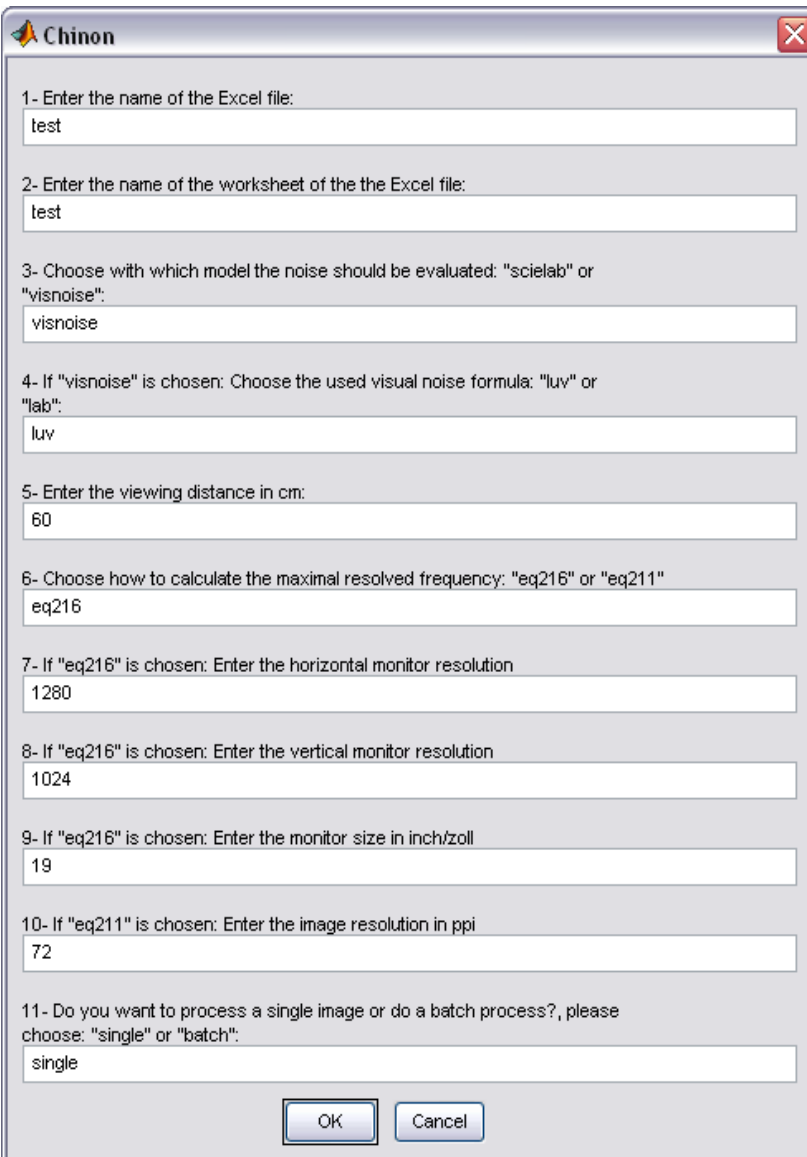
C122. Installation

- first install the application of Matlab® in order to be able to run `chinon` then. So double click on `MCRInstaller.exe` and follow the instructions.
- Then go in the folder `chinon` and double click on the `chinon.exe` data. It should then run the programm Chinon. A command window should open, but do not worry about.
- the `source` folder contains the code of the `chinon` programm in the Matlab® so called `m.file`.

C2. How to use Chinon

C21. Settings of Chinon

After double click on `chinon.exe`, the following window should open:



The screenshot shows a dialog box titled "Chinon" with a close button in the top right corner. The dialog contains 11 numbered input fields for configuration, followed by "OK" and "Cancel" buttons at the bottom.

- 1- Enter the name of the Excel file:
test
- 2- Enter the name of the worksheet of the the Excel file:
test
- 3- Choose with which model the noise should be evaluated: "scielab" or "visnoise":
visnoise
- 4- If "visnoise" is chosen: Choose the used visual noise formula: "luv" or "lab":
luv
- 5- Enter the viewing distance in cm:
60
- 6- Choose how to calculate the maximal resolved frequency: "eq216" or "eq211"
eq216
- 7- If "eq216" is chosen: Enter the horizontal monitor resolution
1280
- 8- If "eq216" is chosen: Enter the vertical monitor resolution
1024
- 9- If "eq216" is chosen: Enter the monitor size in inch/zoll
19
- 10- If "eq211" is chosen: Enter the image resolution in ppi
72
- 11- Do you want to process a single image or do a batch process?, please choose: "single" or "batch":
single

Buttons: OK, Cancel

Figure C.01: window of the settings of the Chinon programm.

Enter your settings:

Setting 1: the results of the measurement of Chinon are reported in an Excel® table, which is created automatically in the current folder of Chinon.

Setting 2: if the Excel® table already exists and you want to add some new measurements as worksheet, just enter a new name for the worksheet, while keeping the same name for the Excel® table. Still the report will occur in the current folder of Chinon.

Setting 3: refer to chapter 2 [paragraph 2.5.2] (step 9 of the human visual algorithm). Here you have to choose with which model, you want your image be evaluated. Keep in mind that the S-CIELabDE2000 model requires a noisy image and its corresponding noise free image. A spatially complex frequency pattern can be present in the image data. While the visual noise measurement model requires only one noisy image, but the evaluated image must be a uniform patch.

Setting 4: refers to chapter3 [paragraph 3.1.1], this only apply if you choose to evaluate your images with the visual noise measurement model.

Setting 5 to 10: refers to chapter 2 [paragraph 2.5.2] (step5). Here you need to enter the setting of your experiment or the use of your image, from which depends the smallest resolvable pattern.

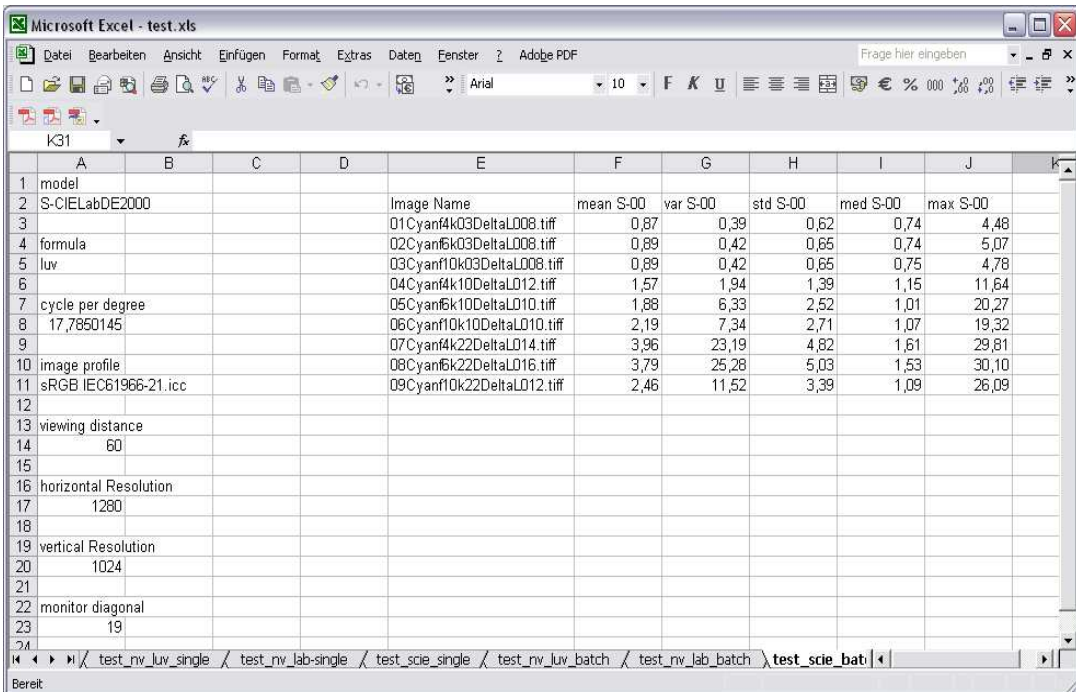
Setting 11: for experiment you may need to evaluate many images, so you can choose if you would like to do a single image processing or a batch processing of your images. When you choose the single process, while running Chinon will display the image you have chosen

After choosing all the settings, click on „OK“. First another window will open and ask to choose the profile that is embedded in your images. You can brows through your computer. Then another window will open asking you to choose the image with noise or the folder containing the noisy images, depending on which process you choose to evaluate your images.

For the batch process be sure that all the images you want to be evaluate are all in the same folder. Then if you have choose to evaluate your images with S-CIELabDE2000 model another window will open and ask you to choose the image or the folder of your noise free image. In the last case, be sure that you have the same number of noisy images and corresponding noise free images in both folders and inside the folder in the same order.

C22. How Chinon returns the Results

After chinon evaluates your image you can open your Excel® table, which lays in the current folder of chinon.



	A	B	C	D	E	F	G	H	I	J
1	model									
2	S-CIELabDE2000				Image Name	mean S-00	var S-00	std S-00	med S-00	max S-00
3					01Cyan4k03DeltaL008.tiff	0,87	0,39	0,62	0,74	4,48
4	formula				02Cyan6k03DeltaL008.tiff	0,89	0,42	0,65	0,74	5,07
5	luv				03Cyanf10k03DeltaL008.tiff	0,89	0,42	0,65	0,75	4,78
6					04Cyan4k10DeltaL012.tiff	1,57	1,94	1,39	1,15	11,64
7	cycle per degree				05Cyan6k10DeltaL010.tiff	1,88	6,33	2,52	1,01	20,27
8	17,7850145				06Cyanf10k10DeltaL010.tiff	2,19	7,34	2,71	1,07	19,32
9					07Cyan4k22DeltaL014.tiff	3,96	23,19	4,82	1,61	29,81
10	image profile				08Cyan6k22DeltaL016.tiff	3,79	25,28	5,03	1,53	30,10
11	sRGB IEC61966-21.icc				09Cyanf10k22DeltaL012.tiff	2,46	11,52	3,39	1,09	26,09
12										
13	viewing distance									
14	60									
15										
16	horizontal Resolution									
17	1280									
18										
19	vertical Resolution									
20	1024									
21										
22	monitor diagonal									
23	19									

Figure C.02: figure of how the results of the evaluation of the images with Chinon are reported in the table Excel®.

Notice that the previously set parameters in the window chinon has been reported in the Excel® Table. Depending on the chosen model, the visual noise value or the colour difference as mean, variance, standard deviation, median or maximlum error values have been reported adverse to the images' name.

Referring to point 1 and 2, for instance in this case (figure C.02) the results have been reported in an already existing Excel table named „test“ in a new worksheet named „test_scie_batch“.

C23. Notice to avoid any Problems while running Chinon

- Make sure that your image is a RGB data file and that it has a tiff or jpeg format.
- Do not forget to close your Excel® table if you want a worksheet to be added to it, otherwise while running chinon will ask you if you would like to replace you entire Excel® table.
- Be careful by naming your profile, Matlab does not allow any data name with any symbol like dot or semicolon (this apply also when you enter a Excel and a worksheet name). Make sure that you have a valid data ending with *.icc or *.icm.
- At the points 3, 4, 6 and 11, you are asked to choose between either way, be sure that you enter the asked option as it is spelled between the quotation mark, otherwise Chinon will not run.

Appendix D: Colour Transformation Matrices

D1. Chromatic Adaptation Matrices to transfer the Tristimulus Values, X, Y and Z into the Cone Space L, M, and S

D11. von Kries Matrix

- *p109 : ICC.1:2001-12, File Format for Color Profiles (Version 4.0.0)*
<http://www.color.org/newiccspec.pdf>
- *Measuring Colour, R.W.G. Hunt, Ellis Horwood, Series, Applied Science and Industrial Technology, (p71) [4]*

$$M_{\text{von Kries}} = \begin{bmatrix} 0,40024 & 0,70760 & -0,08081 \\ -0,22630 & 1,16532 & 0,04570 \\ 0,0 & 0,0 & 0,91822 \end{bmatrix} \quad (\text{D1.01}_1)$$

It exists another variant of the von Kries matrix, which is slightly different as the one above.

- *Principles of Colour Technology, Billmeyer and Saltzman's, Roy S. Berns, 3rd Edition, John and Wiley, 2000 (pp204-205)[5]*

$$M_{\text{von Kries}} = \begin{bmatrix} 0,3897 & 0,6890 & -0,0787 \\ -0,2298 & 1,1834 & 0,04640 \\ 0,0000 & 0,0000 & 1,0000 \end{bmatrix} \quad (\text{D1.01}_2)$$

This matrix is used in the algorithm of the model of the visual system.

D12. Smith-Porkony cone space matrix

- *Human Color Vision, 2nd Edition, Peter K. Kaiser and Robert M. Boyton, Optical Society of America (p557) [13]*

$$M_{Smith\ Porkony} = \begin{bmatrix} 0,15516 & 0,54308 & -0,03287 \\ -0,15516 & 0,45692 & 0,03287 \\ 0,0000 & 0,0000 & 0,01608 \end{bmatrix} \quad (D1.02)$$

D13. Bradford Transformation

- *The Reproduction of Colour, R.W.G. Hunt, Sixth Edition, John Wiley and Sons Ltd, West Sussex, England, 2004.p590 [7]*
- *Colour Appearance Model, Fairchild Mark. D., Addison Wesley Longman, Inc (1998, p379) [3]*

The chromatic adaptation Bradford transform is a modified von Kries transformation, which uses some a set of responses R, G, B based on the eye's sensitivity curves, but unlike the cone responses L, M, S, they have some negative spectral values. Moreover an exponential non-linearity has been added to short-wavelength sensitive channel.

$$M_{Bradford} = \begin{bmatrix} 0,8951 & 0,2664 & -0,1614 \\ -0,7502 & 1,7135 & 0,0367 \\ 0,0389 & -0,0685 & 1,0296 \end{bmatrix} \quad (D1.03)$$

Using linear transform matrices (like von Kreis transform), reference and test states are interchangeable. Using matrices with non-linear factor (like Bradford transform) care must be taken by interchanging the reference with the tests. Actually the Bradford chromatic-adaptation transform is used to go from the source viewing conditions to the reference viewing conditions.

D14. The Hunt-Pointer-Estevez Transformation

- *Fairchild, Mark D. 2005 : Color Appearance Models, second edition, John Wiley & Sons, Chichester, West Sussex (p379). [3]*

The Bradford responses are not physiologically plausible cone responsivities (they have negative values at many wavelengths), that is why the Bradford chromatic adaptation transform is then scaled to the Hunt-Pointer-Estevez cones responses, prior to the application of a non linear response compression.

$$M_{\text{Hunt Pointer Estevez}} = \begin{bmatrix} 0,38971 & 0,68898 & -0,07868 \\ -0,22981 & 1,18340 & 0,04641 \\ 0,0000 & 0,0000 & 1,0000 \end{bmatrix} \quad (\text{D1.04})$$

As we can notice the Hunt-Pointer-Estevez chromatic adaptation transform is very similar to the von Kries Transformation.

D15. the CIECAM02 Matrix

Color appearance Model, Mark D. Fairchild, Second Edition, Wiley and Sons, 2005 West Sussex (p268) [3]

$$M_{\text{CIE CAM02}} = \begin{bmatrix} 0,7238 & 0,4296 & -0,1624 \\ -0,7036 & 1,6975 & 0,0061 \\ 0,003 & 0,0136 & 0,9834 \end{bmatrix} \quad (\text{D1.05})$$

D16. Evaluation of the Matrices

Related to step 2 of the human visual algorithm [paragraph 2.5.2], the chromatic adaptation matrix must be chosen. To do so the LMS coordinates of a white image are calculated with the different matrices.

Table D1.01: cone space coordinates of a white image, tested with the different transformation matrices from the tristimulus values to the cone space responses.

Cone coordinates	Matrix A1.01_1	Matrix A1.01_2	Matrix A1.02	Matrix A1.03	Matrix A1.05
L	1,0127	0,98605	0,6601	0,9647	0,96264
M	0,99267	1,0081	0,3405	0,9901	0,98668
S	0,91824	1	0,01608	1,0084	0,99626

The criteria for choosing the Matrix A1.01_2 rather than the others is that the cone coordinates for a white should be all equal and reaching their maximum toward the value of 1.

D2. Matrix Transforms from the Tristimulus Values to the Opponent Colour Space Coordinates.

D21. Matrix from the Photoshop® Plugin

This matrix is proposed in the text data of the default parameters used in the Photoshop® plugin [16].

$$M_{opposite} = \begin{bmatrix} 0,0 & 1,0 & 0,0 \\ 1,0 & -1,0 & 0,0 \\ 0,0 & 0,4 & -0,4 \end{bmatrix} \quad (D2.01)$$

This matrix has been used in the algorithm of the model of the visual system in the Photoshop® plugin as well as in Chinon.

From the literatures [17] [18] that describe the visual noise measurement, there are two other different matrices, that have been proposed, but which do not issue realistic values for opponent colour space coordinates.

D22. Matrix from the Konica® paper

This matrix is proposed in the Konica® paper from Hung et al [17].

$$M_{opposite} = \begin{bmatrix} 1,0 & 1,0 & 0,0 \\ 0,0 & 0,4 & -0,4 \\ 0,0 & 1,0 & 0,0 \end{bmatrix} \quad (D2.02)$$

D23. Matrix from the Photoshop® Plugin User Guide

This matrix is proposed in the Photoshop® plugin user Guide [18].

$$M_{opposite} = \begin{bmatrix} 0,0 & 1,0 & 0,0 \\ 1,0 & -1,0 & 0,0 \\ 0,0 & 0,4 & 0,4 \end{bmatrix} \quad (D2.03)$$

D24. Matrix from the S-CIELabDE2000 Paper

This matrix is proposed by Faichild; Mark D. in his S-CIELabDE2000 paper [20].

$$M_{opposite} = \begin{bmatrix} 0,297 & 0,72 & -0,107 \\ -0,449 & 0,29 & -0,077 \\ 0,086 & -0,59 & 0,501 \end{bmatrix} \quad (D2.04)$$

This matrix issues quiet realistic results for the opponent colour space coordinates, but does not perform as good as the matrix 2.01.

D25. Evaluation of the Matrices

Related to step 3 of the human visual algorithm [paragraph 252], the opponent colour matrix must be chosen. To do so the opponent colour coordinates of a white image are calculated with the different matrices.

Table D2.01: opponent coordinates of a white image, tested with the different transformation matrices from the tristimulus values to the opponent space responses.

Opponent coordinates	Matrix D2.01	Matrix D2.02	Matrix D2.03	Matrix D2.04
A	0,9999	1,9643	0,99987	0,89933
C1	-0,035529	-0,00004855	-0,035407	-0,2201
C2	-0,000047553	0,99987	0,80004	-0,0058585

The criteria for choosing matrix D2.01, was that the coordinates of a white in the opponent colour space, should have a high value in the achromatic channel, but also both chromatic coordinates going both toward the value of zero.

Appendix E: Visual Noise Scaling with the Human Visual Algorithm

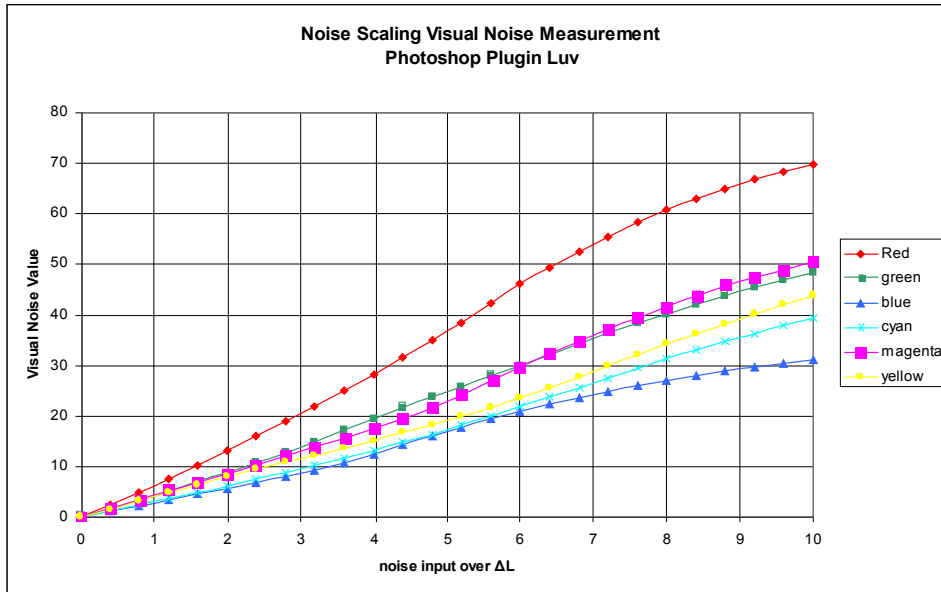
E1. Results for the Visual Noise Measurement Model with the Photoshop® Plugin and Chinon with the Lab formula, and for the S-CIELabDE2000 model.

In paragraph 5.1, the noise scaling with the model S-CIELabDE2000 was determined as the noise input along the luminance, chroma and hue channel in function of the S- Δ E2000 median value, because according to the former results [paragraph 4.2.3.1] the S- Δ E2000 median value is performing better. According to the results, the S- Δ E2000 mean, variance, standard deviation and median value are giving satisfying and similar results as well, that is why the noise scaling was although made as the noise input in function of these grandeurs. Doing so it could be notice that the noise scaling with the S- Δ E2000 mean value is similar to the scaling of the noise with the S- Δ E2000 median value.

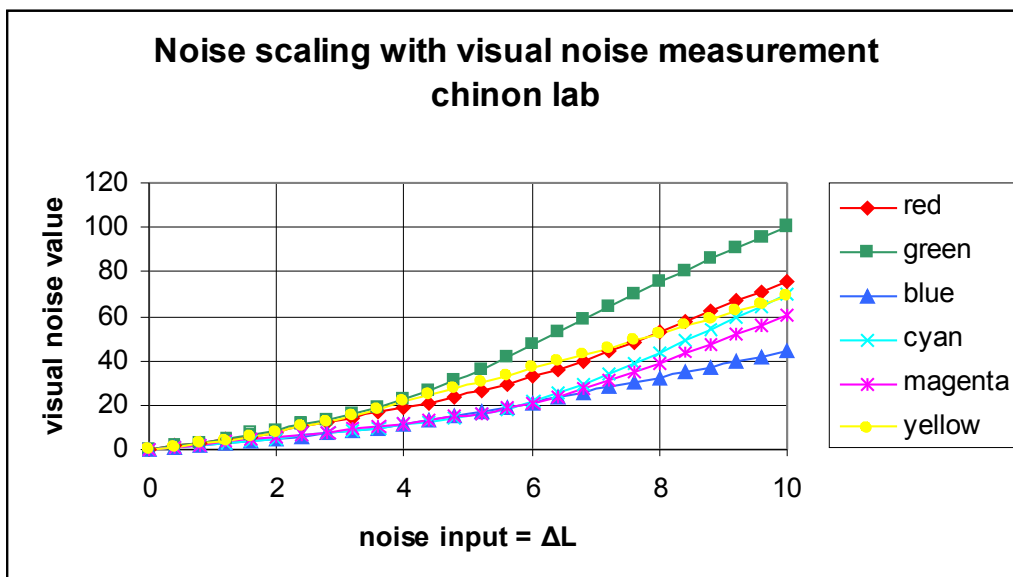
E11.Noise Scaling along the Noise Input LCh for the Colours: Red, Green, Blue, Cyan and Blue.

E111. Noise Input in the Luminance Channel.

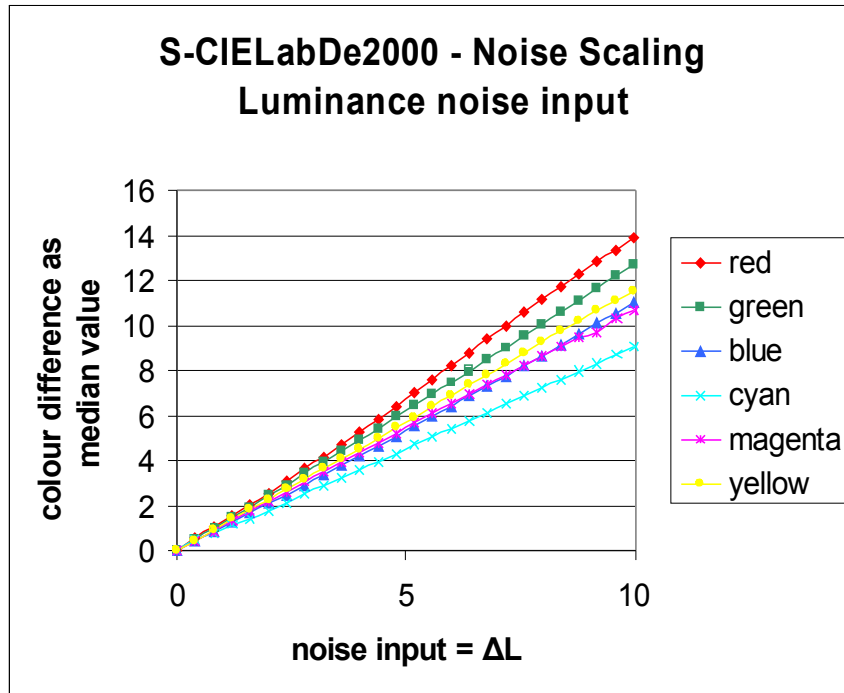
Graph E1.01: Visual noise value from the Photoshop® plugin in function of the noise input along the luminance channel:



Graph E1.02: Visual noise value from Chinon with the Lab formula in function of the noise input along the luminance channel.

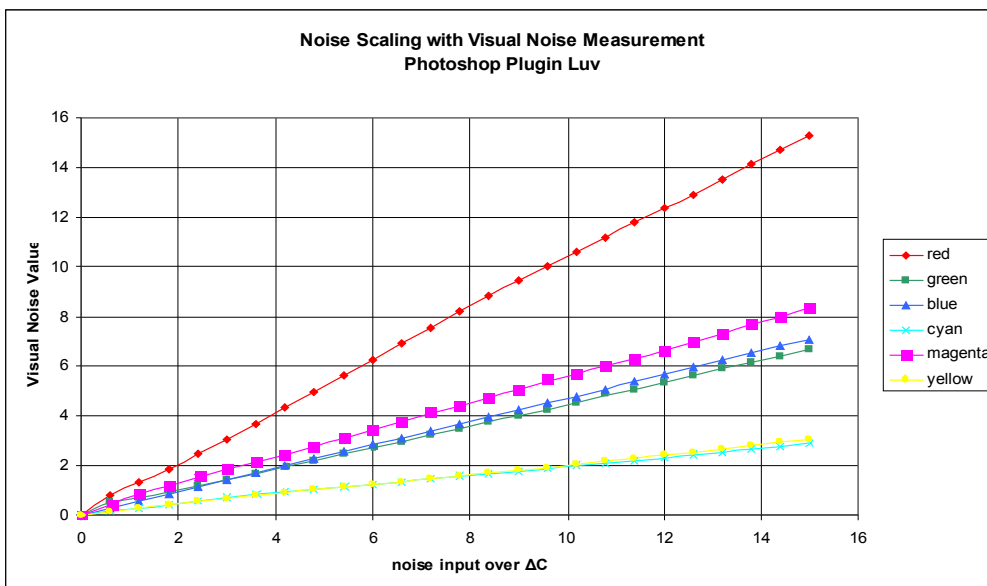


Graph E1.03: colour difference S- ΔE_{2000} as median value in function of noise input along the luminance channel.

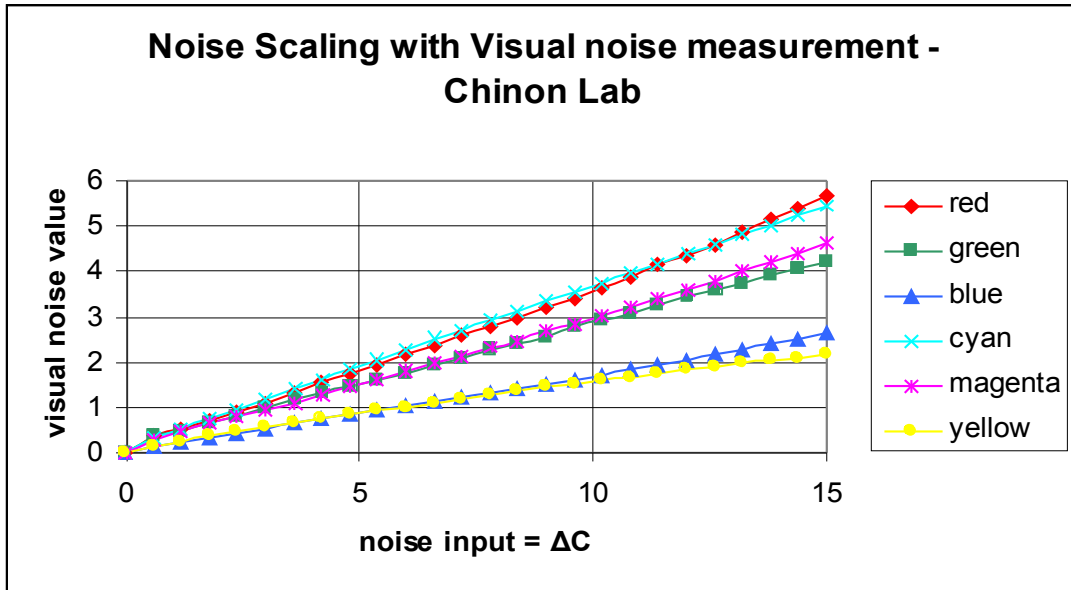


E112. Noise Input in the Chroma Channel

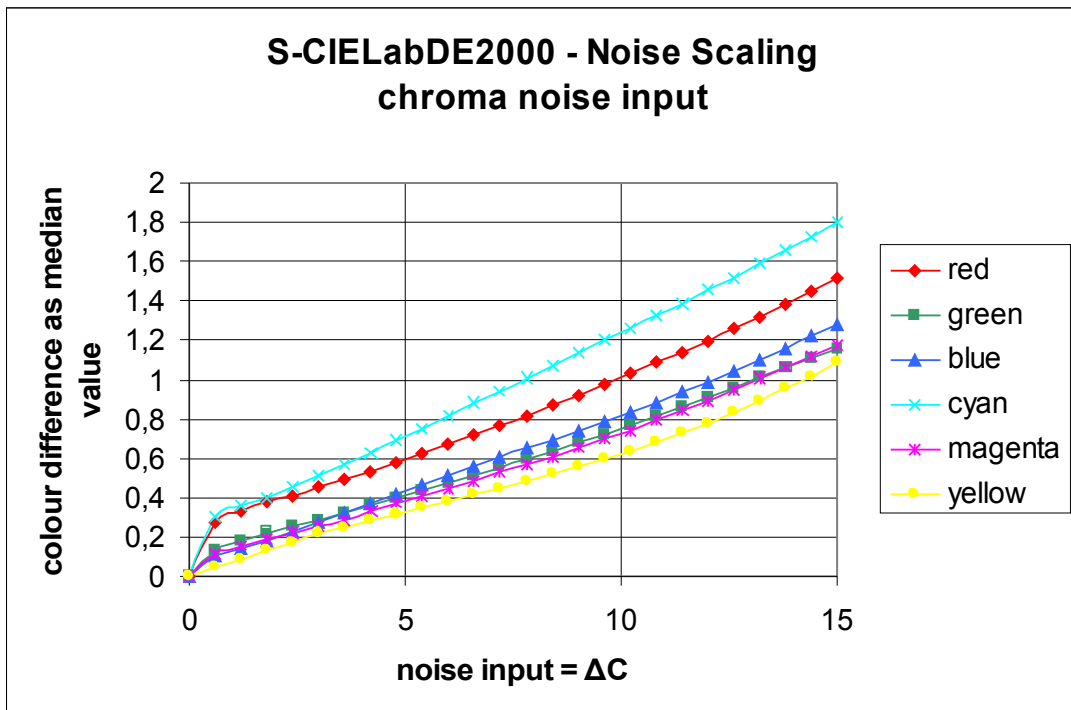
Graph E1.04: Visual noise value from the Photoshop® plugin in function of the noise input along the chroma channel.



Graph E1.05: Visual noise value from Chinon with the Lab formula in function of the noise input along the chroma channel.

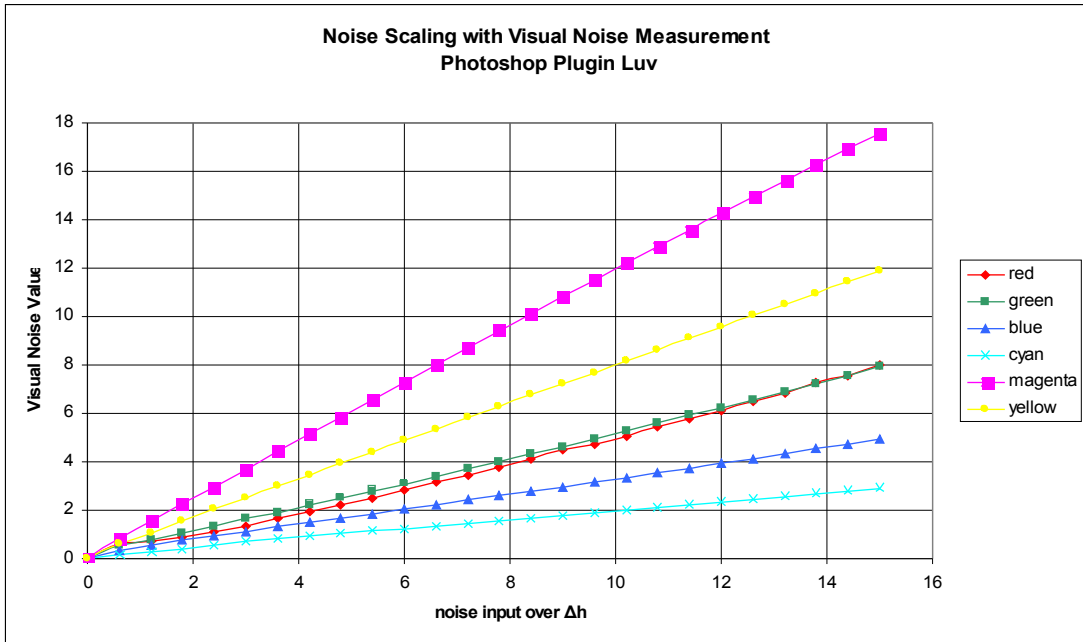


Graph E1.06: colour difference S- ΔE_{2000} as median value in function of noise input along the chroma channel.

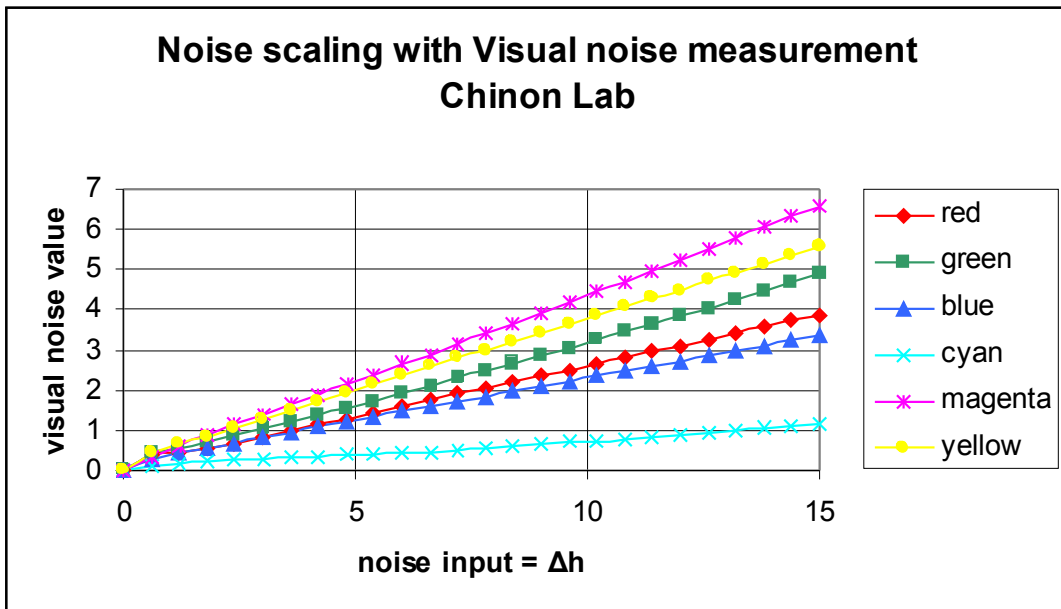


E113. Noise input in the Hue Channel.

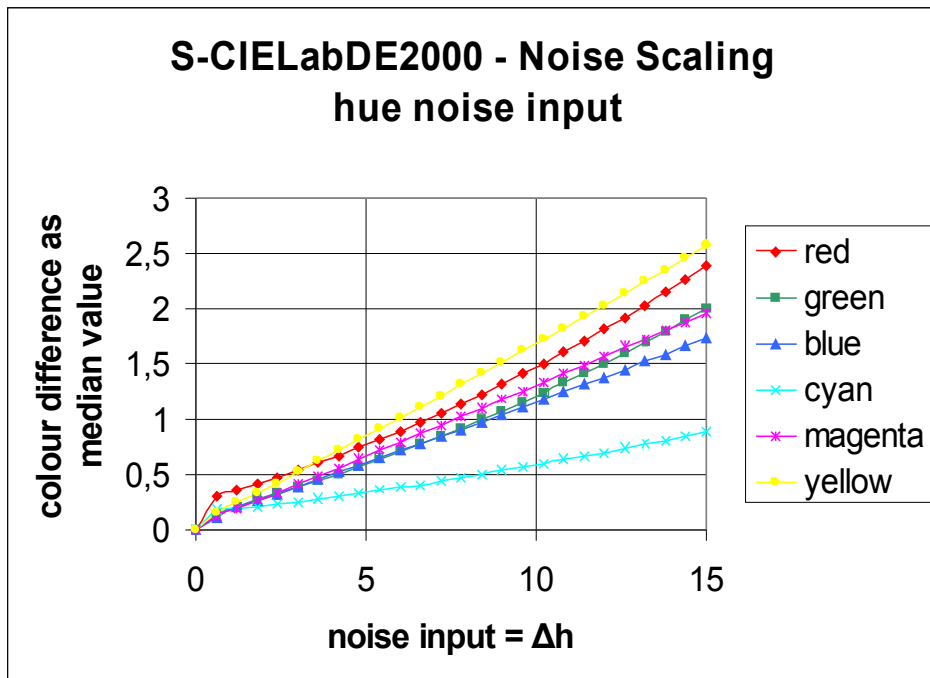
Graph E1.07: Visual noise value from the Photoshop® plugin in function of the noise input along the hue channel.



Graph E1.08: Visual noise value from Chinon with the Lab formula in function of the noise input along the hue channel.



Graph E1.09: colour difference S- ΔE_{2000} as median value in function of noise input along the hue channel.



Appendix F: Investigation of the S-CIELabDE2000 Model.

Here the results of the experiments related to paragraph 4.2.2 are reported for the colours: cyan, red, light grey, and mid-green. Each colour has a rectangular frequency pattern of either 4, 6 or 10 pixels and each a contrast of either 3, 10 or 22%. So there are 9 different patterns of contrast and frequency for each colour.

F1. Cyan

Table F1.01: median value of the colour difference over the pixels for noise input in the luminance, chroma, and hue channel for each of the 9 patterns of contrast and frequency for the colour cyan.

frequency in pixels pro cycle	contrast in %	noise input ΔL	S- ΔE_{200} median	noise input ΔC	S- ΔE_{200} median	noise input Δh	S- ΔE_{200} median
4	3	0,86	1,00	6,92	1,61	15	0,87
6	3	0,82	1,00	7,22	1,69	15	0,87
10	3	0,80	1,00	6,78	1,61	14,86	0,86
4	10	1,16	1,61	8,44	2,21	14,98	0,94
6	10	1,08	1,39	8,47	2,30	14,54	0,93
10	10	0,95	1,32	7,09	1,85	14,39	0,92
4	22	1,49	1,64	10,26	2,60	15	1,13
6	22	1,5	1,85	9,7	2,44	14,88	1,14
10	22	1,21	1,50	8,46	2,16	14,79	1,13

F2. Red

Table F1.01: median value of the colour difference over the pixels for noise input in the luminance, chroma, and hue channel for each of the 9 patterns of contrast and frequency for the colour red.

frequency in pixels pro cycle	contrast in %	noise input ΔL	S- ΔE_{200} median	noise input ΔC	S- ΔE_{200} median	noise input Δh	S- ΔE_{200} median
4	3	0,81	1,24	5,39	0,69	9,61	1,55
6	3	0,89	1,24	5,83	0,72	10,6	1,71
10	3	0,8	1,23	6,18	0,79	10,15	1,69
4	10	1,08	1,60	6,64	0,93	11,1	1,97
6	10	1,03	1,65	6,67	0,95	11,46	2,06
10	10	0,95	1,70	6,12	0,89	10,11	1,89
4	22	1,48	1,96	7,73	1,28	11,57	1,93
6	22	1,42	2,01	7,99	1,26	12,61	2,05
10	22	1,12	1,81	6,54	1,11	11,72	1,95

F3. Mid-green

Table F1.01: median value of the colour difference over the pixels for noise input in the luminance, chroma, and hue channel for each of the 9 patterns of contrast and frequency for the colour mid-green.

frequency in pixels pro cycle	contrast in %	noise input ΔL	S- ΔE_{200} median	noise input ΔC	S- ΔE_{200} median	noise input Δh	S- ΔE_{200} median
4	3	0,82	1,09	11,61	1,31	6,78	0,96
6	3	0,87	1,09	12,86	1,44	8,28	1,16
10	3	0,71	1,09	11,60	1,30	8,27	1,15
4	10	1,18	2,02	13,56	2,21	8,69	1,85
6	10	1,2	1,82	12,55	1,88	9,31	1,83
10	10	0,88	1,32	12,90	2,03	8,03	1,69
4	22	1,53	1,90	13,33	1,59	9,85	1,44
6	22	1,50	1,88	13,44	1,62	9,22	1,37
10	22	1,16	1,48	13,63	1,63	9,35	1,39

F4. Light grey

Here we only report the values for noise input in luminance.

Table F1.01: median value of the colour difference over the pixels for noise input in the luminance, chroma, and hue channel for each of the 9 patterns of contrast and frequency for the colour light-grey.

frequency in pixels pro cycle	contrast in %	noise input ΔL	S- ΔE_{200} median
4	3	0,81	1,08
6	3	0,90	1,08
10	3	0,75	1,07
4	10	1,13	1,50
6	10	1,15	1,51
10	10	1,16	1,04
4	22	1,52	1,85
6	22	1,52	1,60
10	22	0,88	1,48

F5. Mid-green

Table F1.01: median value of the colour difference over the pixels for noise input in the luminance, chroma, and hue channel for each of the 9 patterns of contrast and frequency for the colour mid-green.

frequency in pixels pro cycle	contrast in %	noise input ΔL	S- ΔE_{200} median	noise input ΔC	S- ΔE_{200} median	noise input Δh	S- ΔE_{200} median
4	3	0,82	1,09	11,61	1,31	6,78	0,96
6	3	0,87	1,09	12,86	1,44	8,28	1,16
10	3	0,71	1,09	11,60	1,30	8,27	1,15
4	10	1,18	2,02	13,56	2,21	8,69	1,85
6	10	1,2	1,82	12,55	1,88	9,31	1,83
10	10	0,88	1,32	12,90	2,03	8,03	1,69
4	22	1,53	1,90	13,33	1,59	9,85	1,44
6	22	1,50	1,88	13,44	1,62	9,22	1,37
10	22	1,16	1,48	13,63	1,63	9,35	1,3